E2F6: A Unique Regulator of Post-natal Cardiac Growth, Death and Function

Jennifer Lynn Major

Thesis submitted to the Faculty of Graduate and Postdoctoral Studies
in partial fulfillment of the requirements for the
PhD degree in Cellular and Molecular Medicine.

Department of Cellular and Molecular Medicine
Faculty of Medicine
University of Ottawa

FOR HUNTER.

AUTHORIZATIONS

Title: The E2F Pathway in Cardiac Development and Disease
Author: Jennifer Rueger
Publication: Springer eBook
Publisher: Springer
Date: Jan 1, 2011

Logged in as:

Jennifer Major

LOGOUT

Order Completed

Thank you for your order.

This Agreement between Jennifer L Major ("You") and Springer ("Springer") consists of your license details and the terms and conditions provided by Springer and Copyright Clearance Center.

Your confirmation email will contain your order number for future reference.

Printable details.

License Number	4022540005708
License date	Jan 05, 2017
Licensed Content Publisher	Springer
Licensed Content Publication	Springer eBook
Licensed Content Title	The E2F Pathway in Cardiac Development and Disease
Licensed Content Author	Jennifer Rueger
Licensed Content Date	Jan 1, 2011
Type of Use	Thesis/Dissertation
Portion	Figures/tables/illustrations
Number of figures/tables/illustrations	2
Author of this Springer article	Yes and you are a contributor of the new work
Order reference number	
Original figure numbers	Figures 1,2
Title of your thesis / dissertation	E2F6: A Regulator of Cardiac Growth, Differentiation, and Death
Expected completion date	Oct 2016
Estimated size(pages)	200

Requestor Location	Jennifer L Major Attn: Jennifer L Major
Billing Type	Invoice
Billing address	Jennifer L Major Canada Attn: Jennifer L Major
Total	0.00 CAD

ORDER MORE CLOSE WINDOW

Title: Interplay between the E2F pathway and β-adrenergic signaling in the pathological hypertrophic response of myocardium

Author: Jennifer L. Major,Maysoon Salih,Balwant S. Tuana

Publication: Journal of Molecular and Cellular Cardiology

Publisher: Elsevier

Date: July 2015

Order Completed

Thank you for your order.

This Agreement between Jennifer L Major ("You") and Elsevier ("Elsevier") consists of your license details and the terms and conditions provided by Elsevier and Copyright Clearance Center.

Your confirmation email will contain your order number for future reference.

Printable details.

License Number	4022531001921
License date	Jan 05, 2017
Licensed Content Publisher	Elsevier
Licensed Content Publication	Journal of Molecular and Cellular Cardiology
Licensed Content Title	Interplay between the E2F pathway and β-adrenergic signaling in the pathological hypertrophic response of myocardium
Licensed Content Author	Jennifer L. Major,Maysoon Salih,Balwant S. Tuana
Licensed Content Date	July 2015
Licensed Content Volume	84
Licensed Content Issue	n/a
Licensed Content Pages	12
Type of Use	reuse in a thesis/dissertation
Portion	full article
Format	electronic
Are you the author of this Elsevier article?	Yes
Will you be translating?	No

Order reference number	
Title of your thesis/dissertation	E2F6: A Regulator of Cardiac Growth, Differentiation, and Death
Expected completion date	Oct 2016
Estimated size (number of pages)	200
Elsevier VAT number	GB 494 6272 12
Requestor Location	Jennifer L Major Attn: Jennifer L Major
Total	0.00 CAD

ORDER MORE CLOSE WINDOW

Author Self-Archiving Policy

This policy sets out the ways in which Oxford University Press journal authors may self-archive versions of their work on their own webpages, on institutional webpages, and in other repositories. Please be aware that policies and embargo periods may differ from journal to journal, so ensure that you have selected the correct journal policy.

Abstract and Citation information

Authors may reuse the Abstract and Citation information (e.g. Title, Author name, Publication dates) of their article anywhere at any time including social media such as Facebook, blogs and Twitter, providing that where possible a link is included back to the article on the OUP site. Preferably the link should be, or include, the Digital Object Identifier (DOI) which can be found in the Citation information about your article online.

Author's Original Version

The Author's Original Version (AOV) is defined here as the un-refereed author version of an article completed before submission of the article to the journal. This is sometimes referred to as the "preprint" version. The author accepts full responsibility for the article, and the content and layout is set out by the author.

Authors may reuse the AOV anywhere at any time, providing that once the article is accepted they provide a statement of acknowledgement, and that once the article has been published this acknowledgement is updated to provide details such as the volume and issue number, the DOI, and a link to the published article on the journal's website:

> *This article has been accepted for publication in* [Journal Title] *Published by Oxford University Press*.

Accepted Manuscript

The accepted manuscript (AM) is the final draft author manuscript, as accepted for publication by a journal, including modifications based on referees' suggestions, before it has undergone copyediting, typesetting and proof correction. This is sometimes referred to as the post-print version.

Immediately upon publication authors may:

- Immediately upload their AM to their own personal webpage (excluding commercial websites and repositories)
- Immediately upload their AM to their institutional repository on the proviso that it is not made publically available until after the specified embargo period

After the embargo period authors may:

- Upload their AM to institutional repository or other non-commercial repositories and make it publicly available. Accepted Manuscripts may not be uploaded to commercial websites or repositories, unless the website or repository has signed a licensing agreement with OUP allowing posting. For Profit social networking sites such as Researchgate and Academia.edu are considered "commercial" platforms.

Embargo periods

Embargo periods may vary between journals. For details of a journal's specific embargo period, please see the information for each individual title on our **Accepted Manuscript embargo** page.

When uploading an accepted manuscript to a repository, authors should include the following acknowledgment as well as a link to the published version in the journal. This will connect the published version to the AM version in the repository and help ensure that the article is cited correctly.

> *This is a pre-copyedited, author-produced version of an article accepted for publication in [insert journal title] following peer review. The version of record [insert complete citation information here] is available online at: xxxxxxx [insert URL and DOI of the article on the OUP website].*

Version of Record

The Version of Record (VOR) is defined here as the final typeset and edited version of the journal article that has been made available by OUP by formally and exclusively declaring the article "published". This includes any 'advanced access' article even before the compilation of a volume issue.

The VOR as it appears in the journal following copyediting and proof correction may not be deposited by authors in institutional repositories or posted to third party websites and made publicly available unless the article is published on an Open Access model licence that allows for such posting. Authors may share their VOR with private groups within their institution or through private groups on non-commercial platforms that are signatories to the STM Voluntary principles for article sharing on Scholarly Collaboration Networks (SCN). The VOR may not be posted to Commercial Platforms, either publically or privately unless they have signed a direct agreement with OUP.

ABSTRACT

Rationale/Background: The adult mammalian heart has a very limited potential for regeneration due to cardiomyocyte cell cycle withdrawal which occurs shortly after birth. One potential avenue to repair the heart following stress/injury is to reprogram pre-existing cardiomyocytes to re-enter the cell cycle. The E2F family is a group of transcription factors which ubiquitously regulate the cell cycle, but it has previously been difficult to fully appreciate their role in the post-natal myocardium due to either redundancy or embryonic lethality of genetic models. Thus we generated a dominant negative model of the E2F/Rb pathway via expression of the unique transcriptional repressor E2F6 in postnatal myocardium. E2F6 transgenic (Tg) mice developed dose dependent Dilated Cardiomyopathy (DCM) and sudden death without hypertrophy or apoptosis. This was accompanied by the partial loss of E2F3 (critical for cardiac development) and connexin-43 important for metabolic and electrical coupling.

Methods/Results: In this thesis E2F6-Tg mice were examined for markers of cardiac differentiation/ function and exposed to stressors to evaluate the capacity for the E2F pathway to regulate cardiomyocyte growth (isoproterenol) and death (doxorubicin and cobalt chloride). E2F6-Tg mice were twice as sensitive to isoproterenol as their Wt counterparts due to the observed activation of a β_2-adrenergic survival pathway. Cardiac hypertrophy in E2F6-Tg mice was accompanied by the rescue of E2F3 expression. Treatment of neonatal cardiomyocytes isolated from Wt and E2F6-Tg pups with cobalt chloride revealed a protective effect for E2F6 against apoptosis. Doxorubicin exposure

led to the loss of E2F6 protein and abolished its protective effect. Examination of neonatal hearts and cardiomyocytes isolated from them demonstrated a shift in the cell cycle and metabolic profiles of E2F6-Tg myocardium. Tg cardiomyocytes show decreased glycolysis and a dramatic increase in the regulator of ketolysis, β-hydroxybutyrate dehydrogenase (BDH1), prior to DCM. The substrate of BDH1 (β-hydroxybutyrate) was demonstrated to influence the levels of CX-43 in cardiomyocytes. E2F6 also deregulated expression of T-cap which has been linked to human DCM.

Conclusions: I provide evidence that the E2F pathway can regulate growth, death, and differentiation through a variety of mechanisms which link the cell cycle and metabolism to growth and survival to critically govern post-natal cardiac function. Furthermore, I reveal a new biomarker (BDH1) for early DCM which may be useful in diagnosis/ treatment of idiopathic cases of disease.

TABLE OF CONTENTS

LIST OF TABLES

LIST OF FIGURES

LIST OF ABBREVIATIONS

2-DG	2-deoxy glucose
α-MHC	Alpha myosin heavy chain
AKT	Protein Kinase B
β-OHB	Hydroxybutyrate
Anti-A	Antimycin-A
Bcl2	B-cell lymphoma 2
Blm2	Bloom syndrome 2 homologue
BW	Body weight
BDH1	B-hydroxybutyrate dehydrogenase 1
β_1AR	B_1-Adrenergic receptor
β_2-AR	B_2-Adrenergic receptor
Blm2	Bloom syndrome 2 homologue
BSA	Bovine serum albumin
cAMP	Cyclic AMP
CDK	Cyclin dependent kinase
CDKI	Cyclin dependent kinase inhibitor
CHF	Congestive heart failure
Chk1	Checkpoint Kinase 1
CREB	cAMP response element-binding protein
CX-43	Connexin-43 (gap junction α1)
CVD	Cardiovascular disease
DCM	Dilated cardiomyopathy
Dnaja3	Chaperone protein hsp40
Dox	doxorubicin
ECAR	Extracellular acidification rate
Echo	Echocardiography
EF	Ejection fraction
ERK (1/2)	Extracellular Receptor kinase (p44/p42)
FBS	Fetal bovine serum
FCCP	Carbonyl cyanide-4-phenylhydrazone
FS	Fractional shortening
GAPDH	Glyceraldehyde 3-phosphate dehydrogenase
GLUT4	Glucose transporter 4
HAT	Histone acetyl-transferase
HCM	Hypertrophic cardiomyopathy
HDAC	Histone deacetylase
HF	Heart failure
Iso	isoproterenol
IVSs	Interventricular septum thickness (systole)
IVSd	Interventricular septum thickness (diastole)
NCM	Neonatal cardiomyocyte
MAPK	Mitogen activated protein kinase
MI	Myocardial infarction

Myc-E2F6	E2F6 derived from transgene tagged with myc
OCR	Oxygen consumption rate
OXCT1	succinyl-CoA: 3-oxoacid-CoA transferase
Pal	palmitate
PDE4B	Protein phosphodiesterase 4B
PDK4	Pyruvate dehydrogenase kinase 4
PKA	Protein Kinase A
Pln	phospholamban
LV	Left ventricle
LVW	Left ventricle weight
LVEDs	Left ventricle end diameter (systole)
LVEDd	Left ventricle end diameter (diastole)
Rad51	Recombinant protein A
Rb	Retinoblastoma gene
RT-q-PCR	Reverse transcription quantitative polymerase chain reaction
SEM	Standard error of the mean
Ser	serine
Src/ c-src	Proto-oncogene tyrosine-protein kinase
T-cap	Teliothenin (titin cap)
TnI	Troponin I
TnT	Troponin T
Tg	Transgenic
Wt	Wild type

ACKNOWLEDGEMENTS

I would like to extend my sincere gratitude to the many people in my life who have helped me.

I would like to thank my supervisor: Dr. Balwant Tuana for giving me the opportunity to work on such a unique project in his lab, for his guidance as well and freedom to design and test my own ideas. I would also like to than Maysoon Salih- without her help and advice I do not think I could have finished this thesis. I would also like to thank all current and past members of the Tuana lab especially to Aaraf for all his help with the BDH1 project and to both him and Taha for great discussions and being my IT support. Thank-you to Mayra and Jana, I learned so much from both of you.

Thank-you to my best friends: Megan, Andrea, and Khierstyn, my sister Cyndi and my mother-in-law Ruth for always having my back whatever the problem.

Thank-you to my parents, Dan and Jan Rueger, for always pushing me to do my best and reach my potential. I'm so grateful to have such loving and supportive parents.

Thank-you to my wonderful husband Shane Major for being my partner and my support through school and life.

Thank-you to my daughter Roxy for being the sunshine in my life.

Thank-you Hunter for always believing in me, you taught me so much-

This is for you kiddo!

GENERAL INTRODUCTION

Cardiovascular diseases are the leading cause of non-communicable disease deaths, killing 17.5 million people world-wide in 2012 (1). In Canada, research and medical intervention has extended life for patients with cardiovascular disease (CVD) such that the survival rate has increased by 75% in the past six decades (2). Although such an improvement is astounding, it also means that there is a high rate of Canadians living with CVD and that produces an estimated economic burden of $20.9 billion annually. Furthermore, the quality of life for those patients with CVD and heart failure is lessened.

The heart is a highly specialized organ whose function is to pump blood which will be delivered to the whole body providing both oxygen and nutrients. The mammalian heart is a four chambered organ consisting of numerous cell types. The contractile cells which make up the bulk of the weight are cardiomyocytes. The basic contractile unit of the cardiomyocyte is called the sarcomere, which is organized into thick (actin) and thin (myosin) filaments giving cardiac muscle its striated appearance. In order for cardiomyocytes to communicate with one another and exert force they have a highly developed cell membrane called the sarcolemma which has deep invaginations called t-tubules which are rich in proteins and ion channels for excitation-contraction coupling. Cardiomyocytes also have gap junctions which form channels across cells allowing for communication between cardiomyocytes. The main gap junction protein expressed in the ventricles (the cardiac chambers which pump blood to the body) is connexin43. Such a

specialized force comes at a cost: metabolism, which is why ~40% of cardiomyocyte volume is occupied by mitochondria.

In order for appropriate differentiation and post-natal cardiac development to proceed, cardiomyocytes withdraw from the cell cycle shortly after birth. There is evidence indicating a limited amount of cardiomyocyte division in adult myocardium, but it is generally believed that growth in the adult heart is restricted to hypertrophy (3,4). This leaves the heart very sensitive to injury, since there is a limited potential to divide and replenish damaged tissue. Thus following injury, such as myocardial infarction, acute toxin/viral exposure, or long term exposure to stresses caused by chronic hypertension, chemotherapy, etc. the heart undergoes cardiac remodeling in an attempt to rescue function. This usually involves the induction of the pathological hypertrophic program. While initially this may be beneficial, it ultimately causes disorganization of the contractile apparatus resulting in inadequate pump function, chamber dilation, and cell death leading to heart failure (HF).

A tremendous amount of research has gone into the use of stem cells to replenish the heart mainly including the use of non-embryonic stem cells derived from bone marrow and induced pluripotent stem cells (5). While studies have demonstrated the therapeutic effects of these techniques they are limited by the ability of the cells to remain in the heart as well as the many barriers in place to collecting and using stem cells in humans. Another avenue to repair the heart is a cell cycle based approach to stimulate pre-existing cardiomyocytes to re-enter the cell cycle to divide. Recent studies have demonstrated that, for a brief window of time, neonatal mice have the potential to regenerate lost/damaged cardiac tissue (6). Cell lineage tracing revealed that the newly

regenerated cardiac tissue consisted of cells that came from pre-existing cardiomyocytes and not stem cells (7). Finally, the promotion of physiological over pathological hypertrophy and the inhibition of apoptosis is an attractive way to save the failing heart. In order to achieve this thorough understanding of the cardiac cell cycle, in particular the switch from a proliferative to differentiated state that happens in the perinatal period is essential.

The Cell Cycle

The cell cycle is a tightly regulated process which exists in five phases and has numerous checkpoints to inhibit abnormal cell proliferation. It begins in Gap 1(G_1) during which cells grow and prepare for cell division. Cells which remain in G_1 for extended periods of time (such as cardiomyocytes) can exit the cell cycle and enter G_0, after which they may re-enter the cell cycle or differentiate. When the appropriate growth cues are received cells pass through a restriction point in G_1, after which they are committed to the cell cycle. The next stage is the synthesis (S) phase in which DNA is duplicated, followed by a second preparatory phase Gap 2 (G_2). Next chromatin is condensed and assembled at the mitotic plate (mitosis) and DNA and cellular components are separated into two daughter cells in a process called cytokinesis. In the post-natal heart cardiomyocytes can pass through the cell cycle without cytokinesis in a process called endo-reduplication resulting in bi-nucleation.

Cell cycle regulation is managed in large by cyclin dependent protein kinases (CDKs) which phosphorylate a wide range of proteins leading to the appropriate expression of genes for coordinated induction and passage through the cycle. CDKs are

activated by the binding of cyclins whose type and level of expression fluctuates throughout the cycle. During G_1 cyclin D associates with CDK4 and CDK6, which is important for passage through the G_1/S restriction point. During S phase cyclins E or A associate with CDK2 to create the S phase promoting factor, and cyclin B or A associates with CDK1 to promote mitosis. While the embryonic heart contains large amounts of cyclins and CDKs, they are down-regulated in quiescent adult cardiomyocytes, which correlates with cell cycle withdrawal (8).

CDK inhibitors (CDKIs) negatively regulate CDKs by competing with cyclins for binding, thereby blocking cell cycle progression. They exist in two groups: Cip/Kip (p21, p27, and p57) which broadly inhibit all CDKs and the Ink4 family (p15, p16, p18, and p19) which selectively inhibit CDK4/6. In contrast to cyclins, Cip members are highly expressed in adult cardiomyocytes which have permanently withdrawn from the cell cycle (8).

Together cyclins and CDKIs respond to cellular signals to activate or inactivate the appropriate CDK complexes throughout the cell cycle, and this appears to be crucial to cardiac development. Deletion of CDK2 and CDK4 is embryonic lethal due to cardiac defects, and hyperplasia is observed in mice which over express cyclin D and CDK2 (8). These defects have been attributed to the deregulation of the pocket protein Rb, and consequently its effect on the E2F pathway. In fact, the pocket protein and E2F families are amongst the most widely studied targets of CDK complexes. This is because the E2F/Pocket protein families play a pivotal role in cell cycle control by regulating the expression and repression of genes involved in cellular proliferation, differentiation, and death.

The E2F Family

The E2F family is a group of transcription factors which regulate the expression of genes which are involved in a wide variety of cellular processes including but not limited to cellular proliferation, checkpoint control, differentiation, and apoptosis. The family consists of nine members (including two forms of E2F3) which are expressed in both tissue and temporal specific manners allowing for the complex regulation of mammalian tissues. In the past, E2Fs were generally categorized as transcriptional activators (E2F1-3a) or repressors (E2F3b-E2F8) based on their capacity to activate gene expression and drive cell proliferation in conditions of over-expression. It is now more widely recognized that these categories are over-simplistic and in reality the outcome of gene expression will be dictated by numerous factors including tissue type, temporal expression, and the availability of other transcription factors.

E2F structure

All E2F family members share a conserved winged helix motif for DNA binding **(Figure 1)**. E2F1-6 also share a differentiation protein (DP) dimerization domain consisting of a leucine zipper and a marked box motif. These family members require heterodimerization with DP proteins to form functional DNA binding complexes. Instead of binding to DP proteins, E2F7 and E2F8 have two DNA binding complexes which allow them to form homo and heterodimers with one another (9,10).

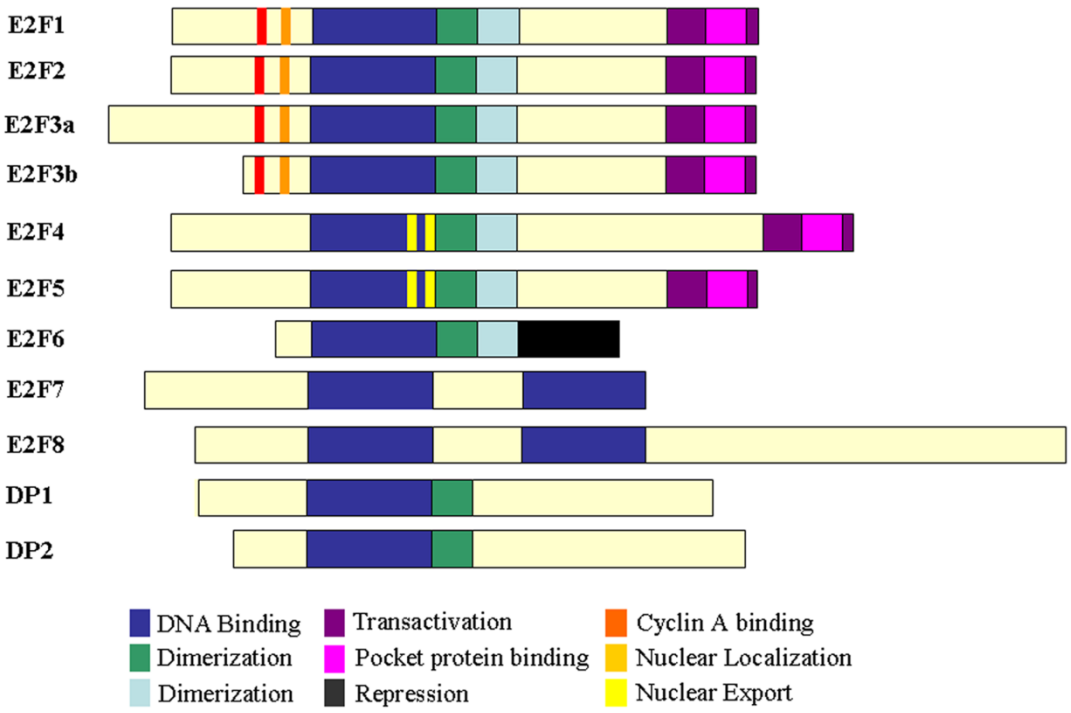

Figure 1: ***E2F/DP family Structure.*** Schematic of the E2F and DP family members. All members share a DNA-binding domain and E2F1–6 dimerize with DPs through their dimerization domain in order to form functional DNA-binding heterodimers. E2F7 and E2F8 do not bind to DPs and instead have two DNA-binding domains. E2F1–5 share a C-terminal domain that is responsible for transcriptional transactivation which also contains a pocket-protein-binding domain. E2F1–3 share a cyclin-A-binding motif as well as a nuclear localization signal in their amino-terminal while E2F4 and E2F5 share nuclear export signals embedded in the DNA-binding domain. The C-terminus of E2F6 contains a domain important for the recruitment of polycomb proteins for gene repression (11).

At their C-terminus E2F1-5 have a transactivation domain in common which allows them to recruit the basal transcriptional machinery to activate gene expression **(Figure 1 and 2)**. Additionally, E2Fs may recruit histone acetyltransferases to relax

chromatin architecture, thereby facilitating gene expression (12). This is particularly important at G_1/S phase of the cell cycle to drive growth and proliferation **(Figure 2)**. Within the transactivation domain is a pocket protein binding motif, which when occupied by the pocket proteins (Rb, p130, and p107) inhibits transcriptional activity. The pocket proteins are able to recruit chromatin remodeling proteins such as histone deacetylases (13) and methyltransferases (14) to silence gene expression. Repression of E2F is crucial during G_0 and early G_1 phases of the cell cycle in order to block proliferation (tumor suppressor) and also to achieve differentiation **(Figure 2)**. In order to drive proliferation pocket proteins must dissociate from E2Fs, which is achieved by the cyclin dependent kinases, which phosphorylate pocket proteins when appropriate growth cues are received.

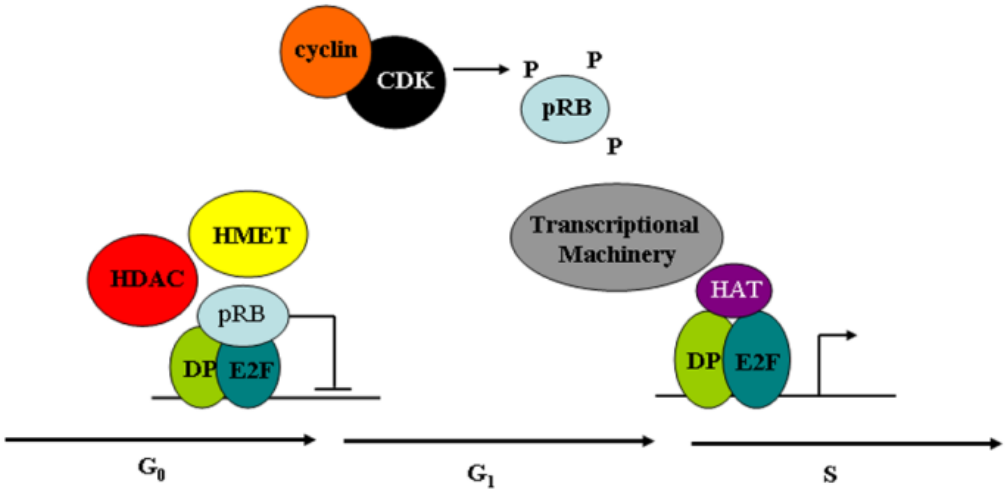

Figure 2: ***The E2F/RB pathway is regulated throughout the cell cycle.*** During G_0 E2F's transactivation domain is masked by pocket protein binding, resulting in E2F responsive gene repression. Pocket proteins can recruit histone deacetylases (HDACs) and histone methyltransferases (HMETs) to actively repress gene activity by chromatin remodeling. As cells transition into G_1/S phase, pocket proteins become phosphorylated by cyclin/CDK complexes freeing E2F/DP complexes. Histone acetyl transferases (HATs) are recruited to open chromatin architecture and the basal transcriptional machinery activates the E2F-responsive genes necessary for cell cycle progression. (11)

E2F6: A non-classical E2F family member

The non-classical E2Fs include E2F 6-8 which do not contain transactivation or pocket protein binding domains **(Figure 1)**, and thus are not regulated by the conserved E2F/Rb pathway. This adds another layer of complexity for E2F mediated gene regulation, and makes them unique targets for modulation of the E2F pathway.

E2F6 was the first non-classical E2F family member to be recognized in the late 1990's. Ectopic E2F6 was capable of repressing luciferase expression constructs containing E2F-binding elements, leading to its recognition as a potent transcriptional repressor (15,16,17,18). In support of its role as a repressor it has been demonstrated by immunoprecipitation to interact with a group of chromatin remodeling enzymes called the polycomb group (PcG) proteins. This group is responsible for the formation and maintenance of heterochromatin during development (19). E2F6 interacts directly with various members including Bmi1 and RYBP (20) and has also been isolated in PcG like complexes (21). It was previously demonstrated that E2F6 only binds to promoters during G_1 (22,23) at which time it is normally up-regulated (18,24). Since then E2F6 has been isolated in repression complexes during G_0 as well (25,26). These complexes also include other transcription factors such as Myc and Mga. Thus it seems highly plausible that interactions with other proteins in different cell types and conditions could also influence the behavior of E2F6.

The effect of E2F6 on the cell cycle is not entirely clear, but several studies have demonstrated that it may delay progression in particular conditions. In growth arrested NIH 3T3 cells, E2F6 expression delayed G_1 exit while unsynchronized NIH 3T3 and SAOS-2 cells were not affected by E2F6 (27). In another study over-expression of E2F6 in unsynchronized U-2 OS led to a delay in S-phase exit (15). In contrast, embryonic fibroblasts from $E2F6^{-/-}$ mice did not display any alteration in the cell cycle even under conditions of growth arrest (28). This can likely be attributed to functional compensation by other E2F family members such as E2F4. This was demonstrated in a chromatin

immunoprecipitation (ChIP) study in which E2F4 replaced E2F6 at gene promoters during G_1 and S phase in its absence (23).

The functional redundancy of E2F family members was highlighted in a ChIP study in which E2F1, 4, and 6 were detected at similar gene promoters in HeLa and GM cells (29). Surprisingly, 60% of the promoters E2F6 was detected at were genes which were actively transcribed, providing evidence that E2F6 does not always behave as a potent transcriptional repressor. Intriguingly, in Ntera2 cells E2F6 was the only E2F family member which was detected at promoters of a unique set of genes (involved in cell adhesion and glycoproteins), suggesting a novel role for gene regulation in these cells (29).

E2F Family Member Functions

Given the size of the E2F/Rb families it is not surprising that there is a large level of redundancy. This allows for complex gene regulation and given the importance of the pathways regulated by E2F is likely intended to safeguard against disease due to mutation. Despite the redundancy, individual knockouts have revealed some specific roles for family members. A list of phenotypes associated with each family member is described in **Table 1**.

Table 1. ***Individual E2F/ Pocket protein family member knockouts.***

Gene	Phenotype	Reference
E2F1	Higher tumor incidence in adults	(30) (31)
E2F2	Increased susceptibility to infections, late-onset auto-immune disease	(32)
E2F3	100% embryonic lethal in 129/sv pure strain. 75% embryonic lethality in C57BL/6 × 129/sv. Cardiac proliferation defects. Congestive heart failure in adults.	(33) (34) (35)
E2F4	Defects in erythrocyte and gut epithelial differentiation. Early death due to increased susceptibility to infection.	(36)
E2F5	Choroid plexus differentiation defect leading to non-lethal hydrocephalus.	(37)
E2F6	Homeotic transformations of the axial skeleton, defects in spermatocyte differentiation.	(28)
E2F7	No defects noted.	(38)
E2F8	No defects noted.	(38)
Rb	$Rb^{-/-}$ embryonic lethal, $Rb^{-/+}$ develop pituitary and thyroid cancer	(39,40)
p130	No defects noted.	(41)
p107	No defects noted.	(42)

The individual knockout studies reveal that only one E2F family member, E2F3, is required for viability. Double and triple knockout **(Table 2)** of E2Fs reveal that the requirement for E2F3 is related to the timing of its expression during development, since E2F1 and E2F2 can compensate for its loss when under the control of the E2F3a promoter (43). In the case of E2F repressors, there is less room for error. Deletion of

more than one member in a subgroup (i.e. E2F4 and E2F5 or E2F7 and E2F8) is lethal **(Table 2)**. Since Rb is also required for embryonic viability $Rb^{-/+}$ were studied. Deletion of more than one pocket protein leads to embryonic lethality or cancer **(Table 2 bottom)**. Thus it seems that appropriate repression of the E2F pathway is critical to development.

Table 2. ***Double and Triple E2F/Pocket Protein Knockout Studies.***

Genes	Phenotype	Reference
E2F1;E2F2; E2F3a	Partial embryonic lethal, perinatal lethal. Reduction in white adipose tissue deposits.	(43)
E2F4;E2F5	Embryonic lethal due to differentiation defects.	(44)
E2F7;E2F8	Embryonic lethal. Excess apoptosis (due to increased E2F1 and p53) and blood vessel dilation.	(38)
$Rb^{-/+}$; p130	Increased tumor incidence.	(45)
$Rb^{-/+}$; p107	Embryonic lethal.	(42)
$Rb^{-/+}$;p107	Embryonic lethal. Increased proliferation in CNS and blood vessel endothelial cells, heart defects.	(46)
p130;p107	Neonatal lethal. Deregulated limb development.	(41)

E2F function in the heart

Regulation of the E2F pathway is also critical to normal cardiac development. Deletion of E2F3 leads to partial embryonic lethality due to defects in cardiac proliferation (35). Additionally, mice which survive to adulthood eventually develop dilated cardiomyopathy and die of congestive heart failure late in life. Deletion of pRb

and p107 is also embryonic lethal due to cardiac defects (46), and deletion of pRb (cardiac restricted) and p130 causes abnormal cardiac hyperplasia (47). Furthermore, pRb and p130 were demonstrated to be crucial in the maintenance of post-mitotic function in adult cardiomyocytes (48). Thus appropriate repression of the E2F pathway by pocket proteins is critical during both embryonic and postnatal cardiac development and function.

E2Fs and Heart Failure:

When the heart is challenged by physical or chemical insult its initial response is to remodel to increase cardiac function and output. This involves hypertrophy and shifts in metabolism which although initially believed to be beneficial, eventually lead to disruption of contraction and cell death (discussed below). The E2F/Rb pathway regulates cell growth, death, and differentiation thus it is an attractive target for therapeutic intervention.

Cardiac hypertrophy

Post-natal cardiac growth is restricted to hypertrophy which occurs under normal conditions in response to increasing energy demands such as exercise and pregnancy in what is termed physiological hypertrophy. Hypertrophy can also occur as a response to physical and/or chemical challenges which results in a different set of processes resulting in pathological hypertrophy, which will be discussed below (49,50). Hypertrophy can be further sub-classified by the geometry in which the cardiomyocyte increases its size. In concentric hypertrophy, sarcomeres are added in parallel which leads to a thickening of the myocardial wall and less ventricular space. This occurs in response to pressure

overload such as that caused by hypertension. In eccentric hypertrophy sarcomeres are added in series which results in left ventricle dilation (51,50). This occurs in response to volume overload such as after myocardial infarction and is believed to be a greater risk to the heart.

During hypertrophy the myocardium undergoes major transcriptional changes in which it reverts to a more fetal like gene program to induce cell growth. Some of the major players include the induction of natriuretic peptides ANP and BNP as well as a switch from the α-myosin heavy chain to β-myosin heavy chain (51). It is also associated with an increase in overall protein synthesis and the induction of proto-oncogenes. Pathological cardiac hypertrophy involves a variety of receptors which upon stimulation activate signal transduction pathways (51,50,52) which are briefly summarized below.

One of the main pathways activating cardiac hypertrophy is the increase of intracellular Ca^{2+}which activates the calcineurin/ nuclear factor of activated T-cells (NFAT) pathway. Calcineurin is a serine/threonine phosphatase which causes the de-phosphorylation of NFAT and its subsequent translocation to the nucleus where it can activate hypertrophic gene expression. Increased Ca^{2+} also activates the Ca^{2+}/calmodulin-dependent kinase II (CaMKII) which can induce the transcription factor MEF-2 and the expression of genes involved in hypertrophy.

Hypertrophy can also be stimulated via catecholamines which bind to adrenergic receptors (α and β). Adrenergic receptors belong to the G-protein coupled receptor family which activate the heterotrimeric G-proteins (G_{α}, and $G_{\beta\gamma}$). Upon stimulation, α-adrenergic receptors bind to $G_{\alpha q}$ and activate phospholipase C which produces

diacylglycerol (DAG). DAG activates the mitogen activated protein kinases (MAPK) and protein kinase C which results in hypertrophy and vasoconstriction. The β-adrenergic receptors bind to $G_{\alpha s}$ which activates adenylate cyclase which produces cyclic-AMP (cAMP). This activates the protein kinase A and MAPKs which phosphorylate various proteins resulting in hypertrophy, vasodilation, and increased contraction. Catecholamines also activate the calcineurin/NFAT pathways and CaMKII pathways described above.

Another major activator of cardiac hypertrophy is the release of cytokines, such as the interleukin 6 family (IL-6) and cardiotrophin (CT-1). Cytokines binds to glycoprotein 130 and activate multiple signal transduction pathways including the JAK/STAT, MAPK, and PI(3)K/AKT which activate transcription factors which regulate the expression of genes involved in cell growth.

In addition to the activation of transcription factors (such as MEF-2D, GATA4, and NFAT), transcriptional reprogramming in hypertrophy is aided by changes in chromatin architecture achieved by the competing activities of histone acetyltransferases (HATs) and histone deacetylases (HDACs). Increased HAT activity is associated with the increased transcription of genes involved in cell growth which can induce hypertrophy and occurs after MI. In contrast, class II HDACs are exported from the nucleus during hypertrophy thereby eliminating their inhibitory effect on transcription of pro-hypertrophic genes. Class I HDACs also inhibit gene transcription, but their targets include anti-hypertrophic genes, thus they have a pro-hypertrophic effect.

Given that the E2F/Rb family regulates the transcription of genes involved in cell growth, and their interaction with HATs and HDACs, it is not surprising that they have been implicated in cardiac hypertrophy. In neonatal cardiomyocytes isolated from rats, expression of the classical E2Fs induced hypertrophy and the fetal gene program (53), which was partially recapitulated *in vivo* via adenoviral delivery of E2Fs (54). Furthermore, blocking the E2F pathway via pharmacological inhibition of E2F/DP dimerization blocked neonatal cardiomyocyte growth and induction of the fetal gene program (55). This appears to be clinically relevant as E2F1 and Rb were up-regulated in human congestive heart failure patients, which was reversed after left ventricle assistance device implantation (56) indicating a reversible relationship between E2F and human cardiac hypertrophy.

Cardiac metabolism

It has become increasingly apparent that there is a cross-talk between the cell cycle and metabolism (57,58). In hypertrophy and heart failure changes in metabolism are also observed (59) which may in part reflect the alterations in gene expression observed when the heart reverts from its differentiated state to a more "fetal like" growth state as described above. Such changes can have a drastic effect on the heart, which beats ~100000 times per day, requiring an enormous amount of energy, while holding only a small ATP reserve. In fact, the heart accounts for ~10% of the body's total energy expenditure although it only makes up ~0.5% of the actual body weight (60). In the fetus, and immediately following birth, the majority of the heart's energy supply is glucose, with less than 20% of the heart's ATP production coming from fatty acid

oxidation (61). As cardiomyocytes differentiate lipid oxidation increases to account for ~70% of the hearts energy utilization, which can increase further during exercise.

In general, during heart failure there is a decrease in lipid oxidation (62,61). Many studies indicate that glycolysis is increased (as are many fetal genes/states), while others have found that it remains unchanged. It is still up for debate whether these changes are a beneficial or maladaptive, but in advanced heart failure there appears to be a lack of energy in the heart which increases pathogenesis (63). Another major metabolic change in heart failure is insulin resistance which is a major problem when the heart has switched to rely more heavily on glucose (61). Ketone metabolism is increased during glucose scarcity, such as the afore mentioned insulin resistance, as well as in response to fasting and exercise (64). It has also been more recently recognized that ketone metabolism is activated in humans in end stage heart failure and in mice during compensatory hypertrophy (65,66).

Ketones are synthesized in the liver as a byproduct of lipid metabolism, and exist in three main forms: β-hydroxybutyrate (β-OHB) (the most stable and abundant), acetoacetate, and to a much lesser extent acetone. When glucose is scarce, they are exported to the bloodstream where they can be taken up by tissues such as the brain and heart. In order to be oxidized by the tri-carboxylic acid cycle, ketones must be in the form of acetoacetate, thus the β-hydroxybutyrate dehydrogenase (BDH1) is important for the interconversion of β-OHB to acetoacetate. In addition to increased ketolysis, BDH1 was also recently recognized to be up-regulated in HF (66). The level of ketones and their oxidation can impact the heart's ability to uptake and oxidize other nutrients (fatty acids,

glucose, and lactate) thus a better understanding of their part in cardiac metabolism is important.

As mentioned above, there is a cross-talk between metabolism and the cell cycle, thus it comes as no shock that the E2F/Rb pathway has been implicated in both. In particular, the focus has been put on Rb which, in association with E2F1, inhibits oxidative phosphorylation and mitochondrial activity (57). E2F1 can also drive glycolysis via promotion of the pyruvate dehydrogenase kinase 4 and cyclin D. This is especially important in cancer in which deregulation of the E2F pathway can promote proliferation and alter metabolism to shift towards glycolysis promoting tumor growth (57). The role of the E2F pathway in cardiac metabolism remains to be explored.

Apoptosis

Cardiac apoptosis is a major contributing factor to heart failure in particular following myocardial infarction and dilated cardiomyopathy. Since cardiomyocytes have little to no capacity to regenerate, lost cells are replaced with collagen leading to myocardial stiffening and a further reduction in cardiac output.

Apoptosis is a program designed to kill the cell without the release of debris which would cause inflammation (necrosis) (67). In this signaling cascade pro-caspases are cleaved thereby initiating a protein proteolytic cascade, DNA fragmentation, cell shrinking, and membrane blebbing. Apoptosis can be initiated via extrinsic pathways involving death receptors (TNF) and caspase-8, or via intrinsic mechanisms which involve changes in the mitochondria which activate the apoptoptosome and caspase-9. Ultimately both pathways lead to the activation of the “executioner” caspase: capsase-3.

Intrinsic apoptosis can be initiated by negative factors including the withdrawal of growth factors and hormones which normally suppress apoptosis, as well as by positive factors such as hypoxia, radiation, toxins, and free radicals. These stimuli cause changes in the permeability of the outer membrane of the mitochondria triggering the release of pro-apoptotic proteins such as cytochrome c and apoptosis inducing factor (AIF) (67). Cytochrome c binds to the apoptotic protease activating factor (APAF1) and pro-caspase 9 forming the apoptoptosome, while AIF is released at a later stage of apoptosis and causes nuclear fragmentation.

The regulation of apoptotic events is largely regulated by the Bcl-2 family of proteins which consist of both pro (ex. Bax, Bid, Bad) and anti-apoptotic (Bcl-2, Bcl-x) members which regulate the release of cytochrome c. The Bcl-2 families of proteins in turn are principally regulated by the tumor suppressor protein p53, which is deregulated in most cancers.

The E2F pathway is widely recognized to regulate apoptosis (68). Rb is also a tumor repressor which was initially discovered for its mutation in retinoblastoma, and is deregulated in many cancers resulting in aberrant E2F activation and proliferation. In addition to driving proliferation, E2F1 also has the capacity to initiate apoptosis via multiple mechanisms including both p53 dependent and independent actions. E2F1 induces the expression of the cyclin-dependent kinase inhibitor $p14^{ARF}$, which inhibits MDM2 and thereby stabilizes p53 (69,70,71). It also has the capacity to interact directly with p53 through its cyclin-A binding domain (72), thus the availability of cyclin-A is important for regulating E2F1's decision between life and death. E2F1 can also directly

activate the expression of a variety of pro-apoptotic genes including caspases, bnip3, and the p53 homologue: p73 (73,30).

E2F6 has been demonstrated to have anti-apoptotic properties in HEK-293 cells which were treated with UV light (74) or exposed to the hypoxia mimetic agent cobalt chloride ($CoCl_2$) (75). This anti-apoptotic effect was believed to be achieved through interference of the pro-apoptotic E2F1. E2F6 was also linked to prostate cancer and resistance to apoptosis induced by chemotherapeutic agents (76,77,78). In these cases the level of E2F6 is regulated by changes in expression of the microRNAs which targets it: miR-31 and miR-185. When miR-31 is suppressed (by chromatin remodeling) cells are resilient to death due to excess E2F6 (76) while treatment with an HDAC inhibitor induced the activation of miR31 and the resultant loss of E2F6 and apoptosis (77).

Both E2F1 and E2F3 were demonstrated to activate apoptosis in neonatal cardiomyocytes (53), as well as in the adult heart via viral administration (79). In contrast, the role of E2F6 in cardiac apoptosis has yet to be evaluated.

E2F6 and Dilated Cardiomyopathy

Given the importance of the E2F pathway in the heart, and the complexity of the E2F/Rb families we took a novel approach to assess the pathway via over-expression of E2F6 to serve as a dominant negative regulator of the classical E2F pathway. Cardiac specific expression was achieved using the cardiac α-myosin heavy chain promoter which is pre-dominantly expressed in the postnatal period of cardiac development. During my MSc I assessed these mice which developed dose dependent dilated cardiomyopathy associated with the early loss of connexin-43- a regulator of cardiac communication and

contraction, and E2F3, the major regulator of cardiac development (80). Surprisingly, E2F6 expression resulted in the robust induction of gene expression, including E2F responsive pathways, which was presumably due to competition and deregulation of other E2F family members which would normally recruit Rb to repress gene expression. Perhaps even more surprising, was the fact that E2F6-Tg mice displayed no evidence of pathological hypertrophy or apoptosis which are usually enhanced by E2F activity and activated in DCM and HF.

Dilated cardiomyopathy:

Dilated cardiomyopathy (DCM) is the second most common cardiomyopathy in Canada and worldwide. It affects both sexes and is the most prevalent cardiomyopathy in children (81). Approximately 40% of DCM cases are hereditary, many of which are caused by mutations in genes which code for proteins which regulate force generation and transmission such as those expressed in the sarcomere (i.e. troponins I and T, titin, titin-cap, tropomyosin, and myosin heavy chain). Mutations in genes which regulate nuclear structure such as lamin A and emerin also cause DCM. A more exhaustive list can be found in the review published by McNally and colleagues in the *Journal of Clinical Investigation* (82). In addition to mutations, DCM is induced by a variety of factors including myocardial infarction, alcohol and toxins (such as anthracyclines), thyroid disease, chronic hypertension, and viral infections, but in about one third of cases the cause is unknown.

Dilated cardiomyopathy is characterized by the dilation of the left ventricle and thinning of the myocardial wall. This causes disorganization of the sarcomere (the

contractile unit of the heart) and leads to reduced systolic function which in humans is described as a left ventricle ejection fraction of less than 50% and fractional shortening less than 25% (83). DCM can also be accompanied by or cause arrhythmias and blood clots. Since DCM has so many etiologies, histological results vary from patient to patient, but usually cardiomyocyte loss is observed, nuclei are often enlarged and irregularly shaped, and myofibril content is diminished (84). Dilated cardiomyopathy can be a primary disease (most often in the case of genetic mutation) or can follow other cardiovascular diseases and hypertrophy. One of the major problems in treating DCM is that it can be asymptomatic for decades, and at the point in which symptoms arise, a substantial amount of damage has already occurred.

Statement of the problem:

There are no treatments for DCM but current management strategies to improve cardiac function in patients with the disease include β-adrenergic receptor blockers, angiotensin converting enzyme inhibitors, and diuretics. Patients with arrhythmias can also have pace-makers and cardiac defibrillators implanted. The lack of treatment options and mechanistic information about idiopathic DCM warrants interrogation. During my MSc studies I contributed to the development of a mouse model of DCM by targeting the E2F pathway in the postnatal myocardium via the purported repressor E2F6 (80). Contrary to what was expected, these mice presented with an enhanced E2F response and DCM but without changes in cardiac growth or apoptosis. **Thus, I hypothesize that expression of E2F6 in post-natal myocardium would impact growth, death, and differentiation leading to DCM.** Furthermore, I hypothesize that through the exploration

of the E2F6-Tg model I will define how the E2F pathway regulates cardiomyocyte growth, differentiation, and death with the hope of finding novel mechanisms, biomarkers, and potential therapeutic targets for idiopathic DCM.

Objective/ Hypothesis 1:
E2F6 can repress pathological hypertrophy in myocardium.

In order to address if E2F6 could repress hypertrophy in myocardium I evaluated cardiac growth during early post-natal cardiac development to determine if hypertrophy preceded DCM. The capacity of E2F6 to block pathological hypertrophy was assessed via administration of isoproterenol with osmotic mini pumps in Tg mice. These experiments are described in the manuscript entitled "Interplay between the E2F pathway and β-adrenergic signaling in the pathological hypertrophic response of myocardium" which was published in the *Journal of Molecular and Cellular Cardiology* in July 2015 (Chapter 1).

Objective /Hypothesis 2:
E2F6 can repress apoptosis in cardiomyocytes

To determine if E2F6 can attenuate apoptosis in the heart, neonatal cardiomyocytes were isolated from Wt and Tg mice and treated with the anthracycline doxorubicin or the hypoxia agent $CoCl_2$ to induce DNA damage and death. This study is described in the manuscript entitled "E2F6 Protein Levels Modulate the Apoptotic Response in Cardiomyocytes" which is under consideration for publication in *Cardiovascular Research* (Chapter 2).

Objective/ Hypothesis 3:

E2F6 can inhibit the cardiac differentiation program via changes in the cell cycle.

To determine the impact of E2F6 on differentiation I assessed the expression of proteins involved in the cell cycle and metabolism and their impact on the expression of proteins which regulate cardiac contraction. This study is described in the manuscript entitled "E2F6 Impairs Glycolysis and Activates BDH1 Prior to Dilated Cardiomyopathy" which was published in *PLoS One* in January 2017 (Chapter 3) and is also discussed in Chapter 2.

CHAPTER 1

“Interplay between the E2F pathway and β-adrenergic signaling in the pathological hypertrophic response of myocardium”

Major JL, Salih M, and Tuana B.S. (2015) Journal of Molecular and Cellular Cardiology, 84: 179-190.

Author contributions: JL Major performed experiments, analyzed data, and prepared the manuscript under the supervision of BS Tuana. Technical support and advice was provided by Maysoon Salih.

Abstract

The E2F/Pocket protein (Rb) pathway regulates cell growth, differentiation, and death by modulating gene expression. We previously examined this pathway in the myocardium via manipulation of the unique E2F repressor, E2F6, which is believed to repress gene activity independently of Rb. Mice with targeted expression of E2F6 in postnatal myocardium developed dilated cardiomyopathy (DCM) without hypertrophic growth. We assessed the mechanisms of the apparent failure of compensatory hypertrophic growth as well as their response to the β-adrenergic agonist isoproterenol. As early as 2 weeks, E2F6 transgenic (Tg) mice present with dilated thinner left ventricles and significantly reduced ejection fraction and fractional shortening which persists at 6 weeks of age, but with no apparent increase in left ventricle weight: body weight (LVW:BW). E2F6-Tg mice treated with isoproterenol (6.1 mg/kg/day) show double the increase in LVW:BW than their Wt counterparts (32% vs 16%, p-value: 0.007). Western blot analysis revealed the activation of the adrenergic pathway in Tg heart tissue under basal conditions with ~ 2-fold increase in the level of β_2-adrenergic receptors (p-value: 8.9E − 05), protein kinase A catalytic subunit (PKA-C) (p-value: 0.0176), activated c-Src tyrosine-protein kinase (p-value: 0.0002), extracellular receptor kinase 2 (ERK2) (p-value: 0.0005), and induction of the anti-apoptotic protein Bcl2 (p-value 0. 0.00001). In contrast, a ~ 60% decrease in the cardiac growth regulator: AKT1 (p-value 0.0001) and a ~ four fold increase in cyclic AMP dependent phosphodiesterase 4D (PDE4D), the negative regulator of PKA activity, were evident in the myocardium of E2F6-Tg mice. The expression of E2F3 was down-regulated by E2F6, but was restored by isoproterenol. Further, Rb expression was down-regulated in Tg mice in response to

isoproterenol implying a net activation of the E2F pathway. Thus the unique regulation of E2F activity by E2F6 renders the myocardium hypersensitive to adrenergic stimulus resulting in robust hypertrophic growth.

These data reveal a novel interplay between the E2F pathway, β_2–adrenergic/PKA/PDE4D, and ERK/c-Src axis in fine tuning the pathological hypertrophic growth response. E2F6 deregulates E2F3 such that pro-hypertrophic growth and survival are enhanced via β_2-adrenergic signaling however this response is outweighed by the induction of anti-hypertrophic signals so that left ventricle dilation proceeds without any increase in muscle mass.

Abbreviations

- β-AR, beta adrenergic receptor;
- DCM, dilated cardiomyopathy;
- ERK, extracellular receptor kinase;
- PDE4D, 5′3′ cyclic AMP phosphodiesterase 4D;
- PKA-C, protein kinase A catalytic subunit;
- Pln, phospholamaban;
- Rb, retinoblastoma gene product (pocket protein);
- Ser, serine;
- c-Src, protein tyrosine kinase

Keywords

- Hypertrophy;
- β-Adrenergic receptors;
- E2Fs;
- Protein kinase;

- Phosphodiesterase

Introduction

Cardiac stress induces remodeling in an attempt to increase left ventricle mass to improve pump function, which is associated with an increase in cardiomyocyte size, protein synthesis, and changes in gene expression (85) (51). In pathological hypertrophy, reactivation of the fetal gene program occurs to promote cardiac growth in the post-natal heart. While this is believed to initially be an adaptive response to improve cardiac output it causes aberrant protein build up and sarcomere disorganization resulting in inadequate pump function (52). Cardiac hypertrophy can be induced by multiple factors including chronic adrenergic stimulation, growth factors and hormones, as well as, by mechanical stress induced by pressure or volume overload (86).

The E2F/Pocket protein pathway controls cellular growth, differentiation and death in all cells including those of the myocardium (68). *In vivo* loss of function studies have elegantly defined a critical role of the E2F/Pocket protein family members in physiological cardiac growth and development (47), (35)and (46). The classical pathway involves E2F1-5 which transactivate gene expression with their dimerization partners, DP proteins (DP1-3), and are negatively regulated by the pocket proteins Rb, p130, and p107 (68).

Over-expression of the classical E2F family members has been demonstrated to induce hypertrophy and apoptosis in neonatal cardiomyocytes, while inhibition of E2F activity with pharmacological block of heterodimerization with DP is sufficient to inhibit neonatal cardiomyocyte hypertrophy (55), (53) and (54). Further, activation of the classic

E2F/Rb family members has been noted in neonatal cardiomyocytes and mice stimulated with hypertrophic agonists, as well as in human heart failure patients exhibiting hypertrophy (55), (56) and (87). Thus, aberrant E2F expression can alter normal cardiac growth patterns and furthermore, pathological stimuli can impact the E2F pathway. E2F6-8 are unique family members which do not share the transactivation or pocket protein binding domain and thus are able to regulate gene expression independently. E2F6 is as a potent repressor of E2F responsive genes and can induce cell cycle arrest through repression during G_1/S phase of the cell cycle (15), (23), (24), (27) and (17). In order to gauge the role of E2Fs in postnatal cardiac growth and function we previously created a dominant negative transgenic (Tg) mouse model with the cardiac specific expression of E2F6 (80). Expression of E2F6 resulted in dose dependent dilated cardiomyopathy (DCM) and heart failure with sudden death (80). This was associated with the loss of gap junction protein: connexin 43 which has been previously linked to DCM and heart failure (80) (88) and (89). E2F3 was specifically down-regulated in E2F6-Tg myocardium, and studies have shown that E2F3 is a critical regulator of growth and development and its loss leads to DCM (35) and (80).

In addition, E2F6 induced genes involved in the G_1/S transition, increased BrdU incorporation, reactivated the fetal gene program, and activated the extracellular receptor kinase pathway (ERK) in adult myocardium (80). Despite all these indications of cardiac hypertrophy, there was no increase in muscle mass noted in the adult E2F6-Tg myocardium. We hypothesized that deregulation of the E2F pathway rendered Tg mice incapable of orchestrating an increase in muscle mass and instead went straight to cardiac dilation leading to heart failure. In order to test this hypothesis we examined the

compensatory hypertrophic response with a focus on muscle build up in younger E2F6-Tg mice and their response to the known hypertrophic agonist isoproterenol. While no hypertrophy was apparent as early as two weeks, E2F6 expression rendered the myocardium twice as sensitive to isoproterenol and resulted in marked activation of the β-adrenergic signaling pathway on the one hand while increasing PDE4D activity and a decrease in the growth regulator AKT1 on the other. Interestingly, isoproterenol was able to restore the levels of E2F3 which correlated with muscle build up in Tg mice.

Materials and methods

Mice and genotyping

B6C3F1 mice expressing the E2F6 transgene under control of the αMHC promoter and genotyping were previously described (80). The protocol was approved by the University of Ottawa Institutional Care Committee. All surgery was performed under isoflurane anesthesia, and all efforts were made to minimize animal suffering.

Isoproterenol delivery

Isoproterenol delivery was based on two published studies (90) and (91) with the following modifications. Six week old Wt and Tg mice were anesthetized with 2% isoflurane. Mini-osmotic pumps (2001D, Alzet) containing either 0.9% saline or isoproterenol-HCl (Sigma Aldrich) dissolved in 0.9% saline were implanted subcutaneously for eight days. Isoproterenol was delivered at the “low” rate of 6.1 mg/kg/d or the “high” rate of 12.2 mg/kg/d. Mice were subsequently analyzed by echocardiography and/or sacrificed for histological or biochemical analysis.

Echocardiography

Echocardiography was performed on a Vevo 2100 high-resolution imaging system (Visual Sonics, Toronto, ON, Canada) with a 40-MHz probe under 2% isoflurane anesthesia. Cross-sectional M-mode recordings at the midventricular level were taken and used to analyze left ventricle internal dimension, volume, wall thickness, mass, fractional shortening, and ejection fraction with Vevo2100 1.4.1 software.

RNA isolation and reverse transcription-quantitative PCR

Total RNA extraction, first-strand cDNA synthesis, and qRT-PCR were performed as previously described (80). Briefly, RNA was extracted from cardiac lysate using the RNEasy Fibrous Tissue Mini Kit as per the manufacturer's protocol (Qiagen). First-strand cDNA was synthesized from 2 μg RNA and oligoDT with SuperScriptII reverse transcriptase (Invitrogen) as per the manufacturer's protocol. qPCR was performed in the q-Rotor (Qiagen) using Fast Start SYBR Green (Roche). Gene expression was normalized against 18S rRNA, and fold inductions were calculated using the $\Delta\Delta C_t$method. Primer pairs used for qPCR are:

18S: 5′-CAGTTTCAGAGAGGTCTATTGCAC-3′ (sense)

and 5′-GCACTCACATGCCCATACTACATA-3′ (anti-sense)

AKT1: 5-ATAACGGACTTCGGGCTGTG-3′ (sense)

and 5-CTCGAACAGCTTCTCGTGGT-3′ (anti-sense)

ANP 5′-AGAGAGAGAAAGAAACCAGAGTGG-3′ (sense)

and 5′-GTCTAGCAGGTTCTTGAAATCCAT-3′ (anti-sense)

BNP 5′-GCTGGAGCTGATAAGAGAAAAGTC-3′ (sense)

and 5′-CAGGAGGTCTTCCTACAACAATT-3′ (anti-sense)

B_2AR 5′-TGGTGCGAGTTCTGGACTTC-3′ (sense)

and 5′-GATCCACTGCAATCACGCAC-3′ (anti-sense)

PKA-C 5′-AAGAAGGGCAGCGAGCAG-3′ (sense)

and 5′-CGGTGCCAAGGGTCTTGAT-3′ (anti-sense)

Western blot analysis

Following treatment with isoproterenol or saline cardiac lysates were prepared using an electric tissue homogenizer in RIPA buffer containing protease and phosphatase inhibitors (Roche). Protein concentrations were estimated with the BCA kit (Thermo Scientific). Protein (10–40 μg) were resolved on 10% SDS-polyacrylamide gels and transferred to polyvinylidene fluoride membranes. The blots were probed with the antibodies (listed below) which were diluted in TBS-T containing 5% non-fat dry milk. The conversion of ECL substrate (Roche) was detected using film (Denville Scientific). Band signals were assessed by densitometry using Image Lab Software 4.0.1 (Bio-Rad).

The following primary antibodies were used: AKT1 (2938, 1:1000), P-AKT1 (ser-473) (9018, 1:1000), ERK1/2 (4695, 1:4000), P-ERK1/2 (Thr 202/Tyr204) (4370, 1:1500), Non-P-Src(tyr 416) (2102, 1:1000), and P-Src (tyr 416) (6943, 1:1000) were purchased from Cell Signaling, β_1-AR (sc-568, 1: 2000), E2F3 (sc-878, 1:1000), and PKA-C (sc-48412, 1:4000) were purchased from Santa Cruz Biotechnology, PLN (MA3-922, 1:20,000) was purchased from Affinity Bioreagents, P-PLN (ser16) (A010-12, 1:10,000)

was purchased from Badrilla, β_2-AR (ab36956, 1:2000) and α-tubulin (ab176560, 1:30,000) were purchased from Abcam, PDE4D (12918-1-AP, 1:2000) was purchased from Proteintech, GAPDH (RGM2, 1:50,000) was purchased from Advanced Immunochemicals, Rb (554,136, 1:500) was purchased from Badrilla, and anti-myc clone 9E10 (in-house, 1:500) was used for the detection of myc-tagged E2F6. Secondary antibodies: anti-mouse (115-035-003, 1:10,000) and anti-rabbit (111-035-045, 1:10,000) were purchased from Jackson Immunochemicals.

Immunohistochemistry

Hearts were extracted from mice under anesthesia with 2% isoflurane, washed in PBS, and fixed in 10% neutral buffered formalin for 24 h. Hearts were embedded in paraffin blocks and 5μm longitudinal sections were cut and stained with hematoxylin and eosin.

Statistics

All data are presented as means ± se. Two-group comparisons were done using Student's *t* test using Graph Pad Prism (GraphPad, San Diego, CA, USA). A p-value of < 0.05 was considered statistically significant.

Results

DCM without compensatory hypertrophy in E2F6 myocardium

We previously determined that postnatal cardiac expression of E2F6 results in dilated cardiomyopathy (DCM) in the absence of any hypertrophy at the ages of three and six months . We examined left ventricle (LV) structure of Wt and Tg mice at earlier ages to determine if there was a hypertrophic response which preceded the presentation of DCM. Echocardiographic examination of Wt and E2F6-Tg mice aged 2, 6, and 12 weeks

indicates that Tg hearts show statistically significant signs of dilated cardiomyopathy as early as 2 weeks which worsen over time **(Figure. 3)**. At 2 weeks Tg mice display a significant increase in left ventricle internal dimension in both systole (LVIDs) (20% increase p-value: 0.005) and diastole (LVIDd) (11% increase, p-value: 0.04) **(Figure 3A and 3B)**. They also show significant reduction in cardiac function as indicated by a lower ejection fraction (EF) (18% decrease, p-value: 0.004) **(Figure 3E)** and fractional shortening (FS) (21% decrease, p-value: 0.008) **(Figure 3F)** and a statistically significantly thinner LV posterior wall thickness in diastole (LVPWd) (9% decrease, p-value: 0.04) **(Figure. 3D)**. No difference in body weight between Wt and Tg mice was observed at any age (data not shown). We determined any changes in LV hypertrophy by calculating the LV weight (determined by echo): body weight ratio (LVW: BW), and no significant increase was noted at any age in Wt versus Tg hearts **(Figure 3G)**.

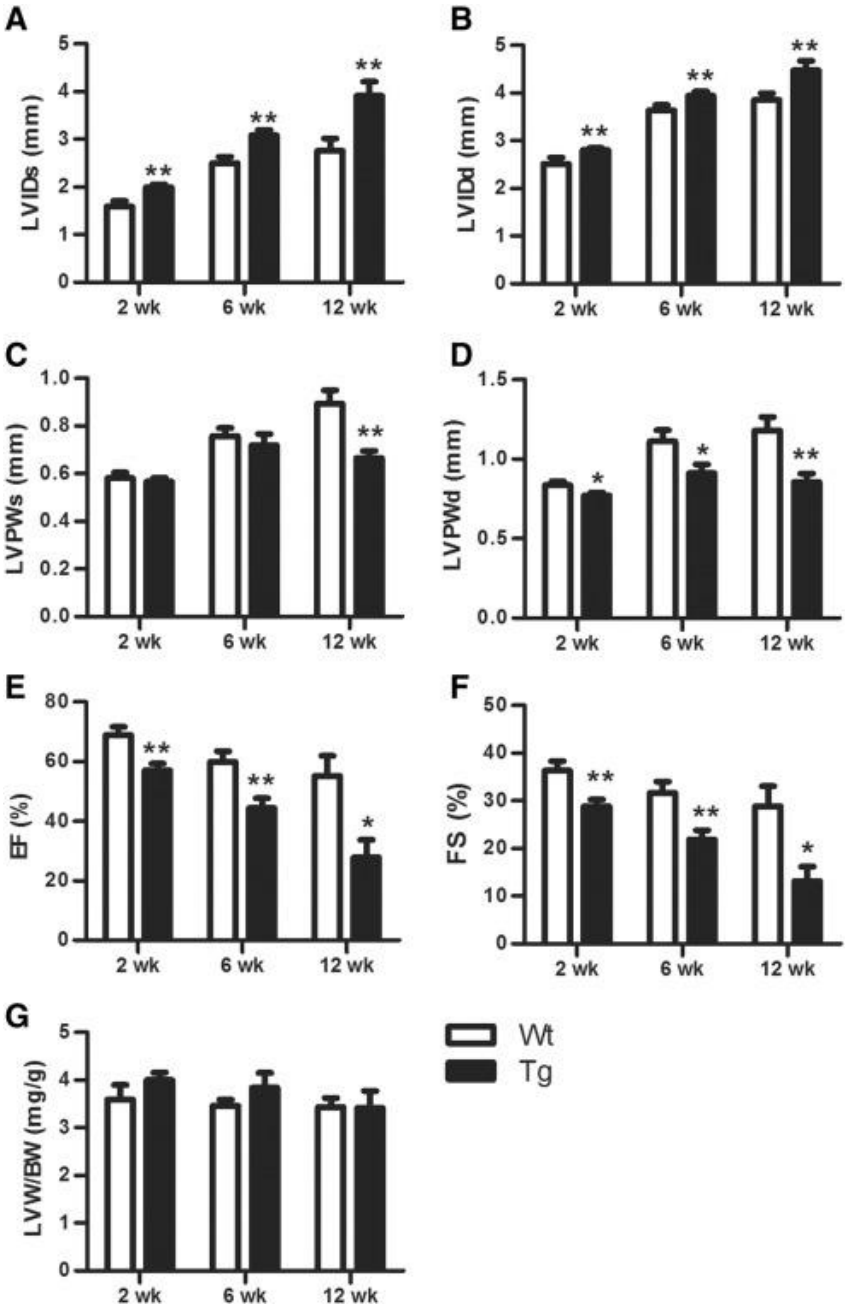

Figure 3. ***E2F6-Tg mice develop early dilated cardiomyopathy without significant compensatory hypertrophic growth***. Echocardiographic examination of Wt (white bar) and Tg (black bar) mice aged 2, 6, and 12 weeks. (A–B) Left ventricle internal diameter in systole (LVIDs) and diastole (LVIDd). (C–D) Left ventricle posterior wall thickness in systole (LVPWs) and diastole (LVPWd). (E) Ejection fraction. (F) Fractional shortening.

(G) Left ventricle weight: body weight. Results are presented as the mean ± sem. *: P < 0.05 *vs* respective Wt, **: P < 0.01 *vs* respective Wt. (2 wk n = 7–9), (6 wk n = 8–10), (12 wk n = 5–6).

Examination of the expression of the fetal genes ANP and β-MHC in 2 week old Wt and Tg myocardium indicated that they remained unchanged **(Appendix 1: Sup Fig 1)**. However, we have previously demonstrated that these genes are markedly reactivated in six week old E2F6-Tg myocardium but in the absence of any hypertrophic growth (80).

E2F6 expression sensitizes the hypertrophic response to isoproterenol

We tested the hypertrophic capacity of 6 week old E2F6-Tg mice by challenging them with the β-adrenergic agonist isoproterenol. E2F6-Tg mice showed a two-fold higher increase in LVW: BW in response to the low dosage of isoproterenol than their Wt counterparts (Wt: 14%, p-value: 0.0144; Tg: 32% increase, p-value 0.0019) **(Figure 4A and 4B)**. Wt mice showed a significant increase in LVPW in response to this dose of isoproterenol (11% increase, p-value: 0.02) **(Figure 4C)** and a slight improvement in cardiac function as assessed by an increase in ejection fraction and fractional shortening **(Figure 4G and 4H)**. In contrast Tg mice did not display an increase in LVPW and instead their hearts became more dilated (LVIDs: 17% increase, p-value: 0.02) **(Figure 4E)** and pumped less efficiently as demonstrated by a lower ejection fraction (37% decrease, p-value: 0.01) **(Figure 4G)** and fractional shortening (39% decrease, p-value: 0.01) **(Figure 4H)**.

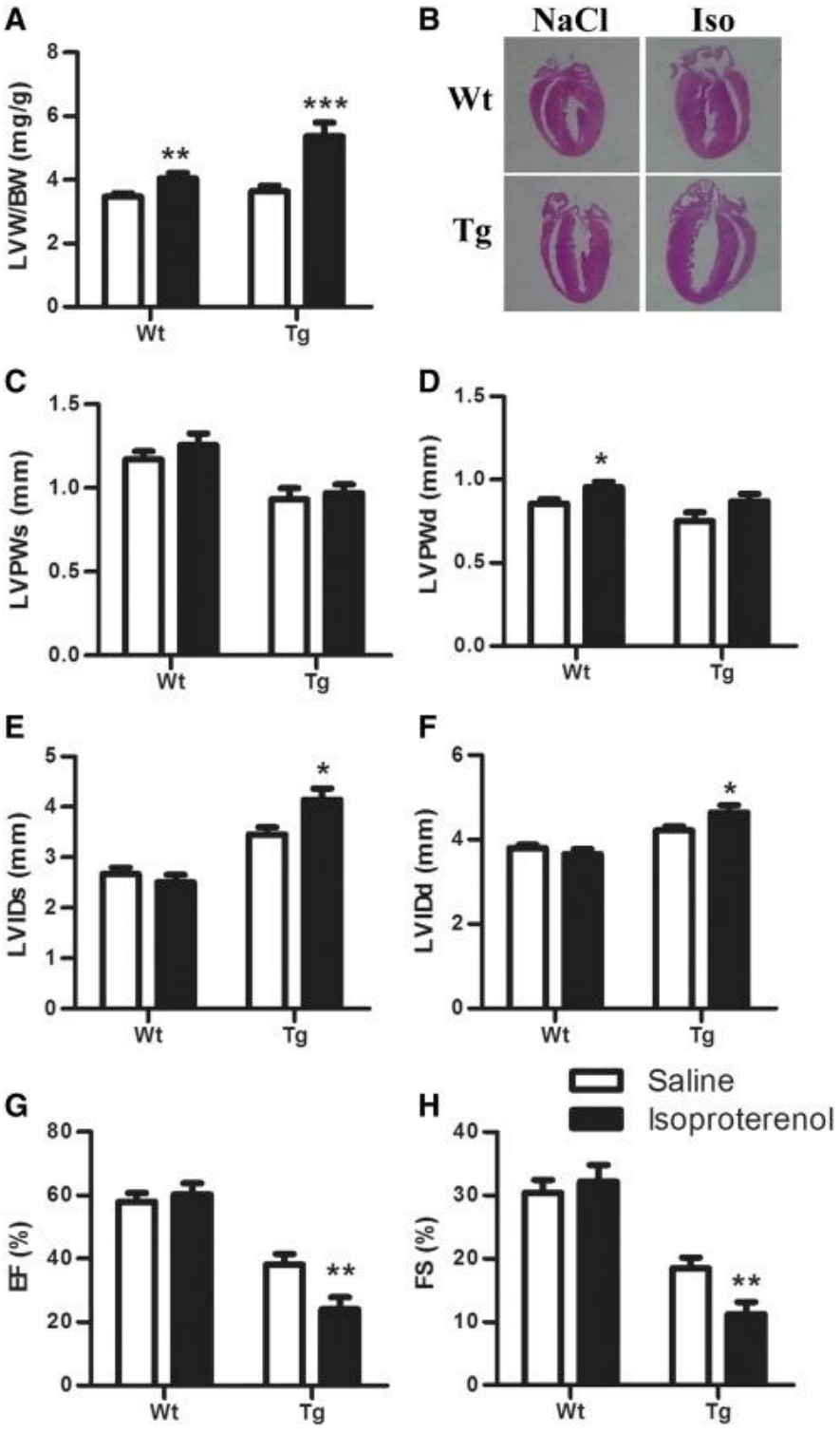
A
LVW/BW (mg/g)
8
6
4
2
0
**
***
Wt
Tg
B
NaCl
Iso
Wt
Tg
C
LVPWs (mm)
1.5
1.0
0.5
0.0
Wt
Tg
D
LVPWd (mm)
1.5
1.0
0.5
0.0
*
Wt
Tg
E
LVIDs (mm)
5
4
3
2
1
0
*
Wt
Tg
F
LVIDd (mm)
6
4
2
0
*
Wt
Tg
G
EF (%)
80
60
40
20
0
**
Wt
Tg
H
Saline
Isoproterenol
FS (%)
40
30
20
10
0
**
Wt
Tg

Figure 4. ***E2F6-Tg mice are twice as sensitive to isoproterenol***. Examination of Wt and Tg mice treated with saline (white bar) or low dose isoproterenol (black bar). (A) Left ventricle weight: body weight. (B) Representative transverse sections of Wt and Tg hearts stained with hematoxylin and eosin following treatment with saline or low dose isoproterenol. (C–H) Echocardiographic examination of Wt and Tg mice treated with saline or isoproterenol. (C–D) Left ventricle posterior wall thickness in systole (LVPWs) and diastole (LVPWd). (E–F) Left ventricle internal diameter in systole (LVIDd) and diastole (LVIDs). (G) Ejection fraction. (H) Fractional shortening. Results are presented as the mean ± sem. (n = 9–11) *: $P < 0.05$ *vs* respective saline, **: $P < 0.01$ *vs* respective saline.

When treated with a higher dose of isoproterenol (12.2 mg/kg/d) both Wt and Tg mice had a 25% mortality rate (2/8). Surviving mice showed a ~ 35% increase in LVW: BW **(Figure 5A)**. Quantitative PCR analysis confirmed our previous results indicating that Tg mice had significantly higher expression of the fetal genes ANP (~ 20 fold, p-value: 0.001) and BNP (~ 5 fold, p-value: 0.026) in saline alone **(Figure 5B and 5C)**. In response to isoproterenol Wt mice show a significant increase in ANP (~ 8 fold increase, p-value 0.05) and BNP (~ 3 fold increase, p-value: 0.03). Echocardiography revealed that only Wt mice show a significant increase in LVPWs (20% increase, p-value: 0.008) in response to "high" isoproterenol **(Figure 5G)**. Both Wt and Tg mice show significant increase in LVIDd **(Figure 5G)** and diminished cardiac function as indicated by a decrease EF and FS in response to high isoproterenol **(Figure 5H and 5I)**.

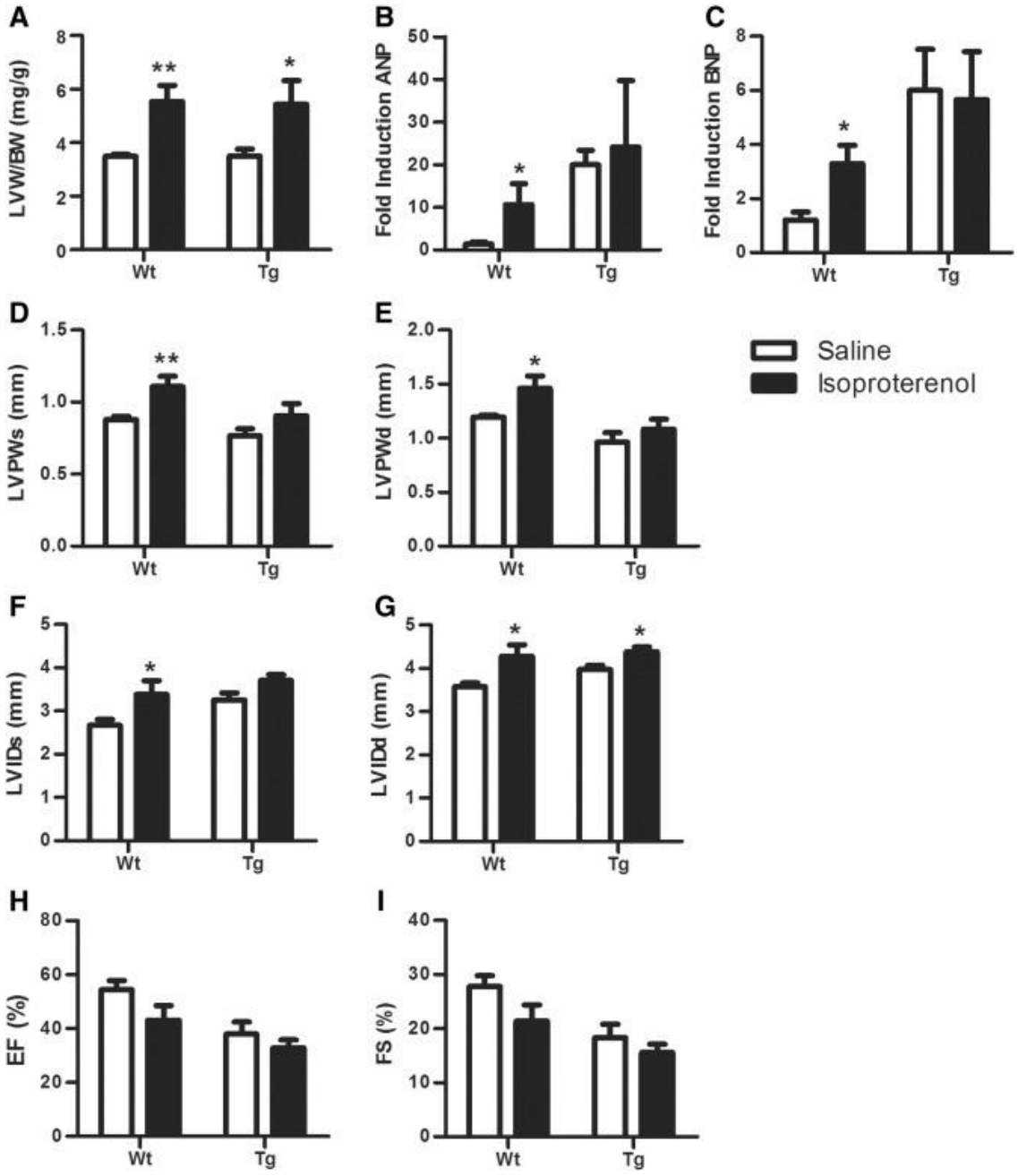

Figure 5. ***High dose isoproterenol induces hypertrophy in Wt and Tg mice***. Examination of Wt and Tg mice treated with saline (white bar) or high dose isoproterenol (black bar). (A) Left ventricle weight: body weight. (B) Fold induction of ANP and (C) BNP transcripts in Wt and Tg mice treated with saline or isoproterenol determined by qPCR in relation to 18SrRNA. (D–E) Left ventricle posterior wall thickness in systole (LVPWs) and diastole

(LVPWd). (F–G) Left ventricle internal diameter in systole (LVIDs) and diastole (LVIDs). (H) Ejection fraction. (I) Fractional shortening. Results are presented as the mean ± sem. (n = 6–7) *: P < 0.05*vs* respective saline, **: P < 0.01 *vs* respective saline.

E2F6 regulates the expression of β-adrenergic receptors

In order to determine why Tg mice were more sensitive to β-adrenergic stimulation we examined the expression of the β-adrenergic receptors. Western blot analysis with anti-β_2-AR revealed polypeptides which migrated with molecular weights of ~ 52, 72, and 150 kDa. The immune-reactivity of the 52 kDa polypeptide was specifically blocked by a peptide designed to squelch the anti-β_2-AR peptide antibodies, thus we analyzed the expression of this protein as the β_2-AR **(Figure 6A)**. Saline treated Tg mice have ~ 2 fold more β_2-AR than their Wt counterparts (p-value: 8.9 × 10E − 05) **(Figure 6A and 6B)**. Both Wt and Tg mice respond to isoproterenol with a significant increase in β_2-AR expression.

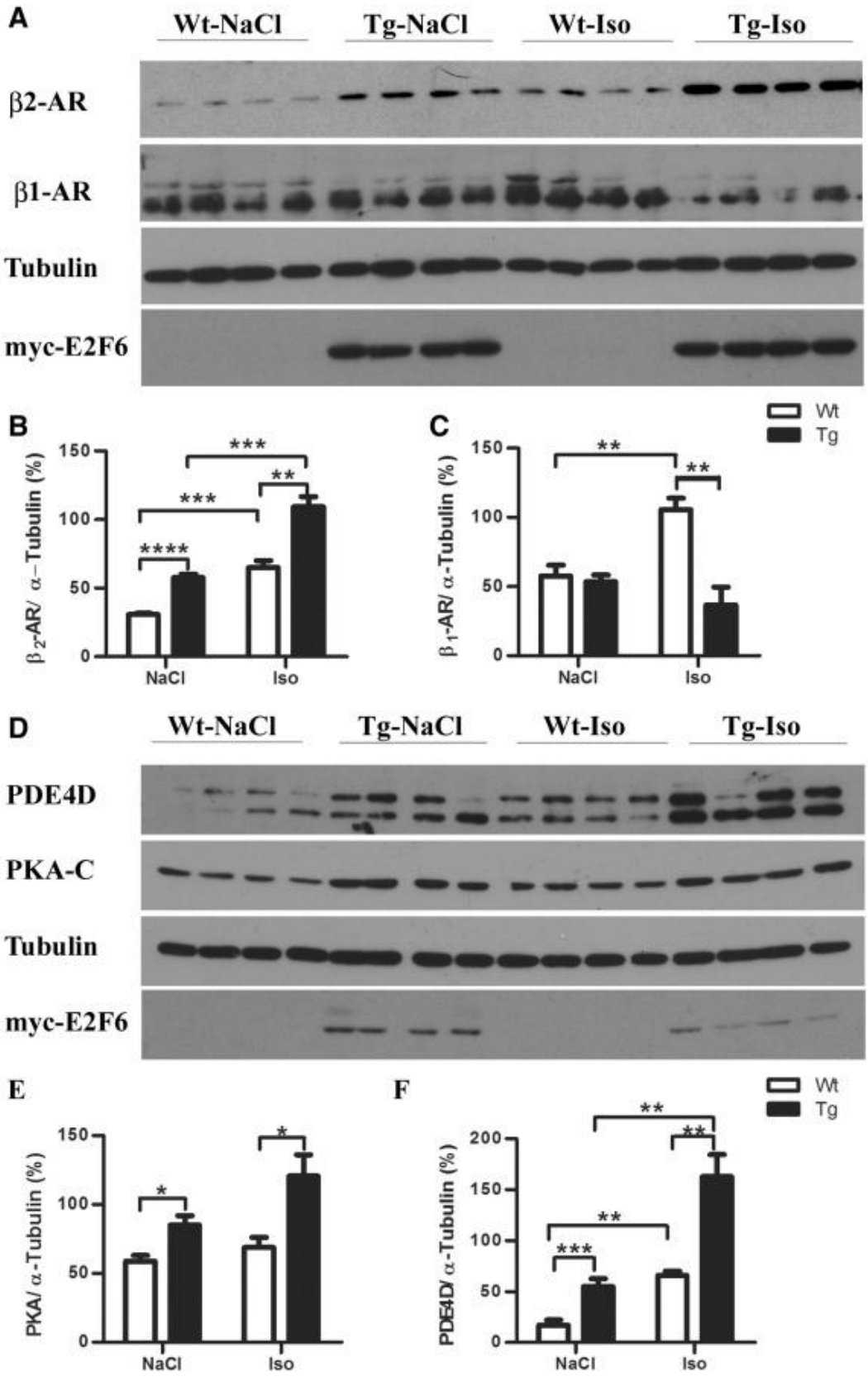
A
Wt-NaCl
Tg-NaCl
Wt-Iso
Tg-Iso
β2-AR
β1-AR
Tubulin
myc-E2F6
B
β2-AR/ α−Tubulin (%)
150
100
50
0
NaCl
Iso
C
Wt
Tg
β1-AR/ α-Tubulin (%)
D
PDE4D
PKA-C
Tubulin
myc-E2F6
E
PKA/ α-Tubulin (%)
F
PDE4D/ α-Tubulin (%)
200

Figure 6. ***β-Adrenergic pathway affected by E2F6 expression***. Heart lysate from Wt and E2F6-Tg mice treated with saline or isoproterenol were analyzed in Western blots followed by quantification using densitometry with α-tubulin as loading control. (A) Immunoblotting with anti-β_2-AR and anti-β_1-AR and densitometric quantification: (B) β_2-AR; (C) β_1-AR. (D) Immunoblotting with anti-PKA-C and anti-PDE4D and densitometric quantification: (E) PKA-C; (F) PDE4D. White bars represent Wt samples and black bars represent Tg samples. Results are presented as the mean ± sem. (n = 4) *: $P < 0.05$, **: $P < 0.01$, ***: $P < 0.0001$.

Immunoblotting with anti-β_1-AR detected several polypeptides. Two polypeptides which migrated at ~ 60 kDa were enriched in isolated microsomes and are similar to what was previously demonstrated in the rat heart **(Figure 6A)** (92). The expression of these polypeptides was approximately the same in Wt and Tg in conditions of saline only, but in response to iso they were significantly increased in Wt cardiac tissue (1.8 fold increase, p-value: 0.005), but not Tg **(Figure 6C)**. This left E2F6-Tg hearts with 65% less β_1-AR (p-value: 0.004) than their Wt counterparts in response to isoproterenol.

E2F6 up-regulates PKA and PDE4D expression in myocardium

Following stimulation, the β-adrenergic receptors activate G-coupled signaling proteins which in turn activate multiple pathways to regulate cell growth vs. death. Adenylate cyclase lies downstream of $G_{\alpha s}$ which synthesizes cyclic AMP-required to activate protein kinase A. Western blot analysis of the catalytic subunit of protein kinase A (PKA-C) revealed a single polypeptide which is ~ 40 kDa, similar to the predicted molecular weight of PKA-C (42 kDa) **(Figure 6D)**, which was up-regulated ~ 1.5 fold in

Tg mice (p-value: 0.0176) under basal conditions **(Figure 6E)**. In response to isoproterenol its levels were increased further in Tg hearts.

We also examined one of the negative regulators of the β-adrenergic pathway—the cAMP-specific 3′5′-cyclic phosphodiesterase—PDE4D. Western blot analysis revealed two polypeptides ~ 90 kDa **(Figure 6D)** which correspond to known cardiac splice variants: PDE4D-5 (higher molecular weight band) and PDE4D-8/9 (lower molecular weight band) (93). An approximately four-fold increase in all splice forms of PDE4D was observed in Tg hearts treated with saline only (p-value: 0.0004) **(Figure 6F)**. In response to isoproterenol both Wt and Tg mice exhibited a significant increase in PDE4D (p-value: 0.006 and 0.0006 respectively) but the difference between Wt and Tg was reduced from 4 fold to 3 fold.

In order to examine the impact of PKA on substrate phosphorylation in E2F6-Tg myocardium we assessed the phosphorylation (ser16) on phospholamban (PLN) a well-known substrate of PKA involved in calcium signaling. Western blot examination of total PLN revealed a polypeptide which migrated just below 10kDa in SDS-PAGE representing the PLN monomer **(Figure 7A)**. Examination with phospho-PLN (ser 16) revealed a single polypeptide which migrated just below 10kDa **(Figure 7A)**. In response to isoproterenol both Wt and Tg hearts showed an increase in phospho: total PLN (WT: 1.5 fold, p-value: 0.05) (Tg: 2.2 fold: p-value 0.008) **(Figure 7B)**.

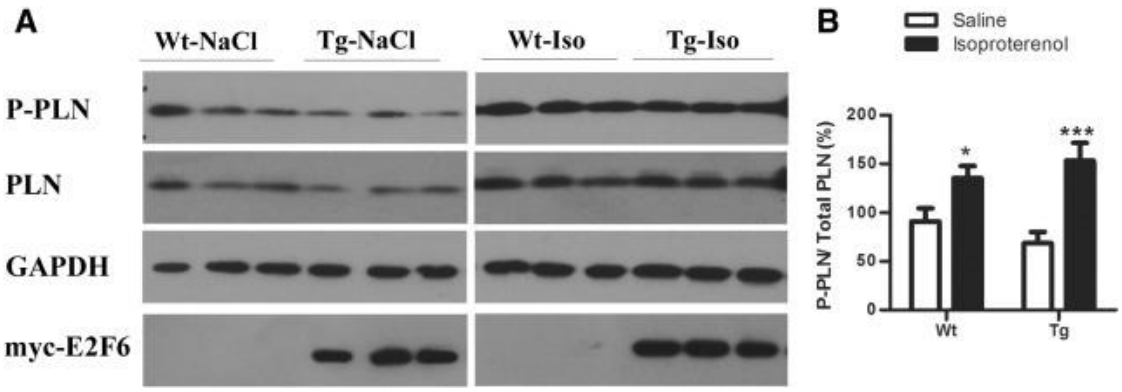

Figure 7. ***Phospholamban is only targeted by PKA in the presence of isoproterenol.*** Heart lysate from Wt and E2F6-Tg mice treated with saline or isoproterenol were analyzed in Western blots followed by quantification using densitometry. (A) Immunoblotting with anti-phospholamban (PLN) and phospho-phospholamban (ser 16) (P-PLN) and (B) Quantification of phospho/total PLN. White bars represent saline treated samples and black bars represent samples. Results are presented as the mean ± sem. (n = 4) *: $P < 0.05$, ***: $P < 0.001$.

E2F6 activates c-Src/ERK and Bcl2 in E2F6-Tg myocardium

In addition to PKA, stimulation of the β-adrenergic pathway has also been reported to activate the c-Src tyrosine kinase which can activate the extracellular receptor kinase (ERK) a known regulator of cardiac growth and survival signaling (94). We previously noted an increase in ERK activation in adult E2F6-Tg myocardium (80). Western blot analysis with phospho-ERK (Thr 202/Tyr 204) and total ERK antibodies revealed a 44 kDa species corresponding to ERK1, and a 42 kDa species corresponding to ERK2 in SDS-PAGE **(Figure 8A)**. Similar to what we previously found in older E2F6-Tg mice, the ratio of phospho-ERK1/ERK1 was not significantly changed in Tg mice **(Figure 8B)**, but ERK2 showed a ~ 9 fold activation (p-value: 0.0005) **(Figure 8C)**.

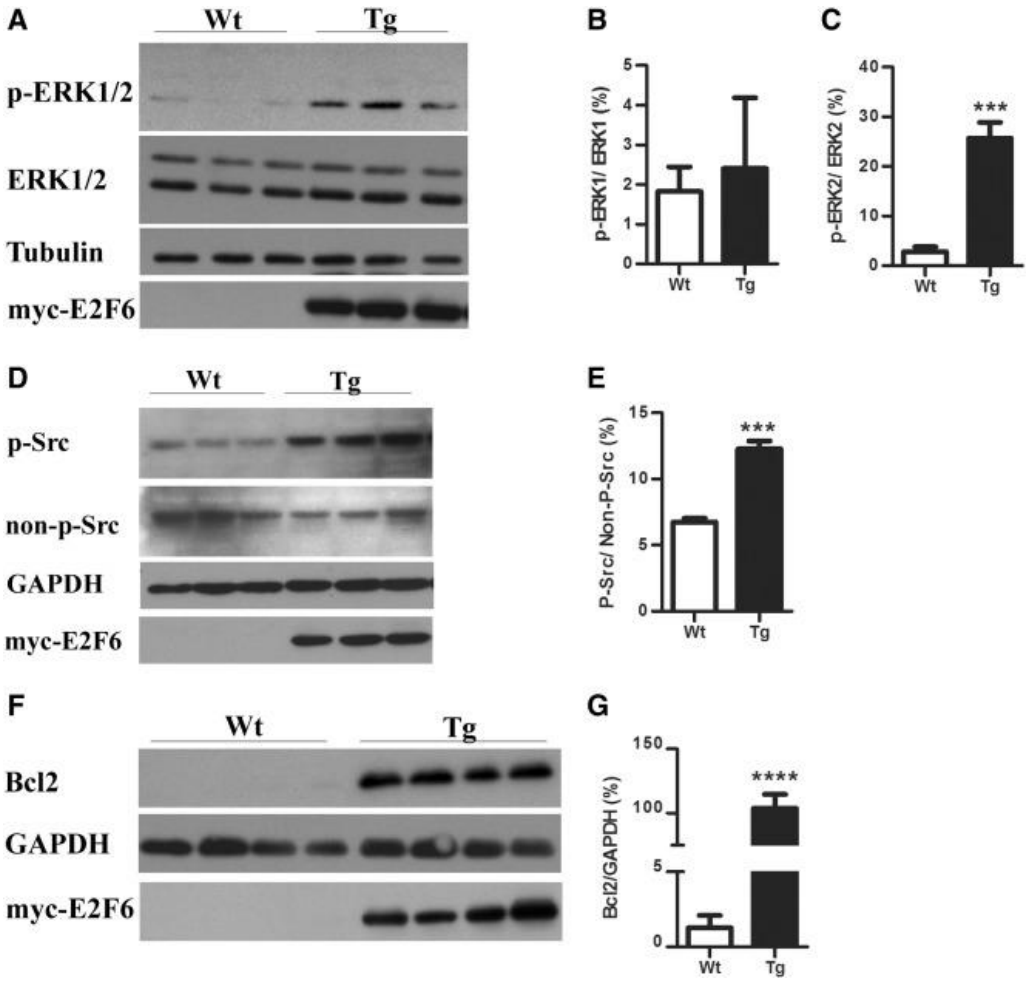

Figure 8. ***Activation of c-Src/ERK/Bcl2 Survival Pathway in E2F6-Tg myocardium.*** Heart lysate from Wt and E2F6-Tg mice treated with saline or isoproterenol was analyzed in Western blots followed by quantification using densitometry with α-tubulin or GAPDH as loading controls. (A) Immunoblotting with anti-phosphorylated ERK1/2 and total ERK1/2 and quantification of (B) phospho-ERK1/ERK1 and (C) phospho-ERK2/ERK2. (D) Immunoblotting with anti-phosphorylated c-Src and non-phosphorylated c-Src and (E) quantification of phospho/non-phosphorylated c-Src. (F) Immunoblotting with anti-Bcl2 and (G) quantification of Bcl2/Tubulin. White bars represent saline treated samples and

black bars represent isoproterenol treated samples. Results are presented as the mean ± sem. (n = 4) ***: P < 0.001, ****: P < 0.0001.

Examination of Wt and Tg hearts with anti-phosphorylated (active) and non-phosphorylated c-Src revealed a doublet ~ 60 kDa, the predicted size of c-Src **(Figure 8D)**. A 2 fold increase in the ratio of phosphorylated c-Src: non-phosphorylated c-Src was noted in Tg mice in comparison to Wt (p-value 0.0002) **(Figure 8E)**.

c-Src/ERK has been demonstrated to activate a survival signal through up regulation of the anti-apoptotic/survival protein, Bcl2 (95). Western blot examination of Bcl2 revealed a single polypeptide ~ 26 kDa which was barely detectable in Wt myocardium, but was induced ~ 100 fold by E2F6 expression (p-value: 0.00001) **(Figure 8F and 8G)**.

E2F6 down-regulates cardiac growth regulator AKT1

Western blot analysis of the major cardiac isoform of AKT involved in cardiac growth—AKT1 (also known as protein kinase B) using a polyclonal antibody revealed 2 polypeptides, one of which was ~ 60 kDa the predicted molecular weight of AKT1 **(Figure 9A)**, the other which was ~ 70 kDa and showed a similar expression pattern. Densitometry of the 60 kDa polypeptide revealed a ~ 60% reduction in the amount of AKT1 in Tg hearts in saline only conditions (p-value: 0.0006) **(Figure 9B)**. Analysis of AKT1 phosphorylation at serine 473, which is necessary for its activation, (with a specific phospho antibody) revealed a 60 kDa phospho-peptide which was reduced in Tg myocardium **(Figure 9C)** by ~ 33% (p-value: 0.04). The ratio of P-AKT1/AKT1 was significantly increased by ~ 1.4 fold in Tg myocardium in saline only conditions (p-value: 0.04) **(Figure 9D)**.

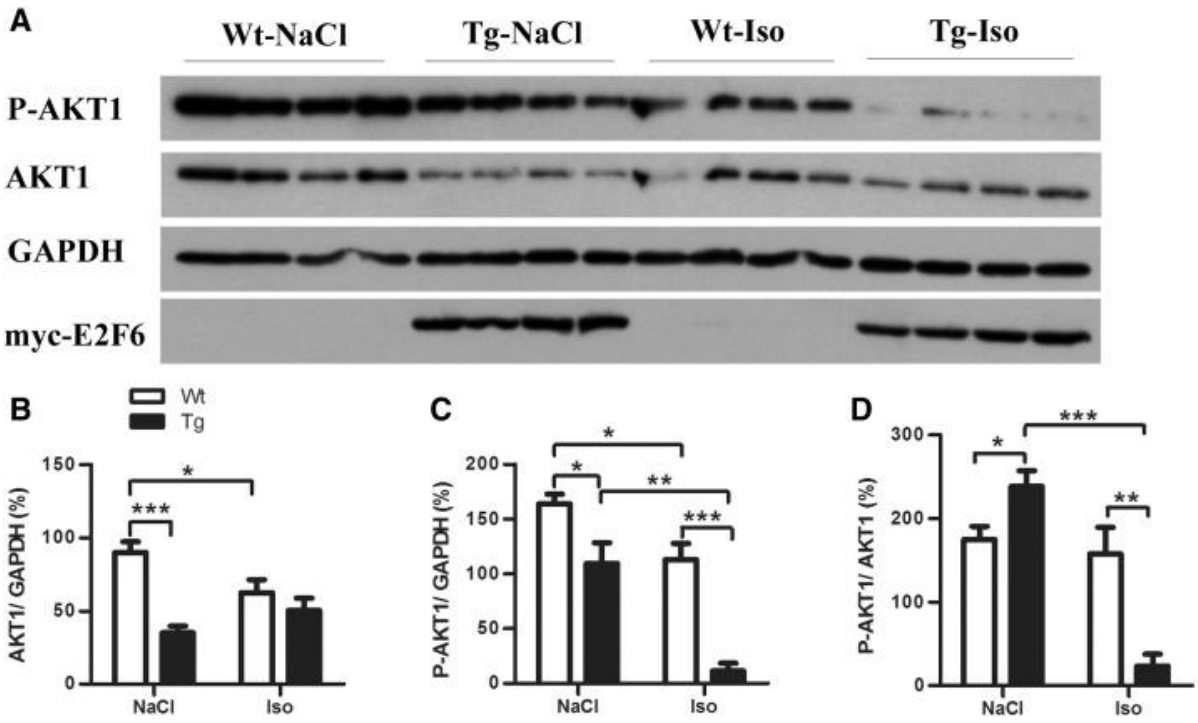

Figure 9. ***AKT1 activity is deregulated in E2F6-Tg myocardium.*** Heart lysate from Wt and E2F6-Tg mice treated with saline or isoproterenol were analyzed in Western blots followed by quantification using densitometry with GAPDH as loading control. (A) Immunoblotting with anti-AKT1 and phospho-AKT1 (ser-473) and quantification of (B) AKT1/GAPDH, (C) phospho-AKT1/GAPDH, and (D) phospho-AKT1/AKT1. White bars represent Wt samples and black bars represent Tg samples. Results are presented as the mean ± sem. (n = 4) *:P < 0.05, **:P < 0.01, ***: P < 0.001.

In response to isoproterenol total AKT1 levels were reduced by ~ 30% in Wt myocardium (p-value: 0.05) while Tg were unchanged such that isoproterenol treatment resulted in Wt and Tg having the same amount of total AKT. In contrast, P-AKT1 was reduced by ~ 90% in Tg myocardium in response to isoproterenol (p-value: 0.003) **(Figure 9A and 9C)** as was the P-AKT1/AKT1 ratio (p-value 0001) **(Figure 9D)**. In Wt hearts, P-

AKT1 was reduced by the same amount as total AKT1 (~ 30%, p-value: 0.009) which resulted in no change in the activation status of AKT1.

E2F6 differentially affects β_2-AR, PKA-C, and Akt1 mRNA

Since E2F6 is believed to serve as a transcriptional repressor, we assessed the transcript levels of various genes whose protein products were deregulated in Tg myocardium to determine if they were modulated at the transcriptional level. QPCR analysis of PKA-C mRNA revealed a ~ 2.5 fold increase in its transcript levels in Tg myocardium **(Figure 10A)** while the β_2-AR and AKT1 mRNA levels were not significantly changed **(Figure 10B and 10C)**.

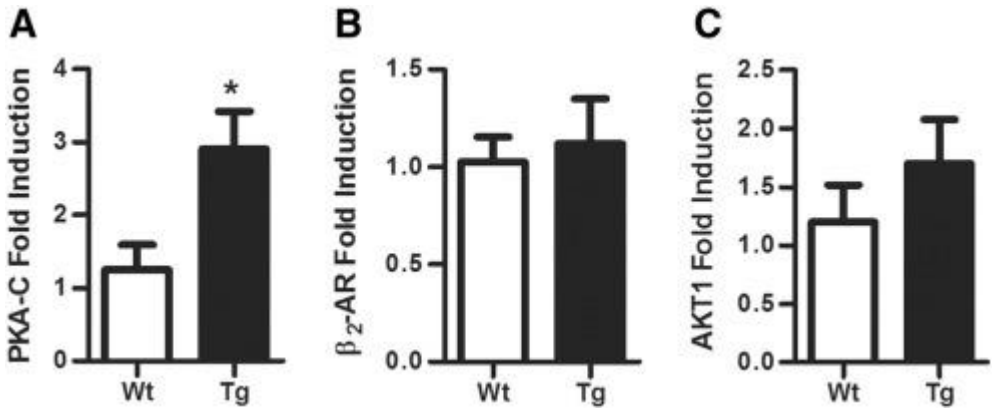

Figure 10. ***Effect of E2F6 on β_2–AR, PKA-C, and AKT1 mRNA.*** QPCR was performed on cDNA from Wt and Tg myocardium to determine the fold induction of **(A)** PKA-C **(B)** β_2-AR and **(C)** AKT1. Fold inductions were calculated in relation to 18sRNA. Results are the mean ± sem. (n = 5) *: $P < 0.05$.

E2F6 deregulates E2F3/Rb expression in myocardium

In order to evaluate the effect of the E2F6 repressor on the E2F pathway in response to hypertrophic stimulation we examined the levels of E2F family members. In particular, we examined the expression of the E2F3 (including E2F3A and E2F3B) since it is the only E2F family member critical to both neo-natal and postnatal cardiac growth, and Rb because it is the major pocket protein expressed in postnatal development (35) and (48). Western blots with anti-E2F3 revealed 3 major bands in cardiac lysates **(Figure 11A)**, which we previously described based on reference to control cell lysates (80). The doublet which appears at ~ 45 kDa represents E2F3B and a higher molecular weight doublet ~ 55 kDa, present at much lower levels, represents E2F3A. A non-specific polypeptide (42 kDa) was detected by this antibody which remained unchanged.

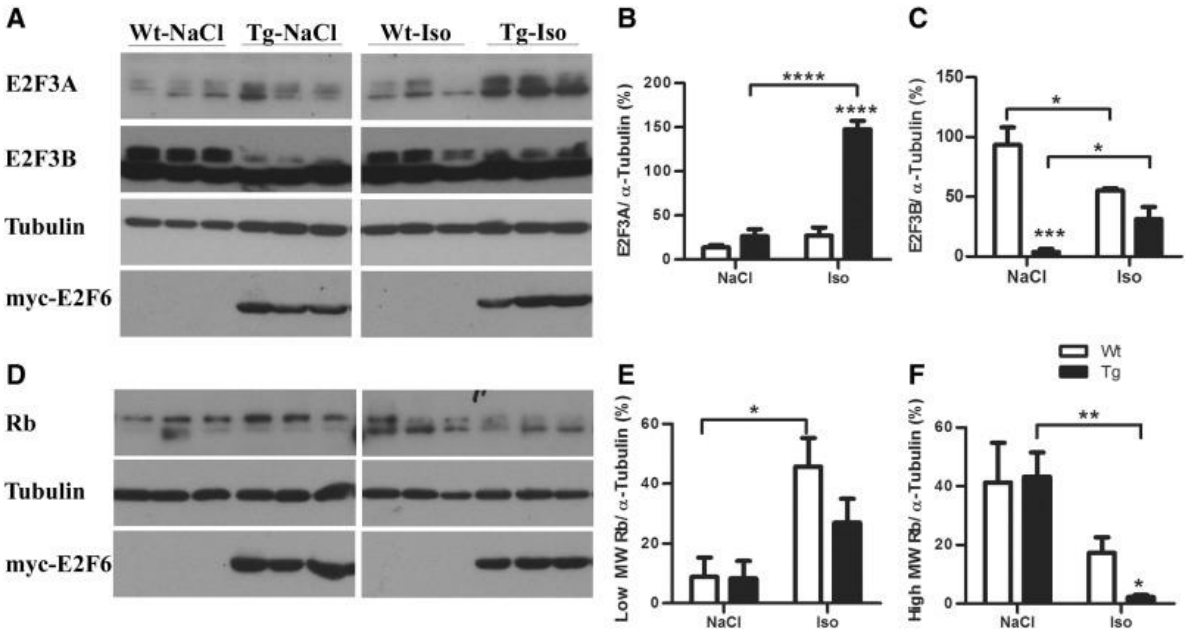

Figure 11. ***Deregulation of E2F3/Rb in Tg Mice under hypertrophic stimulation.*** Heart lysate from Wt and E2F6-Tg mice treated with saline or isoproterenol were analyzed in Western blots followed by quantification using densitometry with α-tubulin as loading control. **(A)** Immunoblotting with anti-E2F3 and quantification of **(B)** E2F3A/α-tubulin and **(C)** E2F3B/α-tubulin. **(D)** Immunoblotting with anti-Rb and quantification of **(E)** high molecular weight Rb/α-tubulin and **(F)** low molecular weight Rb/α-tubulin. White bars represent Wt samples and black bars represent Tg samples. Results are presented as the mean ± sem. (n = 3–4) *: P < 0.05, **: P < 0.01, ***: P < 0.001, ****P < 0.0001.

Similar to what we previously found, E2F3B was drastically reduced (~ 80%, p-value: 0.0001) in Tg hearts under saline conditions **(Figure 11A and 11C)**. Levels of E2F3B were decreased in Wt hearts in response to isoproterenol, and were significantly increased by ~ 8 fold in Tg hearts (p-value 0.04). E2F3A is expressed at low levels in adult myocardium in Wt and Tg hearts and was not different under basal conditions **(Figure 11A**

and 11B). Levels of E2F3A did not change in response to isoproterenol in Wt hearts, but Tg hearts responded with a ~ 6 fold increase in E2F3A (p-value: 6.02E − 05) **(Figure 11B)**. Western blot examination with anti-Rb revealed two polypeptides of ~ 100kDa which likely correspond to the phosphorylated (higher molecular weight) and non-phosphorylated (lower molecular weight) forms of the Rb protein **(Figure 11D)**. Analysis of both higher and lower molecular weight polypeptides revealed no significant changes in Rb under saline conditions. In Wt and Tg myocardium there was a shift from the higher molecular weight polypeptide in saline to the lower molecular weight polypeptide in response to isoproterenol **(Figure 11D)**. In Wt hearts the lower molecular weight polypeptide was significantly increased by 5 fold (p-value 0.02) but not in Tg hearts **(Figure 11E)**. The higher molecular weight polypeptide was significantly reduced in Tg hearts but not Wt resulting in ~ 90% less high molecular weight Rb in isoproterenol treated Tg myocardium (p-value: 0.03) **(Figure 11F)**.

Discussion

Studies here reveal an intriguing cross-talk between the major regulators of cellular growth and death: the E2F pathway, AKT1, and β-adrenergic signaling in the control of pathological hypertrophy in vivo. The targeted expression of E2F6 in mouse myocardium resulted in dilated cardiomyopathy as early as 2 weeks which increased in severity over time in the absence of any change in muscle mass. Surprisingly, these mouse hearts exhibit activation of the β-adrenergic signaling pathway including the specific increase in β_2 receptor protein levels, PKA activity, and c-Src/ERK activation. Despite these indicators of growth, and a re-activation of the fetal gene program, E2F6-Tg mice fail

to elicit any notable cardiac hypertrophy. Activation of the negative regulator of the cAMP pathway, PDE4D, and a reduction in cardiac growth regulator, AKT1, noted in E2F-Tg mouse myocardium may attenuate the pro-hypertrophic growth signals thus potentially limiting any increase in muscle mass. Further, the specific loss of E2F3 which is rescued by adrenergic stimulation suggests that this E2F family member may play a critical role in the hypertrophic response of the postnatal myocardium. The data also imply that normal E2F activity is necessary to fine tune the signals that impinge upon mechanisms encompassing β-adrenergic/PKA/PDE4D, c-Src/ERK, and AKT in control of cardiac hypertrophy. The disruption of the E2F pathway results in an imbalance between pro and anti-hypertrophic signals such that E2F6-Tg mice are unable to mount a compensatory hypertrophic growth response and instead proceed directly to cardiac dilation.

E2F6-Tg hearts show a specific 2-fold up-regulation of the protein levels of β_2 adrenergic receptor under saline conditions while β_1-AR is unchanged. A 1.5 fold increase in the catalytic subunit of PKA protein was also evident and was reflected by a similar increase in transcript levels indicating that E2F6 upregulated its expression via a transcriptional mechanism. E2F6 Tg mice also presented with increased activation of c-Src which is most likely due to phosphorylation by Gα in response to adrenergic stimulation (96). c-Src can activate the mitogen activated protein kinase signaling pathway via the Ras family of small GTPases and β-arrestin resulting in an increase in ERK activity associated with cardiac growth (97) and (98). Thus E2F6 expression stimulated the pro-hypertrophic β_2-adrenergic signaling pathway resulting in PKA and c-Src/ERK activation, but without the expected increase in cardiac muscle mass.

Examination of one of the downstream targets of PKA, phospholamban, revealed that its phosphorylation status at serine 16 was not changed by E2F6 expression. Further, no changes in the phosphorylation of another of PKA's substrates, troponin I, were noted **(Appendix 1: Sup Fig 2)**. This indicates that activation of PKA did not result in the targeted phosphorylation of these protein substrates involved in excitation-contraction coupling. Physiological response to PKA activation requires targeting via A kinase anchoring proteins (AKAPs), thus it is possible that it did not compartmentalize with the appropriate AKAP and substrate (99). Examination of the negative regulator of cAMP signaling, PDE4D, revealed a four-fold increase in its protein levels in E2F6 Tg myocardium. PDE4D was demonstrated to regulate cAMP levels in the sarcoplasmic reticulum micro-domains which contain SERCA2a and phospholamban (100). This suggests that the 4 fold increase in PDE4D in Tg myocardium could result in enhanced cAMP degradation in the domain containing PLN, thus negating any phosphorylation due to the increased PKA.

Another explanation for the discrepancy between pro-hypertrophic signals and the apparent failure to elicit a significant muscle growth response could be the ~ 60% reduction in AKT1, a critical regulator of both physiological and pathological hypertrophy (101). Adrenergic stimulation activates the Phosphatidylinositol 3-kinase which phosphorylates and activates AKT1. AKT1 phosphorylates a negative regulator of cardiac growth: the glycogen synthase GSK3β resulting in its inactivation and allowing for cardiac growth. Thus the down-regulation of AKT1 and its phosphorylation could represent the heart's attempt to counteract the up regulation of the hypertrophic β-adrenergic system in response to deregulated E2F activity.

AKT1 transcript levels were not altered in E2F6 Tg myocardium indicating that its down-regulation involved post-transcriptional mechanisms. Paradoxically, the phosphorylation of AKT1 at serine 473, the site which is necessary for its activity, also targets AKT1 for degradation by the proteasome (102) and (103). Although AKT1 and P-AKT1 were reduced in Tg myocardium, the ratio of P-AKT1/AKT1 was increased suggesting that this could be the potential mechanism for its post-transcriptional loss in Tg myocardium.

It is notable that adrenergic stimulation with isoproterenol did not rescue the levels of AKT1 in Tg myocardium, and decreased AKT1 expression in Wt hearts. These data indicate that the loss of AKT1 may represent a compensatory response to counter adrenergic stimulation, but that it is not sufficient to block hypertrophy. Protein kinase A was increased in both Wt and Tg myocardium following adrenergic stimulation, and PKA targets GSK3β to control muscle growth (104). Thus the up-regulation of PKA in response to isoproterenol may compensate the decrease in AKT1 allowing cardiac hypertrophy to proceed in Wt and Tg mice (104).

Despite the absence of hypertrophy even in very young E2F6-Tg mice, they were capable of mounting a hypertrophic growth response to β-adrenergic receptor stimulation which was much more robust than that observed in their Wt counterparts. The most obvious explanation for this effect is that Tg mice have double the amount of $\beta_2$receptors to respond to the hypertrophic stimulus. Furthermore, the signaling proteins downstream of the β-receptors including PKA, c-Src, and ERK are already activated and primed for signaling in E2F6-Tg myocardium. Thus E2F6 is capable of upregulating the critical components of the pro hypertrophic signaling cascade which are effectively utilized by

isoproterenol enabling an immediate and potent growth response to the drug. PKA-C appears to be activated at the transcriptional level while β_2-AR, c-SRC, and ERK are activated via post-transcriptional mechanisms.

Another key factor contributing to the hyper-sensitivity of Tg myocardium to isoproterenol is that cardiac remodeling has already been activated as have anti-hypertrophic genes ANP and BNP. Isoproterenol does not induce further activation of ANP or BNP transcripts in E2F6-Tg mice, most likely because they are already highly up-regulated. Thus, while isoproterenol induces ANP/BNP and a modest increase in LV muscle mass and cardiac performance in Wt mice, Tg mice have already activated these remodeling genes and proceed directly to a robust hypertrophic response. In fact, the response of Tg mice to low dose isoproterenol is almost indistinguishable to the response of Wt to the high dose which leads to marked LV hypertrophy and decreased contractility that would be expected during heart failure in response to prolonged β-adrenergic stimulation (105). In addition to regulating cardiac growth both E2F and β-adrenergic signaling pathways also regulate cell death. In general, β_1-AR and E2F activation are associated with the induction of apoptosis in cardiomyocytes, while β_2-AR and repression of E2F are believed to enhance survival (95), (106), (73) and (107). In support of this, repression of the E2F pathway via E2F6 led to the specific up-regulation of pro-survival β_2-AR and repressed the induction of pro-apoptotic β_1-AR in response to isoproterenol. The β_2-adrenergic receptor was specifically demonstrated to activate the anti-apoptotic protein Bcl2 via the ERK pathway (95) and both were up-regulated in E2F6-Tg myocardium. In other studies it was demonstrated that the induction of ERK via β_2-AR was dependent on c-Src which is also activated in E2F6-Tg mice and can be induced via mechanical stretch

such as that imposed by dilation (98,108,109). Thus the activation of β_2-AR, c-Src, ERK, and Bcl2 may reflect the attempt of E2F6-Tg myocardium to mount a survival signal following the stress of cardiac dilation which is not related to growth, hence the lack of significant hypertrophy in these mice. In agreement, while ERK is often associated with hypertrophy, $ERK1^{-/-}$ $ERK2^{+/-}$ mice can elicit cardiac growth in response to hypertrophic stimuli, but show increased cell death indicating that ERK is required for survival, but not growth in response to hypertrophic insult (110). Consistent with the activation of a survival pathway, no apoptosis was detected in E2F6 mice at this stage (80), and further, E2F6 has been demonstrated to inhibit apoptosis in cell culture (74,75). We observed an increase in apoptosis in much older mice (6 months), at which point less than 40% of mice are alive, suggesting that apoptosis was a consequence of end stage heart failure and not the underlying cause of the DCM (80).

It is notable that E2F3 null mice which survive into adulthood also develop late onset DCM, which was attributed to the loss of E2F3B (35). E2F6-Tg mice develop a much more severe and earlier onset DCM which is associated with the specific loss of E2F3B as well as the failure to increase the protein levels of the activator E2Fs (80). Thus the specific deregulation of E2F3B by E2F6 induces cardiac dilation in the absence of a compensatory hypertrophic response. Isoproterenol rescues E2F3B expression, induces E2F3A, and attenuates the repressor Rb such that the E2F pathway is restored resulting in a robust hypertrophic response. This study demonstrates that E2F6 can uniquely modulate E2F activity and the hypertrophic response in postnatal myocardium through mechanisms encompassing β-adrenergic signaling and stress related kinases and may serve as a novel target in cardiac remodeling.

Funding sources

This work was funded by operating grants from the Heart and Stroke Foundation of Ontario (54033) to BST.

Disclosures

None.

Acknowledgments

We thank Megan Fortier and Dr. Wael Maharsy for their technical help with echocardiography and the Vevo software.

CHAPTER 2:

“E2F6 Regulates Stress Induced Apoptosis in Cardiomyocytes”

Major JL, Salih M, and Tuana BS. (2017) Cardiovascular Research. Submitted.

Author contributions: JL Major performed experiments, analyzed data, and prepared the manuscript under the supervision of BS Tuana. Technical support and advice were given by Maysoon Salih.

Abstract

Aims: The E2F/Rb pathway regulates cell growth, differentiation, and death. In particular, E2F1 promotes apoptosis in all cells including the heart. E2F6, which represses E2F activity, demonstrates anti-apoptotic properties, but its role in the heart remains to be evaluated. We previously assessed the role of E2F6 in postnatal myocardium in a transgenic (Tg) mouse which developed dilated cardiomyopathy (DCM) in the absence of pathological growth or apoptosis. In this study we evaluate the anti-apoptotic potential of E2F6 in the heart.

Methods and Results: Neonatal cardiomyocytes (NCM) from E2F6-Tg hearts showed significantly less caspase-3 cleavage, a lower Bax/Bcl2 ratio, and improved cell viability in response to various doses of cobalt chloride (CoCl2). In contrast, no difference in apoptotic markers or cell viability was observed in response to Doxorubicin (Dox) between Wt and Tg NCM. Dox caused a rapid and dramatic loss of E2F6 protein in Tg NCM within 6hrs to non-detectable levels at 12 hrs. $CoCl_2$ also promoted a loss of E2F6, but it was still detectable at 24hrs. The level of *e2f6* transcript was unchanged in Wt, but was decreased in Tg NCM in response to Dox which was due to decreased levels of the α-MHC gene (whose promoter was used to drive the E2F6 transgene). In HeLa, Dox induced a dose dependent upregulation of the pro-apoptotic E2F1 protein with a marked reduction in E2F6 levels while $CoCl_2$ caused a reduction in E2F1 without affecting E2F6. In HeLa, Dox induced Checkpoint kinase-1 activation and the loss of E2F6 via post-transcriptional mechanisms. E2F6 up-regulated cyclin-E expression and decreased the contractile protein teliothenin in E2F6-Tg myocardium.

Conclusions: These data imply that E2F6 may serve to protect cardiomyocytes from apoptosis and improve survival although it can adversely impact differentiation leading to DCM. Strategies to modulate its levels may be useful therapeutically to mitigate cell death associated disorders.

Keywords: doxorubicin, cobalt chloride, cell survival, dilated cardiomyopathy, heart failure

Non-standard Abbreviations and Acronyms:

αMHC- alpha myosin heavy chain

Chk- checkpoint kinase

DCM- Dilated Cardiomyopathy

Dox- Doxorubicin

NCM- Neonatal Cardiomyocytes

Rb-Retinoblastoma protein

T-cap- teliothenin

Tg- Transgenic

TnT- troponin T

Introduction

The heart has an estimated cardiomyocyte renewal rate of only ~1%, which is a major obstacle in its repair following ischemia or exposure to toxins which induce apoptosis. (4) Instead of cardiomyocyte proliferation after injury, the dead tissue is replaced with collagen secreted by fibroblasts in a process called fibrosis. (111) This causes the heart to stiffen and lose contractile force which leads to a cycle of blood not being expelled from the heart, cardiomyocyte stretching, and cell death. Thus, finding new ways to promote cardiac survival and limit apoptosis are key to treating the diseased heart.

The E2F/pocket protein pathway is a major regulator of apoptosis in all cell types. (68) The E2F family consists of eight transcription factors which regulate the expression of genes which regulate a multitude of fate decisions in the cell. (112,113) E2Fs1-5 are evolutionarily conserved family members which are negatively regulated by binding of the Retinoblastoma protein (Rb) family (113,112). The induction of apoptosis by E2F1 has been the most extensively studied. E2F1 can induce apoptosis via direct regulation of pro-apoptotic genes including caspases, *bnip3,* and *p73* (73,30). It can also activate apoptosis via expression of the cyclin dependent kinase inhibitor $p14^{ARF}$, thereby inhibiting MDM2 and stabilizing p53, or it can directly bind to p53 via its cyclin-A binding domain to activate p53 dependent apoptosis. (69,70,72,71) Forced expression of E2F1 has been demonstrated to induce apoptosis in neonatal cardiomyocytes as well as in adult myocardium. (53,79,54)

E2F6 is a novel member of the E2F family which is capable of regulating E2F dependent transcription independently of Rb. (15,16,20) It has been demonstrated to be anti-apoptotic in HEK cells against UV damage and the hypoxia mimetic, cobalt chloride, an effect which was partially attributed to its ability to out-compete the pro-apoptotic E2F1. (75,74) The regulation of E2F6 via microRNAs, including miR-31 and miR-185, was related to the efficacy of the chemotherapeutic induction of apoptosis in prostate cancer and triple negative breast cancer respectively. (114,115,78) More recently, it was discovered that the Epstein Barr Virus Nuclear antigen 3 (EBNA3), which is necessary for EBV immortalization and the induction of EBV cancers, binds to and stabilizes E2F6 which inhibited the pro-apoptotic E2F1. (116) These studies suggest that E2F6 is an important player in regulating apoptosis in cancer cells, but there is a lack of information evaluating the potential for E2F6 to regulate apoptosis in the heart.

We previously explored the function of the E2F pathway in the post-mitotic heart via expression of E2F6 in a transgenic (Tg) mouse. Expression of E2F6 led to E2F dependent gene activation including genes involved in the cell cycle and DNA damage repair due to competitive binding for E2F/Rb sites and the down-regulation of cardiac transcriptional regulator: E2F3. (80,35). This resulted in E2F6 dose dependent dilated cardiomyopathy (DCM), surprisingly without the normally expected pathological hypertrophic or apoptotic responses (80).We detected the specific stimulation of a β_2-adrenergic survival signaling pathway in E2F6-Tg myocardium which induced the anti-apoptotic protein Bcl2 via the ERK signaling cascade. In the present study we evaluate the capacity for E2F6 to protect the heart from apoptosis by exposing neonatal cardiomyocytes (NCM) from Wt and E2F6-Tg mice to chemical apoptotic insult.

Materials and Methods

Transgenic (Tg) mice with cardiac specific expression of E2F6 (B6C3F1) were bred with WT and genotyped as previously described (80). Neonatal cardiomyocytes (NCM) were collected from Wt and E2F6-Tg mice as previously described (117). HeLa (Passage 3) were obtained from ATCC and grown in DMEM with 10% FBS. NCM and HeLa were starved for 24 hours prior to the addition of cobalt chloride ($CoCl_2$) (250μM-1000μM) or Doxorubicin (Dox) (0.5μM-1.0μM) for 24hrs unless otherwise indicated. Cell viability was determined using the Cell Titer Blue kit (Promega). Protein and RNA analyses were performed using standard methods as previously described (117). A detailed methods section and lists of primers and antibodies used can be found in the online supplement **(Appendix 2)**.

Results

Genes involved in DNA replication and repair are upregulated in E2F6-Tg myocardium

Previously performed microarray analysis in E2F6-Tg hearts detected a significant induction of genes involved in DNA repair (80). Reverse-transcription real time PCR (RT-qPCR) analysis of Wt and E2F6-Tg myocardium confirmed the up-regulation of: *blm2*- a helicase involved in DNA replication and repair (4-fold increase, $p<0.05$), *rad51*-a recombinase involved in double strand break repair- (2 fold increase, $p< 0.05$), and *chk1*- a cell cycle kinase involved in single strand repair (3.6 fold increase, $p< 0.05$) **(Figure 12).** In contrast, *Dnaja3* (otherwise known as hsp40)-a chaperone protein

involved in apoptosis signaling mRNA levels were not altered in Tg myocardium. **(Figure 12)**.

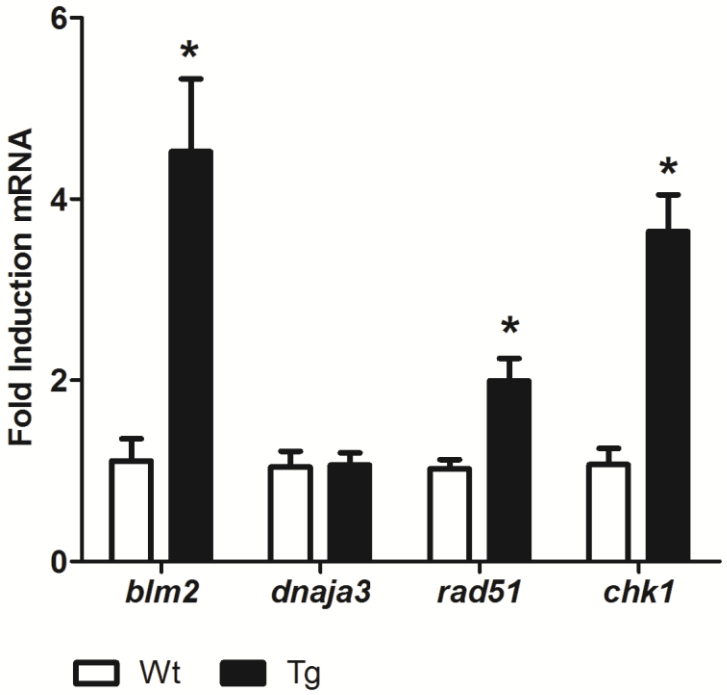

Figure 12. ***E2F6 induces the expression of genes involved in DNA replication and repair in Tg myocardium.*** Fold induction of *blm2*, *rad 51*, *chk1*, and *dnaja3* mRNA in Wt (white bars) and Tg (black bars) neonatal myocardium at post-natal day seven. Fold inductions were calculated in reference to *gapdh*. Results are presented as the mean ± SEM. (n=4-7) *$p<0.05$ vs Wt.

E2F6 protects neonatal cardiomyocytes from cobalt chloride induced apoptosis

E2F6-Tg mice develop early DCM without signs of apoptosis, and with enhanced cell survival programing suggesting that E2F6 may be anti-apoptotic in the heart (80,118). E2F6 was previously demonstrated to have a protective effect against $CoCl_2$

induced apoptosis in HEK-293 cells. (75) In order to determine if E2F6 could serve to protect the heart against apoptosis, neonatal cardiomyocytes (NCM) were isolated from Wt and Tg hearts, exposed to different concentrations of $CoCl_2$, and assayed for cell survival and apoptosis. NCM were exposed to $CoCl_2$ for a 24hr period which was demonstrated to induce apoptosis in H9C2 cells (rat cardiomyocyte line). (119) Cell viability analysis indicated that E2F6 had a significant protective effect on cardiomyocyte survival post exposure to $CoCl_2$ (250,500 and 1000μM) **(Figure 13A)**. E2F6 consistently and significantly increased NCM survival from 12% to as much as 50% at the highest dose of $CoCl_2$ ($p<0.05$) **(Figure 13A)**.

A

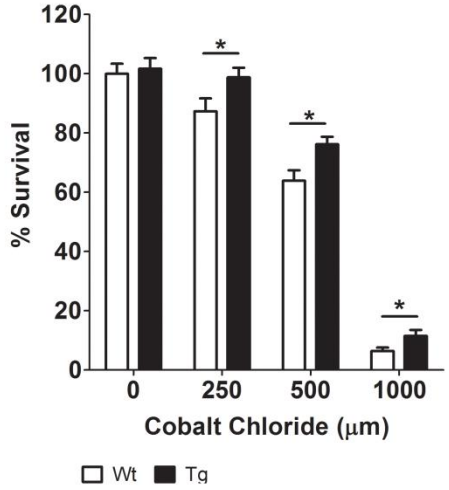
120
100
80
60
40
20
0
% Survival
*
*
*
0
250
500
1000
Cobalt Chloride (μm)
Wt
Tg

B

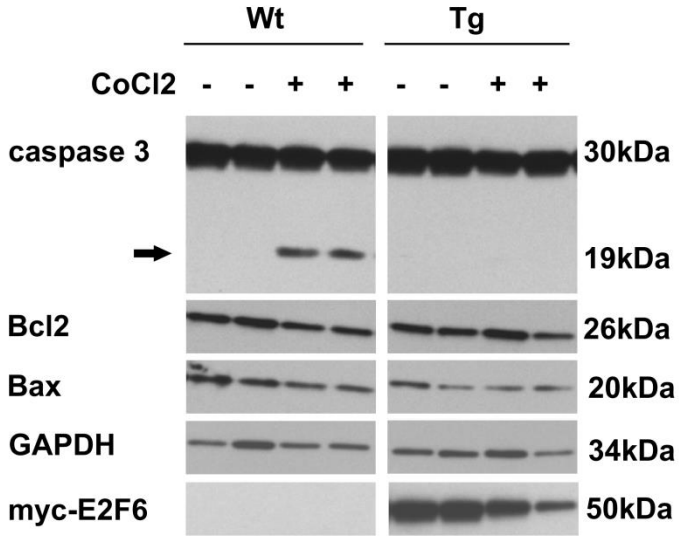
Wt
Tg
CoCl2 - - + + - - + +
caspase 3
30kDa
19kDa
Bcl2
26kDa
Bax
20kDa
GAPDH
34kDa
myc-E2F6
50kDa

C

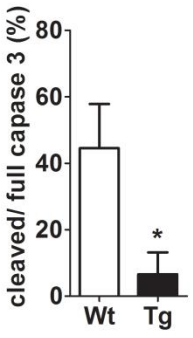
cleaved/ full capase 3 (%)
80
60
40
20
0
*
Wt
Tg

D

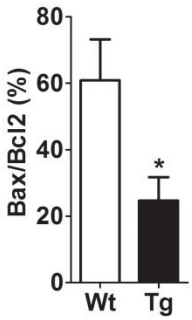
Bax/Bcl2 (%)
80
60
40
20
0
*
Wt
Tg

Figure 13: ***E2F6 protects neonatal cardiomyocytes from cobalt chloride induced apoptosis.*** **(A)** Percent viability of Wt and Tg NCM following 24hr treatment with the indicated amounts of $CoCl_2$. Results are presented as the mean ± SEM (n=8). *p<0.05 vs Wt for each treatment. **(B)** Representative western blot of Wt and Tg NCM lysate following 24hr treatment with 500μM $CoCl_2$ examined with: anti-capsase3, anti-Bax, and anti-Bcl2. Cleaved caspase 3 is denoted by an arrow. GAPDH was used as a loading control. Myc-E2F6 represents E2F6 derived from the transgene. **(C)** Quantification of cleaved caspase 3/full length caspase 3 and Bax/Bcl2 ratios based on densitometry of Wt and Tg cardiomyocytes treated with $CoCl_2$. Results are presented as the mean ± SEM (n=3-4). *p<0.05 vs $CoCl_2$ treated Wt.

To further assess the potential for E2F6 to protect against apoptosis in cardiomyocytes Wt and Tg NCMs were treated with 500μM $CoCl_2$ and examined for molecular markers. While full length caspase 3 (~30kDa) was detected in all samples, cleaved caspase 3 (~19kDa, denoted by arrow) was only detectable in $CoCl_2$ treated samples **(Figure 13B)**. The ratio of cleaved caspase 3/full length caspase 3 was six times greater in Wt in comparison to Tg ($p<0.05$) indicative of less caspase activation and apoptosis in E2F6-Tg NCM **(Figure 13C)**. Western analysis with pro-apoptotic anti-Bax (~20kDa) and anti-apoptotic anti-Bcl2 (~26kDa) (Fig 2B) revealed a significantly lower Bax/Bcl2 ratio in Tg cardiomyocytes (~60% less, $p<0.05$) **(Figure 13C)** also indicative of less apoptosis.

Doxorubicin induces apoptosis in Wt and E2F6-Tg neonatal cardiomyocytes

Wt and Tg NCMs were next exposed to the chemotherapeutic agent doxorubicin which is known to have damaging effects on the heart. (120) Cell viability analysis demonstrated a similar impact on cell survival in Wt and Tg cardiomyocytes treated with 0.5μM or 1.0μM doxorubicin (~75% survival) **(Figure 14A)**. Western blot analysis with anti-caspase 3 detected a similar amount of caspase 3 cleavage in Dox treated Wt and Tg NCMs **(Figure 14B and 14C)**. Similarly, the level of p53 acetylation was equivalent in Wt and Tg Dox treated cells suggesting that E2F6 did not protect cardiomyocytes from Dox induced apoptosis. It is notable that myc-E2F6 protein was undetectable in Tg cardiomyocytes following the doxorubicin treatment **(Figure 14C)**.

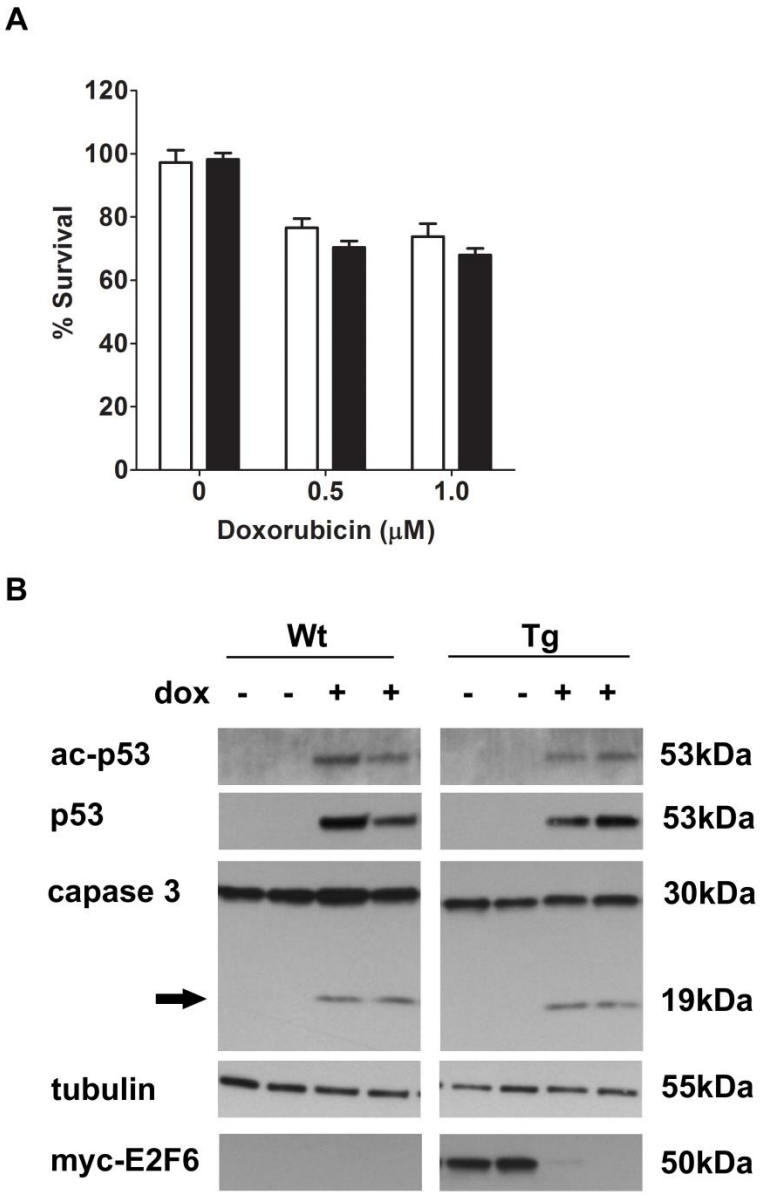
A
120
100
80
60
40
20
0
% Survival
0
0.5
1.0
Doxorubicin (μM)
B
Wt
Tg
dox - - + + - - + +
ac-p53
53kDa
p53
53kDa
capase 3
30kDa
19kDa
tubulin
55kDa
myc-E2F6
50kDa
C
25
20
15
10
5
0
ac-p3/ p53 (%)
Wt
Tg
D
100
75
50
25
0
cleaved/ full capase 3 (%)
Wt
Tg

Figure 14. ***Doxorubicin induces apoptosis in Wt and Tg neonatal cardiomyocytes.*** **(A)** Percent viability of Wt and Tg NCM following 24hr treatment with the indicated amounts of Dox. Results are presented as the mean ± SEM (n=8). *p<0.05 vs Wt for each treatment. **(B)** Representative western blot of Wt and Tg NCM lysate following 24hr treatment with 0.5μM Dox examined with: anti-capsase3, anti-p53, and anti-acetyl-p53. Cleaved caspase 3 is denoted by an arrow. GAPDH was used as a loading control. Myc-E2F6 represents E2F6 derived from the transgene. **(C)** Quantification of cleaved caspase 3/full length caspase 3 and acetyl p53/ p53 ratios based on densitometry of Wt and Tg cardiomyocytes treated with Dox. Results are presented as the mean ± SEM (n=4). *p<0.05 vs Dox treated Wt.

Doxorubicin promotes E2F6 loss in neonatal cardiomyocytes and HeLa

To estimate the effect of Dox on the disappearance of myc-E2F6 protein (derived from the transgene), NCM were isolated from Tg mice and treated with 0.5μM doxorubicin for 0 to 24hrs. Western blot analysis with anti-myc revealed that ~60% of the expressed myc-E2F6 protein was lost by 6 hours (p-value <0.05) and it was virtually undetectable in all samples 12hr post Dox exposure **(Figure 15A and 15B)**. Myc-E2F6 was also decreased in response to $CoCl_2$ (500μM), but there was increased variability between samples and overall was less than that observed in response to Dox **(Figure 15C, 15D, and 13B).**

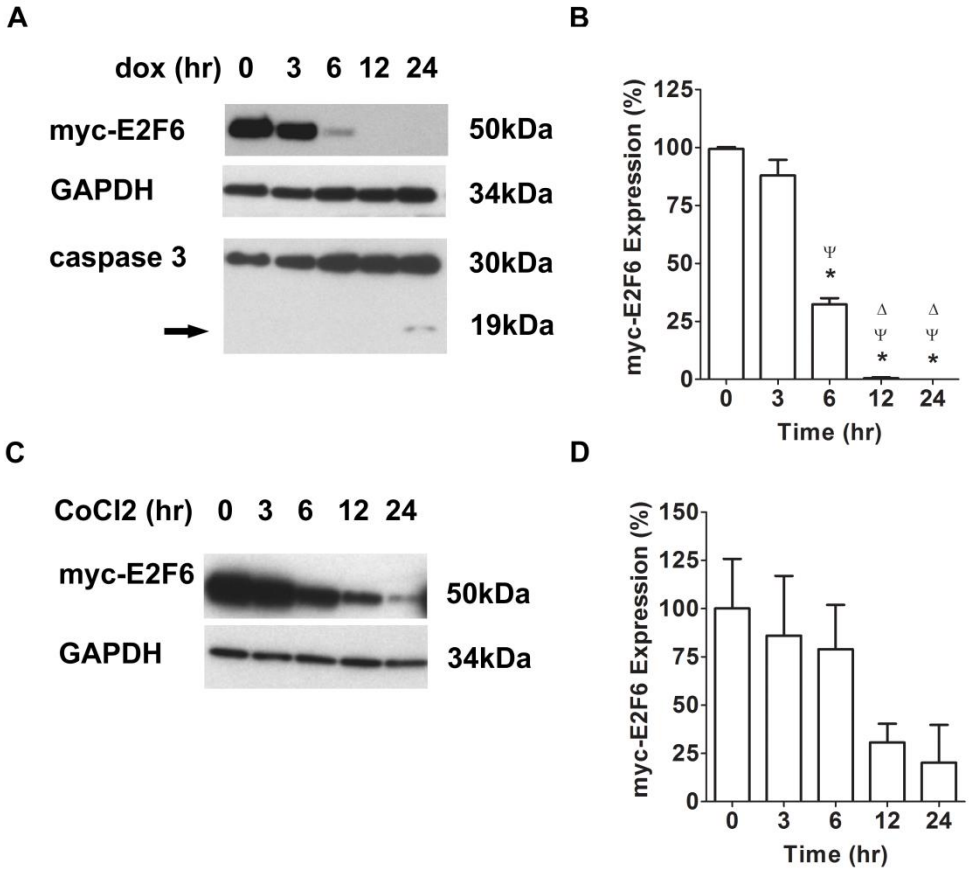

Figure 15. Transgenic *E2F6 protein is lost in response to apoptotic agents.* (A) Representative western blot of Tg NCM lysate treated with 0.5μM doxorubicin for 0-24 hours examined with anti-myc and anti-caspase 3. Cleaved caspase 3 is denoted by an arrow. GAPDH was used as a loading control. **(B)** Quantification of myc-E2F6 protein levels in response to doxorubicin. Results are presented as the mean ± SEM (n=3). *p<0.05 vs time 0. **(C)** Representative western blot of Tg NCM lysate treated with 500μM $CoCl_2$ for 0-24 hours examined with anti-myc. GAPDH was used as a loading control. **(D)** Quantification of myc-E2F6 protein levels in response to $CoCl_2$. Results are presented as the mean ± SEM (n=3). *p<0.05 vs time 0.

To determine if the effects on E2F6 were specific to cardiomyocytes or the transgene itself, we treated HeLa cells with Dox or $CoCl_2$ and examined endogenous levels of E2Fs. Doxorubicin exposure (24hr) led to the dose-dependent down-regulation of endogenous E2F6 protein in these cells **(Figure 16A and 16B)**. In contrast, the pro-apoptotic E2F1 was up-regulated in HeLa in response to doxorubicin treatment **(Figure 16A and 16B)**. $CoCl_2$ had no effect on endogenous E2F6 protein levels in HeLa while E2F1 protein levels were decreased **(Figure 16C and 16D)**.

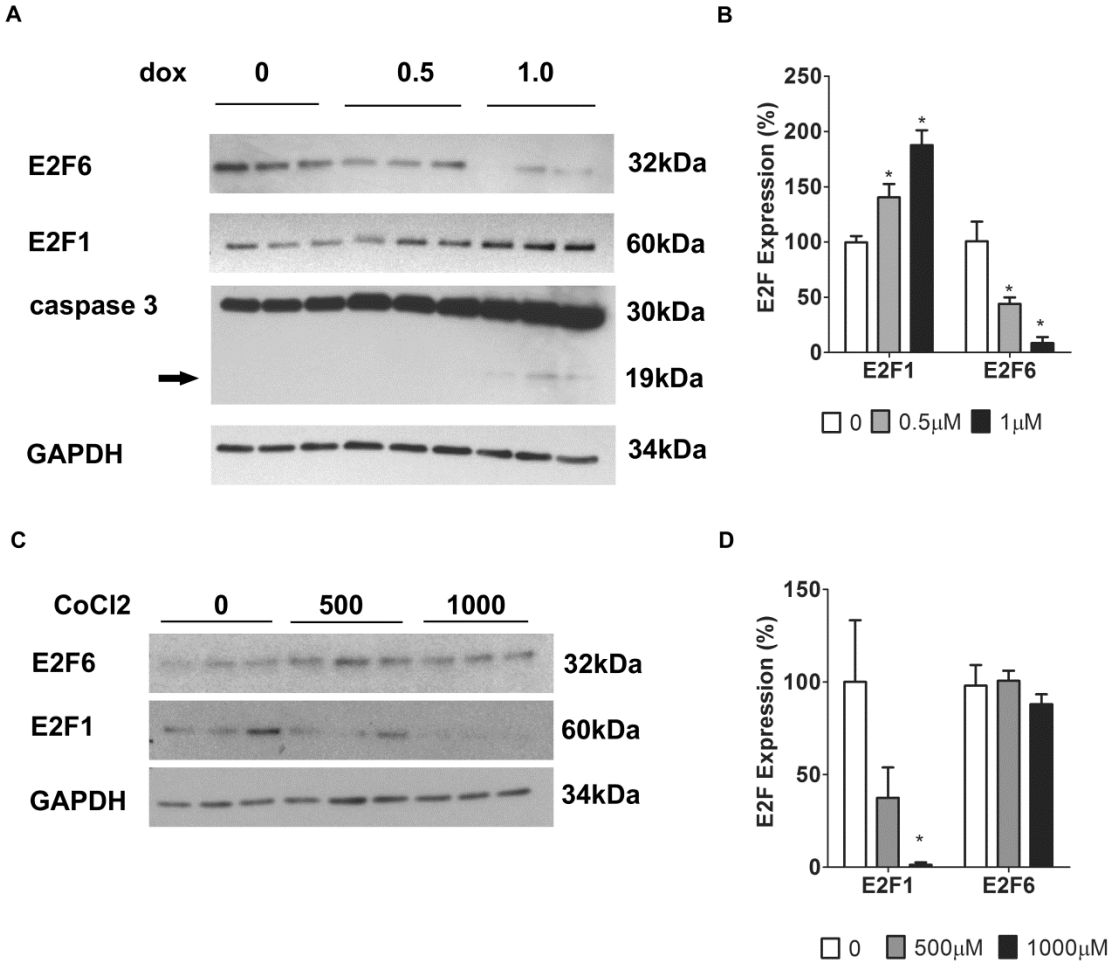

Figure 16. ***E2F6 and E2F1 protein levels are deregulated by apoptotic agents in HeLa cells.*** **(A)** Representative western blot of HeLa following 24hr treatment with the indicated amounts of doxorubicin examined with: anti-E2F6, anti-E2F1, and anti-caspase 3. Cleaved caspase 3 is denoted by an arrow. GAPDH was used as a loading control. **(B)** Quantification of E2F6 and E2F1 protein levels in HeLa in response to Dox. Results are presented as the mean ± SEM (n=3). *p<0.05 vs untreated. **(C)** Representative western blot of HeLa following 24hr treatment with the indicated amounts of $CoCl_2$ examined with anti-E2F6 and anti-E2F1. GAPDH was used as a loading control. **(D)** Quantification of E2F6 and E2F1 protein levels in HeLa in response to $CoCl_2$. Results are presented as the mean ± SEM (n=3). *p<0.05 vs untreated.

Dox promotes E2F6 down-regulation via post-transcriptional mechanisms

RT-qPCR was performed on RNA isolated from HeLa cells to determine if the Dox mediated deregulation of E2F6 and E2F1 were via transcriptional or post-transcriptional mechanisms. No significant changes in either *e2f6* or *e2f1* transcripts were observed in response to 0.5μM or 1μM doxorubicin **(Figure 17A)** suggesting that their levels are regulated post-transcriptionally in HeLa. Transcript levels of *e2f6* were not examined in response to $CoCl_2$ since the protein was stable.

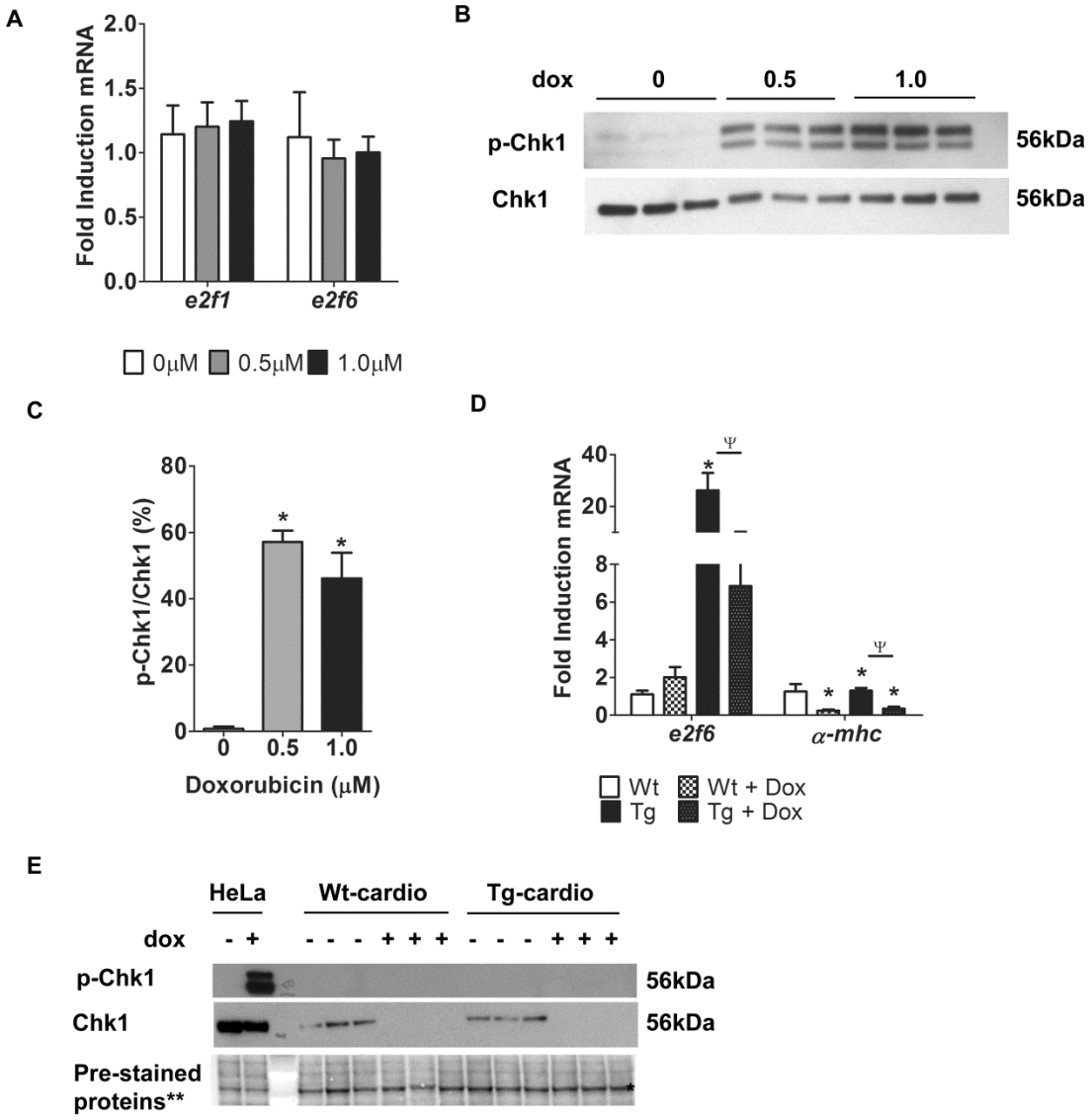

Figure 17. ***Mechanisms of E2F regulation in HeLa and cardiomyocytes.*** **(A)** Fold induction of *e2f1* and *e2f6* mRNA in HeLa following 24hr treatment with Dox. Fold inductions were calculated in reference to *gapdh*. Results are presented as the mean ± SEM (n=8). *p<0.05 vs untreated. **(B)** Western blot of HeLa lysate following 24hr treatment with doxorubicin examined with anti-Chk1 and anti-p-Chk1. **(C)** Quantification of p-Chk1/Chk1 in HeLa. Results are presented as the mean ± SEM (n=3). *p<0.05 vs untreated. **(D)** Fold induction of *e2f6* and *α-mhc* mRNA in Wt and Tg NCM

following 24hr treatment. Fold inductions were calculated in reference to *18S*. Results are presented as the mean ± SEM (n=6). *p<0.05 vs Wt untreated. ΨP<0.05 vs Tg untreated. **(E)** Western blot of Wt and Tg NCM lysate following 24hr treatment of doxorubicin examined with anti- Chk1 and anti- p-Chk1. ** Loading control is section of total protein on blot using pre-stained protein loading buffer (Instant Bands, EZ Biolab).

It was demonstrated that E2F6 is phosphorylated by the Checkpoint kinase (Chk1) following DNA replication stress which led to its dissociation from DNA. (121) Since Chk1 is also activated by DNA damage, (122) and its mRNA was upregulated in E2F6-Tg mice **(Figure 12)** we predicted that Chk1 might be involved in the post-transcriptional regulation of E2Fs by Dox. Western blot with anti-Chk1 in HeLa detected a polypeptide ~56kDa which was not altered by dox treatment **(Figure 17B)**. Western blot with anti-p-Chk1 (active) detected a doublet ~56kDa which showed a robust increase in response to Dox **(Figure 17B)**. The overall ratio of p-Chk1/Chk1 was significantly increased by Dox in HeLa **(Figure 17C)**.

We next examined NCM to determine the mechanism of E2F6 loss and if it was similar to that observed in HeLa. RT-qPCR indicated that E2F6-Tg NCM have ~26 fold higher levels of *e2f6* transcript due to the transgene (p<0.05), but this level drops to only six fold higher (p<0.05) following exposure to doxorubicin **(Figure 17D)**. In contrast, the level of endogenous *e2f6* in Wt-NCM did not significantly change in response to dox exposure **(Figure 17D)**. We next examined α-Myosin heavy chain (αMHC) transcript levels to determine if the E2F6 transgene was reduced due to a change in its promoter (αMHC). RT-qPCR revealed that the levels of *α-mhc* transcript were reduced by 80% in response to dox in both Wt and Tg NCM **(Figure 17D)**.

Western blot examination of Chk1 in NCM revealed that it is expressed at similar levels in Wt and Tg cells, but is not detectable following exposure to doxorubicin **(Figure 17E)**. The phosphorylated form of Chk1 was not detected in treated or untreated NCM **(Figure 17E)**.

E2F6 impacts differentiation to induce dilated cardiomyopathy

Our data in cardiomyocytes above and those reported by others in different cell types indicate that E2F6 has anti-apoptotic properties, which may explain why E2F6-Tg mice do not display the increased levels of apoptosis usually observed in DCM. Since apoptosis is not the underlying cause of DCM in Tg hearts we examined other mechanisms and noted that the G_2/M cyclin, cyclin-B1, was specifically down-regulated in E2F6-Tg myocardium implying a change in the cell cycle (117). Further analysis by western blot shows that the S phase cyclin, cyclin-E1, is up-regulated by ~4 fold (p-value <0.05) in E2F6-Tg pup hearts **(Figure 18A and 18B)**.

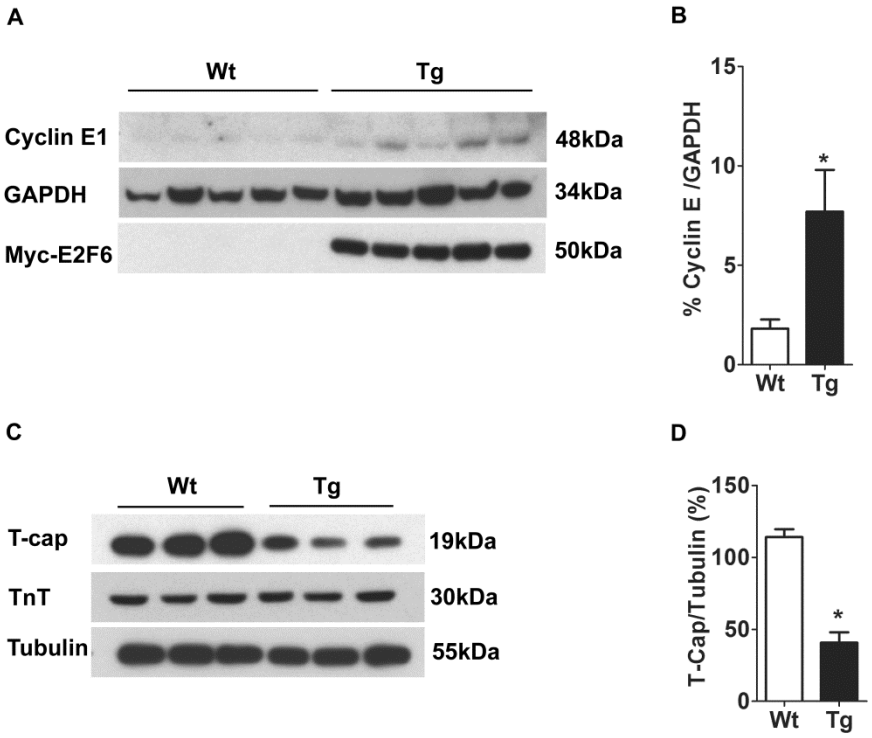

Figure 18. ***E2F6-Tg hearts show alteration in cell cyclins and cardiac proteins.*** **(A)** Representative western blot of Wt and Tg cardiac tissue examined with anti-cyclin-E1. GAPDH was used as a loading control. Myc-E2F6 represents E2F6 derived from the transgene. **(B)** Quantification of cyclin-E1 protein levels. Results are presented as the mean ± SEM. (n=5). *p<0.05 vs Wt. **(C)** Representative western blot of Wt and Tg cardiac tissue examined with anti-T-cap and anti-TnT. Tubulin was used as a loading control. **(D)** Quantification of T-cap protein expression. Results are presented as the mean ± SEM. (n=3). *p<0.05 vs Wt.

As changes in cell cycle dynamics can lead to changes in differentiation we examined cardiac specific gene expression in E2F6-Tg mice. Our initial microarray analysis predicted the down-regulation of the sarcomere protein, teliothenin, otherwise known as titin-cap (T-cap) (80).Western blot analysis with anti T-cap detects a

polypeptide ~19kDa which is down-regulated by ~70% in E2F6-Tg myocardium ($p<0.05$) **(Figure 18C and 18D)**. No change was observed in another sarcomere protein, Troponin-T (TnT), levels in E2F6 hearts **(Figure 18C)**.

Discussion

The E2F pathway is known to critically regulate proliferation, apoptosis, and differentiation thus it has been studied extensively in cancer biology in terms of inhibiting growth and increasing death in tumors. In fact, almost all cancers are associated with aberrant E2F/Rb activity. (123,124) Less is known about how the E2F pathway affects apoptosis in the myocardium, and even less is known about how the atypical E2Fs, such as E2F6, contribute to apoptosis in the heart. In recent studies we manipulated the E2F/Rb pathway *in vivo* in the postnatal heart by expressing the repressor E2F6 (80,117,118).While the E2F pathway was deregulated and the mice presented with DCM, there was surprisingly no significant increase in apoptosis which is normally a hallmark of the disease. In the current study we find that E2F6 confers some resilience towards cobalt chloride induced apoptosis in cardiomyocytes, but not to doxorubicin. This specific protection appears to be related to the levels of E2F6 protein (derived from the transgene) which are more profoundly downregulated following doxorubicin exposure compared with $CoCl_2$ thereby suggesting that E2F6 may serve to protect. In HeLa cells Dox differentially impacts endogenous levels of the E2Fs by upregulation of the pro-apoptotic E2F1 while downregulating E2F6. By contrast, $CoCl_2$ treatment in HeLa caused no change in E2F6 and decreased the levels of apoptotic-E2F1 implying protection.

Mechanism of E2F deregulation during apoptosis

It does not appear that E2F6 levels are decreased by caspase 3 given that its down-regulation in both HeLa and cardiomyocytes occurs prior to the activation of the protease. It was demonstrated that E2F6 is phosphorylated by the Chk1 kinase (in response to DNA replication stress) which resulted in its inability to bind to gene promoters and an increase in E2F1 activity. (121) In our study we found that the activation status of Chk1 (p-Chk1) is increased in HeLa in response to Dox at the same time as E2F6 is down-regulated and E2F1 is up-regulated. Thus it is possible that Chk1 plays a part in E2F deregulation in response to Dox. In support, Chk1 and Chk2 were demonstrated to phosphorylate and stabilize E2F1 promoting apoptosis. (125,126) Furthermore, endogenous *e2f6* transcript levels remain unaltered in both HeLa and Wt-NCM suggesting it is normally regulated at the post-transcriptional level.

Although Chk1 has the potential to regulate E2F in HeLa, it does not appear to do so in myocardium, as it is down-regulated in response to Dox in both Wt and Tg NCM. Instead, myc-E2F6 protein levels are reduced via transcriptional mechanisms which are likely related to the 80% reduction in *α-mhc* transcript since the transgene is under control of its promoter.

E2F6 protects cardiomyocytes from apoptosis via multiple mechanisms during cardiac development

In our previous studies we uncovered the activation of a survival pathway involving β_2-AR, c-src, ERK, and the 100-fold increase in Bcl2, supporting the notion that E2F6 may confer resilience against cell death in the heart (118). In culture the overall

Bax/Bcl2 ratio was decreased in Tg NCM in response to dox, but without drug treatment there was no difference in Bcl2 levels. The discrepancy in Bcl2 levels can be attributed to that fact that the β_2-AR survival pathway is likely only induced later on in E2F6-Tg myocardium to compensate and protect against the stretch caused by DCM. In support of this we did not observe the activation of the stretch sensitive c-src in neonatal Tg hearts **(Appendix 2: Sup Fig 3)**.

E2F6 induces DCM via deregulation of cell cycle not apoptosis

In cultured cardiomyocytes E2F6 likely protects via inhibition of E2F1 as was previously demonstrated in HEK-293 cells. (75,74) In older neonates we observed the activation of a DNA replication and repair gene profile. This activation could reflect a cell survival pathway and/or a defect in the cell cycle, which is supported by the observed changes in cyclin E and B1. A delay in cell cycle re-entry was observed in NIH-3T3 cells over-expressing E2F6 following serum starvation implying that E2F6 does have the capacity to alter cell cycle dynamics. (16)

Thus the DCM initiated by E2F6 appears to be related to changes in differentiation program which impacts the function of critical proteins such as connexin-43, involved in cardiomyocyte communication, and BDH1, involved in metabolic signaling (80,117). Our data here further support this notion since the muscle specific T-cap, involved in contraction, was significantly downregulated by E2F6. This is particularly notable as mutations in T-cap as well as the proteins it interacts with (titin and CSRP-encoded muscle LIM protein) are detected in human dilated and hypertrophic cardiomyopathy. (127,128) Any defect in differentiation is likely linked to the down-

regulation of E2F3 in Tg myocardium (80,118), and the displacement of Rb (which cannot interact with E2F6), which normally represses E2F gene expression during cardiac and skeletal muscle development. (35,129,130,47)

Conclusions

In summary, the data here support a role for E2F6 levels in cardiac cell survival and the potential for protection in drug induced cell death. Our data is consistent with findings in other cell types where E2F6 has been implicated in attenuating apoptosis. The data suggests multiple mechanisms by which E2Fs modulate cell growth, survival and function in early and postnatal cardiac development.

Sources of Funding

This work was supported by an operating grant (540033) from the Heart and Stroke Foundation of Canada to BST.

Conflict of Interest

None declared.

CHAPTER 3:

"E2F6 Impairs Glycolysis and Activates BDH1 Expression Prior to Dilated Cardiomyopathy"

Major JL, Dewan A, Salih M, Leddy JJ, and Tuana BS. (2017) PLOS ONE.12 (1): e0170066.

Author contributions: JL Major collected, analyzed data, and prepared the manuscript. Aaraf Dewan aided in performing the Seahorse fatty acid and glucose oxidation experiments and their data analysis. Technical support and advice were given by Maysoon Salih. Dr. John Leddy aided in statistical analysis of Figure 23 and editing. All experiments, data analysis, and manuscript preparation were done under the supervision of BS Tuana.

Abstract

Rationale- The E2F pathway plays a critical role in cardiac growth and development, yet its role in cardiac metabolism remains to be defined. Metabolic changes play important roles in human heart failure and studies imply the ketogenic enzyme β-hydroxybutyrate dehydrogenase I (BDH1) is a potential biomarker.

Objective- To define the role of the E2F pathway in cardiac metabolism and dilated cardiomyopathy (DCM) with a focus on BDH1.

Methods and Results- We previously developed transgenic (Tg) mice expressing the transcriptional repressor, E2F6, to interfere with the E2F/Rb pathway in post-natal myocardium. These Tg mice present with an E2F6 dose dependent DCM and deregulated connexin-43 (CX-43) levels in myocardium. Using the Seahorse platform, a 22% decrease in glycolysis was noted in neonatal cardiomyocytes isolated from E2F6-Tg hearts. This was associated with a 39% reduction in the glucose transporter GLUT4 and 50% less activation of the regulator of glucose metabolism AKT2. The specific reduction of cyclin B1 (70%) in Tg myocardium implicates its importance in supporting glycolysis in the postnatal heart. No changes in cyclin D expression (known to regulate mitochondrial activity) were noted and lipid metabolism remained unchanged in neonatal cardiomyocytes from Tg hearts. However, E2F6 induced a 40-fold increase of the *Bdh1* transcript and 890% increase in its protein levels in hearts from Tg pups implying a potential impact on ketolysis. By contrast, BDH1 expression is not activated until adulthood in normal myocardium. Neonatal cardiomyocytes from Wt hearts incubated with the ketone β-hydroxybutyrate (β-OHB) showed a 100% increase in CX-43 protein

levels, implying a role for ketone signaling in gap junction biology. Neonatal cardiomyocyte cultures from Tg hearts exhibited enhanced levels of BDH1 and CX-43 and were not responsive to β-OHB.

Conclusions- The data reveal a novel role for the E2F pathway in regulating glycolysis in the developing myocardium through a mechanism involving cyclin B1. We reveal BDH1 expression as an early biomarker of heart failure and its potential impact, through ketone signaling, on CX-43 levels in E2F6-induced DCM.

Introduction

The failing heart shows transcriptional and metabolic remodeling which may have detrimental effects on cardiac function (59,131). Given the extensive energy requirements of the heart, and its limited ATP reserve, understanding the mechanisms which regulate cardiac metabolism is critical to the understanding of heart function and failure (132,62). In the normal adult heart, fatty acid oxidation accounts for up to 90% of the ATP production while glycolysis supplies the remainder. (61). The heart shows a remarkable capacity to adapt to substrate utilization under stress. In the failing heart, a reduction of fatty acid oxidation and changes in glycolysis are observed (61,63). It was recently demonstrated that there is an increase in ketone metabolism and the ketogenic enzyme, β-hydroxybutyrate dehydrogenase 1 (BDH1), in human and mouse heart failure (133,134,66,65).

Ketones are synthesized in the liver and exist in three main forms: β-hydroxybutyrate (β-OHB) the most stable and abundant form, acetoacetate, and acetone (135). Ketone bodies arise from the incomplete oxidation of long chain fatty acids. They

are utilized as an alternative energy source when glucose is scarce, such as during fasting, exercise, and in many disease states such as diabetes (135,136). Glucose is a vital nutrient source in the developing heart and during heart failure, thus ketones could be an important alternative energy source during metabolic stress (59). It is therefore critical to understand how the heart uses ketones to adapt to substrate utilization during cardiac development and disease.

The E2F family is a group of nine transcription factors which regulate cell proliferation, hypertrophy, and death (113,68). Recently, the transcriptional activator, E2F1, has been demonstrated to promote glycolysis via regulation of the pyruvate dehydrogenase kinase (PDK4) and inhibition of histone deacetylases (HDACS) to regulate metabolism (137,138,139,140). In association with its modulator, Retinoblastoma protein (Rb), E2F1 can also repress oxidative phosphorylation (141,142). E2F6 is a unique E2F family member which is believed to repress E2F responsive genes independently of Rb (27,20). We previously examined the contribution of the E2F pathway in post-natal mouse myocardium by cardiac specific expression of E2F6 which led to the early-onset of dilated cardiomyopathy (DCM) without hypertrophy or apoptosis (80). Contrary to expectation, E2F6-Tg mice showed activation of E2F responsive genes (80). This was achieved via down-regulation of E2F3 (critical for cardiac development) and competitive binding at E2F sites which are normally repressed via E2F/Rb in the post-natal heart (143,75,27). In essence, E2F6 serves as a dominant negative of E2F/Rb in the heart.

E2F6-Tg mice display an early reduction in connexin-43 (CX-43) and reduced conductivity which is a hallmark of DCM and heart failure (35). Here we further examine

the changes in the post-natal myocardium of E2F6-Tg mice with the view to define early bio-markers and novel pathways which may be useful for understanding and treating idiopathic DCM. We note the early induction of BDH1 in neonatal Tg myocardium and a relationship between ketones and CX-43 expression in cardiomyocytes. We further note that deregulation of the E2F pathway impairs glycolysis which may have triggered the induction of BDH1 and the resulting changes in CX-43 leading to DCM.

Methods

Mice and Genotyping

Previously described Tg mice with cardiac specific expression of E2F6 (under control of the α-Myosin heavy chain promoter) (B6C3F1) were bred with WT (B6C3F1) mice (80). All animal work was conducted according to the University of Ottawa's institutional animal care committee guidelines. The protocols were approved by the University of Ottawa's institutional animal care committee: cmm-1725, cmm-1723. All possible steps were taken to ameliorate animal suffering. Mouse pups were euthanized by decapitation. Adult mice were euthanized via carbon dioxide inhalation. Approximately 110 mice were used in this study. This number was required in order to obtain sufficient sample size for appropriate biochemical and statistical analyses.

Genotyping was performed via DNA extraction from mouse ear (adult) or tail (pup) clip and PCR using the Phire Tissue Direct (Thermo Scientific) kit as per the manufacturer's instructions. Primers spanning the 6^{th} intron of E2F6 were used (ATCACAGTACATATTAGGAGCAC- sense, and GGTGCGGCTACCAGTCTACA–

anti-sense) which result in the amplification of a long fragment (988bp) in Wt mice and a long and short fragment (342bp) in Tg mice which were separated on a 1.3% agarose gel.

RNA Analyses

RNA was extracted from cardiac lysate at post-natal day 7 using the RNEasy Fibrous Tissue Mini Kit as per the manufacturer's protocol (Qiagen). First-strand cDNA was synthesized from 2μg RNA and oligoDT with SuperScriptII reverse transcriptase (Invitrogen) as per the manufacturer's protocol. qPCR was performed in the q-Rotor (Qiagen) using Fast Start SYBR Green (Roche) according to the manufacturer's instructions. Gene expression was normalized against *Gapdh*, and fold inductions were calculated using the $\Delta\Delta C_t$ method. Primer pairs used for qPCR are: *Bdh1*: AAGCACTGGAAGCAGACACAT (sense), ACACTTAGGGCTTTTCCTGGG (anti-sense), *Oxct1*: CTGGAGTTTGAGGACGGCAT (sense), TCCGCATCAGCTTCGTCTTT (anti-sense), *GLUT4*: GCAGATCGGCTCTGACGATG (sense), GCCACGTTGCATTGTAGCTC (anti-sense), and *Gapdh*: GCAGTGGCAAAGTGGAGATT (sense) and TCTCCATGGTGGTGAAGACA (anti-sense).

Western Blot

Neonatal cardiomyocytes were rinsed twice with PBS and frozen at -80^{o}C. Plates were thawed on ice in RIPA (50mM Tris (pH 7.4), 1mM EDTA, 150μM NaCl, 0.25% deoxycholic acid, 1% NP-40) containing protease and phosphatase inhibitors (Roche). Plates were scraped and lysates were syringed with a 21G needle. Cardiac lysates were

prepared with an electric tissue homogenizer in RIPA with protease and phosphatase inhibitors.

Cardiac and cell lysates were centrifuged at 12800g for 10min at 4^{o}C. Protein concentrations were determined using the BCA assay (Thermo Scientific). Lysates (13-50ug) were run on gradient (5-15%) SDS-PAGE gels in 3X loading dye (Cell Signaling). Gels were transferred to PVDF membrane (Millipore) in transfer buffer (25mM Tris, 190mM Glycine, 20% methanol) overnight at 4^{o}C. Membranes were blocked in TBST (1M Tris, 290mM NaCl, 0.1% Tween, pH7.2) with 5% milk. The blots were probed with primary and secondary antibodies (listed below) which were diluted in TBST with 5% milk. The conversion of ECL substrate (Roche) was detected on film. Band signal intensities were quantified by densitometry using Image Lab Software4.0.1 (Bio-Rad).

The following primary antibodies were used: GLUT4 (2213, 1:1000), AKT2 (6063, 1:1000), p-AKT2 (ser 479) (8599, 1:1000), cyclin D1 (2978, 1:1000), cyclin D3 (2936, 1:2000), and cyclin B1 (4138, 1:1000) were purchased from Cell Signaling, BDH1 (MA5-15594, 1:1000) and GAPDH (MA5-15738, 1:5000) were purchased from Thermo Scientific, CX-43 (ab11370, 1:100000) was purchased from Abcam, OXCT1 (12175-1-AP , 1:10000) was purchased from Proteintech, and myc (which detects myc-tagged E2F6) (11667149001, 1:2000) was purchased from Roche. Secondary antibodies anti-mouse (115-035-003, 1:15000) and anti-rabbit (111-035-045, 1:15000) were purchased from Jackson Immunochemicals.

Neonatal Cardiomyocyte Isolation and Treatment

Hearts were collected from Wt and Tg mice at post-natal day 1 following decapitation. Hearts were rinsed in HBSS and incubated in 0.5% trypsin dissolved in HBSS overnight at 4^{o}C while genotyping was performed. Hearts were grouped in twos or threes (by genotype) for digestion with 0.5% Collagenase type II (Gibco) dissolved in HBSS (4x10min). Cells were collected after each digestion via centrifugation at 3000g for 3 minutes and resuspended in DMEM supplemented with 10% FBS, 1% penicillin/streptomycin, and 1% non-essential amino acids. Total suspensions were plated on uncoated 10cm dishes to remove fibroblasts (45min x2). Cardiomyocytes were seeded onto 0.1% gelatin coated plates (300000/well on XF^{e}24 well plate for Seahorse metabolic analysis, or 1x10^{6}/well on 6 well plates for ketone treatment) and allowed to attach for 48 hours in a 37^{o}C incubator with 5% CO_2.

Paired neonatal cardiomyocytes were treated with or without 3.8mM β-hydroxybutyrate (Sigma) dissolved in water for 24 hours, or used for glycolysis and fatty acid oxidation measurements (described below).

Seahorse Glycolysis Measurement

Cardiomyocyte media was replaced with bicarbonate and glucose free DMEM containing 2mM glutamine. The extracellular acidification rate (ECAR) was measured using an XF^{e}24 Extracellular Flux Analyzer (Seahorse Bioscience). Triplicate pre-injection readings were taken to establish a baseline, followed by triplicate reading after sequential treatment with 20mM glucose, 2mg/mL oligomycin, and 100mM 2-deoxy-glucose. ECAR was corrected to baseline pre-injection measurements.

Seahorse Fatty Acid Oxidation Measurement

Cardiomyocytes were starved for 24hr in substrate limited medium (DMEM, 0.5mM glucose, 1.0mM Glutamine, 0.5mM L-carnitine, 1% FBS) and replaced with fatty acid oxidation assay medium (111mM NaCl, 4.7mM KCl, 1.25mM $CaCl_2$, 2.0mM $MgSO_4$, NaH_2PO_4, 2.5mM glucose, 0.5mM L-carnitine, and 5mM HEPES). Cardiomyocytes were treated with or without 40μM etomoxir for 15min. The oxygen consumption rate (OCR) was measured using the XF^e24 Extracellular Flux Analyzer (Seahorse Bioscience). Triplicate pre-injection readings were recorded to establish baseline and cardiomyocytes were sequentially treated with either 17μM BSA or 100 μM palmitate conjugated to BSA and: 2mg/mL oligomycin, 1μM Carbonyl cyanide-4-trifluoromethoxy phenylhydrazone, and 1μM Antimycin-A. OCR was corrected to baseline pre-injection measurements.

Statistical Analyses

All data were analyzed with a student t-test with the exception of the protein expression data in **(Figure 23D)** which was analyzed with a two way mixed ANOVA with repeated measures. The level of significance was set at $P<0.05$ in all cases.

Results

E2F6 Induces the Early Expression of BDH1 in Neonatal Myocardium

E2F6 expression in postnatal myocardium led to dose dependent DCM associated with decreased levels of CX-43 (80). Our previous microarray results predicted the up-regulation of *Bdh1* in E2F6-Tg hearts thus we performed RT-q-PCR on mRNA collected

from Wt and Tg pup hearts for validation. A 40 fold increase of *Bdh1* transcript was detected in Tg myocardium ($P<0.05$) **(Figure 19A)**. BDH1 protein was barely detectable in Wt pup hearts but was markedly upregulated by 890% ($P<0.05$) in E2F6 Tg hearts at post-natal day 1 (P1) **(Figure 19B and 19C)**. Since BDH1 is up-regulated in the failing adult human heart (65) we examined its expression at 6 weeks of age, at which time Tg mice show full onset of DCM (118). Western blot analysis did not reveal any difference in BDH1level between Tg and Wt hearts at this time **(Figure 19B and 19C)**.

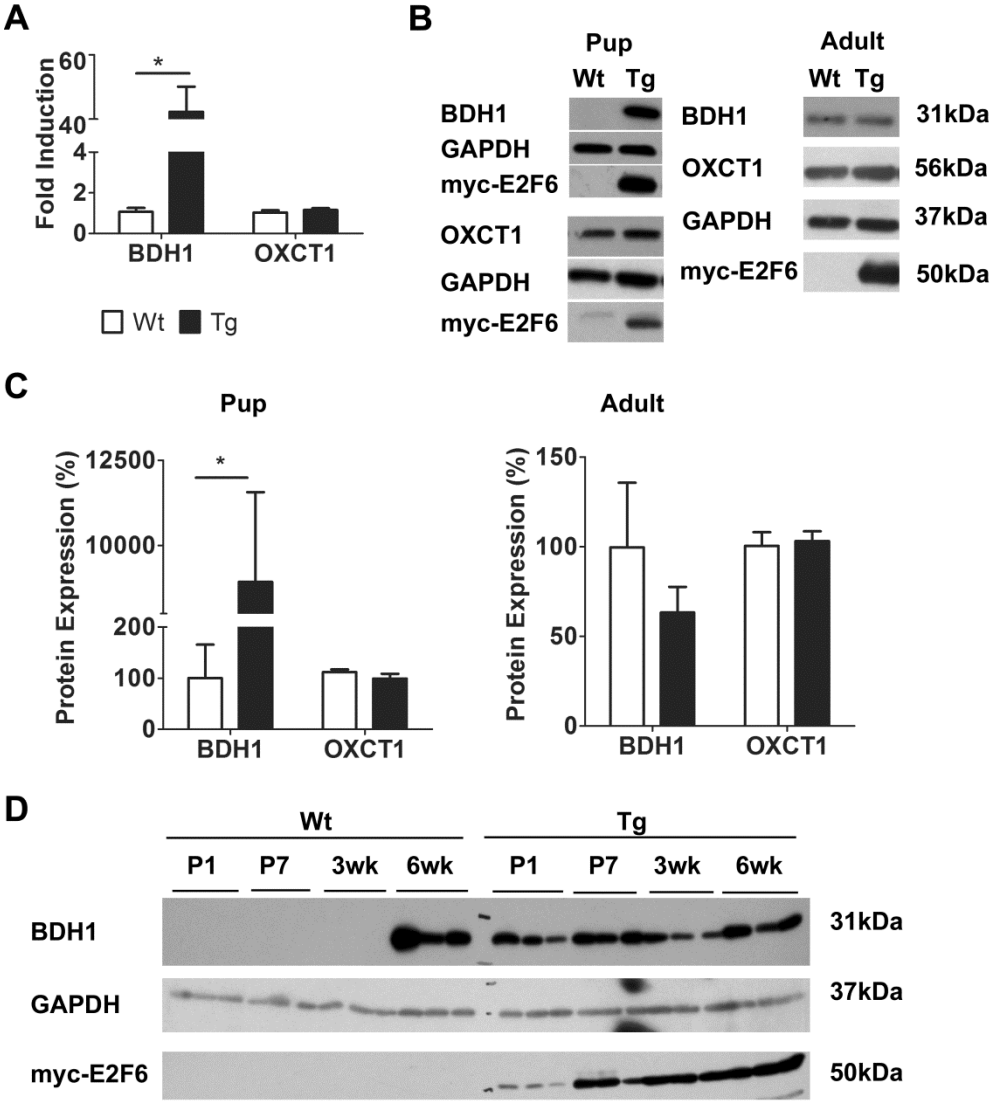

Figure 19. ***E2F6 Activates BDH1 Expression in Neonatal Myocardium.*** (**A)** *Bdh1* (β-hydroxybutyrate dehydrogenase 1) and *Oxct1* (succinyl-CoA: 3-oxoacid-CoA transferase) transcript levels in Wt and Tg myocardium 7 days after birth. Expression is normalized to *Gapdh*. Results represent mean±SEM values (n=5-7). (**B)** Representative immunoblots of protein from Wt and Tg mouse myocardium at post-natal day 1 (pups) and 6wks of age (adult) examined with the anti-BDH1 and anti-OXCT1. (**C)** Densitometric quantification of BDH1 and OXCT1 expression from immunoblots. Expression is normalized against GAPDH. Results represent mean±SEM values (n=4). (**D)** Immunoblot of protein from Wt and Tg myocardium with BDH1 at the indicated time points after birth.*$P<0.05$.

We next examined the developmental expression of BDH1 protein in post-natal myocardium between P1 and 6wks. In normal developing myocardium BDH1 protein is undetectable at P1 and appears at 6 weeks of age **(Figure 19D)**. On the other hand, in E2F6-Tg hearts, BDH1 expression appears to be maximally expressed as early as P1 with this level maintained at P7, 3 weeks, and 6 weeks. It should be noted that symptoms of DCM arise as early as 2 weeks in E2F6-Tg mice (118), thus BDH1 is markedly elevated prior to the early development of DCM and maintained at this level into adulthood **(Figure 19D)**.

The induction of BDH1 expression by E2F6 was specific since the succinyl CoA: 3-oxoacid CoA transferase (OXCT1) (another rate limiting enzyme in ketone metabolism) was not changed at the mRNA **(Figure 19A)** or protein level in heart tissue from pup or adult E2F6-Tg mice **(Figure 19B and 19C)**.

E2F6 Impairs Glycolysis in Neonatal Cardiomyocytes

Since ketone metabolism is increased when glucose is scarce, we measured glycolysis in in Tg mice to gauge whether changes in glycolytic rates may have stimulated BDH1 expression. We used the Seahorse method to monitor the extracellular acidification rate (ECAR) as a measure of glycolysis which produces lactic acid. In nutrient starved neonatal cardiomyocytes (pre-injection) ECAR measurements were similar in Wt and Tg, but Tg ECAR readings were lower following the addition of glucose and oligomycin (inhibitor of ATP synthase that drives glycolysis) **(Figure 20A)**. The competitive inhibitor of glucose, 2-Deoxy-glucose (2-DG), caused the ECAR readings to return to baseline in both Wt and Tg cardiomyocytes demonstrating the specificity of the experiment to glucose **(Figure 20A)**. Calculation of basal glycolysis revealed a 22% decrease in E2F6 expressing cardiomyocytes ($P<0.05$) **(Figure 20B)**. No significant changes in glycolytic capacity or reserve were noted.

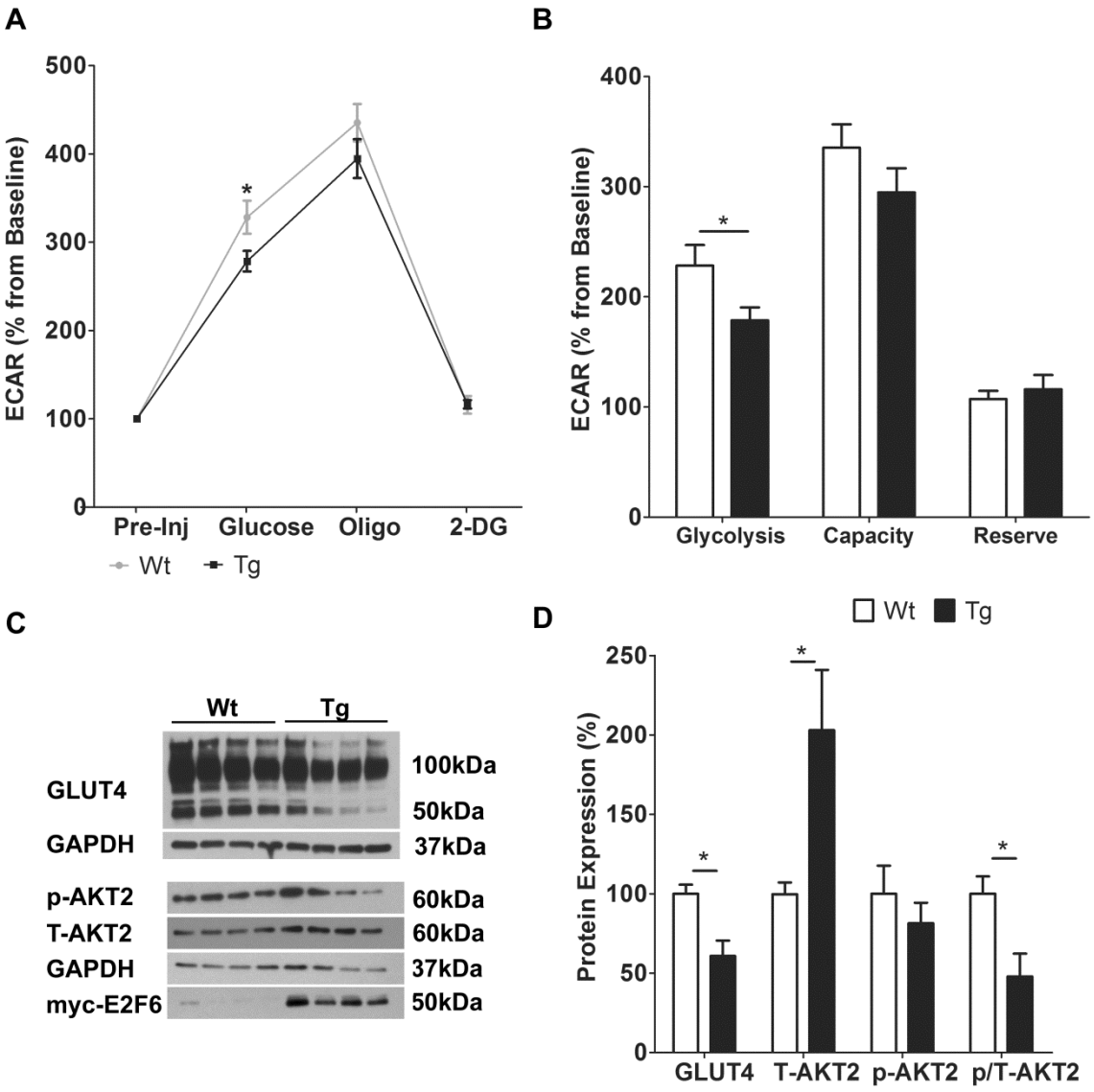

Figure 20. ***E2F6 Impairs Glycolysis in Neonatal Cardiomyocytes.*** (**A)** Glycolytic rates for Wt and Tg neonatal cardiomyocytes pre-injection, and following the sequential addition of: glucose, oligo (oligomycin), and 2-DG (2-deoxy glucose). ECAR (extracellular acidification rate) is normalized against pre-injection rates. Results represent mean±SEM values (n=8). (**B)** Glycolytic measurements (basal glycolysis, glycolytic capacity, glycolytic reserve) in Wt and Tg neonatal cardiomyocytes. (**C)** Representative immunoblot analyses of protein extracts from Wt and Tg myocardium at

postnatal day 1 with anti: GLUT 4 (glucose transporter 4), T-AKT2 (total protein kinase B), and p-AKT2 (phospho (ser 474)- protein kinase B). (**D)** Densitometric quantification of immunoblots. Expression is normalized against GAPDH (n=4). *$P<0.05$.

Glucose entry into cardiomyocytes is a rate limiting step in glycolysis, thus we examined changes in the cardiac glucose transporter: GLUT4.Western blot analysis of protein isolated from Wt and Tg myocardium at P1 with anti-GLUT4 detected a GLUT4 monomer of ~50kDa and high molecular weight polypeptides which are GLUT4 oligomers **(Figure 20C)**. Quantification of all polypeptides revealed a 39% decrease in total GLUT4 protein ($P<0.05$) (Fig 2D). RT-q-PCR revealed no change in *GLUT4* transcript levels in Tg myocardium **(Appendix 3: Sup Fig 4)** indicating its loss is post-transcriptional.

We also examined the expression of another major regulator of glucose metabolism: AKT2 (also known as protein kinase B). Western blot analysis with anti-total AKT2 (T-AKT2) revealed a 100% increase in E2F6-Tg hearts ($P<0.05$), while analysis of phosphorylated (active) AKT2 revealed no change **(Figure 20C and 20D)**. The ratio of phospho: total AKT2 was decreased by ~50% ($P<0.05$) in Tg myocardium indicating less AKT2 activation as a fraction of the total AKT2 pool **(Figure 20D)**.

E2F6 Does Not Impact Fatty Acid Oxidation in Neonatal Cardiomyocytes

In the failing human heart the up-regulation of BDH1 is believed to be an adaptation to a decrease in lipid metabolism (134,66). Thus, we also assessed lipid metabolism in neonatal cardiomyocytes from Wt and Tg mice. We used the seahorse method to measure the oxygen consumption rate (OCR) which revealed no change in

fatty acid oxidation in E2F6-expressing cardiomyocytes at pre-injection, or following the sequential addition of palmitate (fatty acid), oligomycin (inhibitor of ATP synthase), Carbonyl cyanide-4-phenylhydrazone (FCCP/uncoupler) or antimycin-A (electron transport chain inhibitor) **(Figure 21)**. Cardiomyocytes treated with etomoxir (inhibitor of fatty acid entry) showed no significant increase in OCR beyond baseline, thereby demonstrating the specificity of the experiments to fatty acids **(Appendix 3: Sup Fig 5)**.

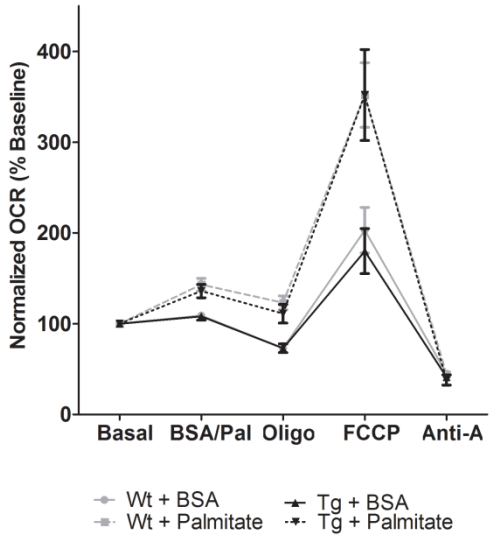

Figure 21. ***E2F6 Does Not Impact Fatty Acid Oxidation in Neonatal Cardiomyocytes.*** Oxygen consumption rate (OCR) in Wt and Tg neonatal cardiomyocytes following 24hr glucose starvation. Results were normalized against baseline (pre-injection). Cardiomyocytes were sequentially incubated with BSA or palmitate, oligo (oligomycin), FCCP (Carbonyl cyanide-4-phenylhydrazone), and Anti-A (Antimycin-A). Results represent mean±SEM values (n=7-8).

E2F6 Deregulates Cyclin Expression in Myocardium

The E2F/Rb pathway is believed to drive glycolysis via the transcriptional regulation of cyclins (144). Thus, we examined the expression of various cyclins in Wt and Tg myocardium at post-natal day 1. Cyclin D1 and D3 expression levels were not altered in cardiac tissue from E2F6-Tg mice **(Figure 22A)** while cyclin B1 was reduced by 70% in E2F6-Tg myocardium (P<0.05) **(Figure 22A and 22B)**.

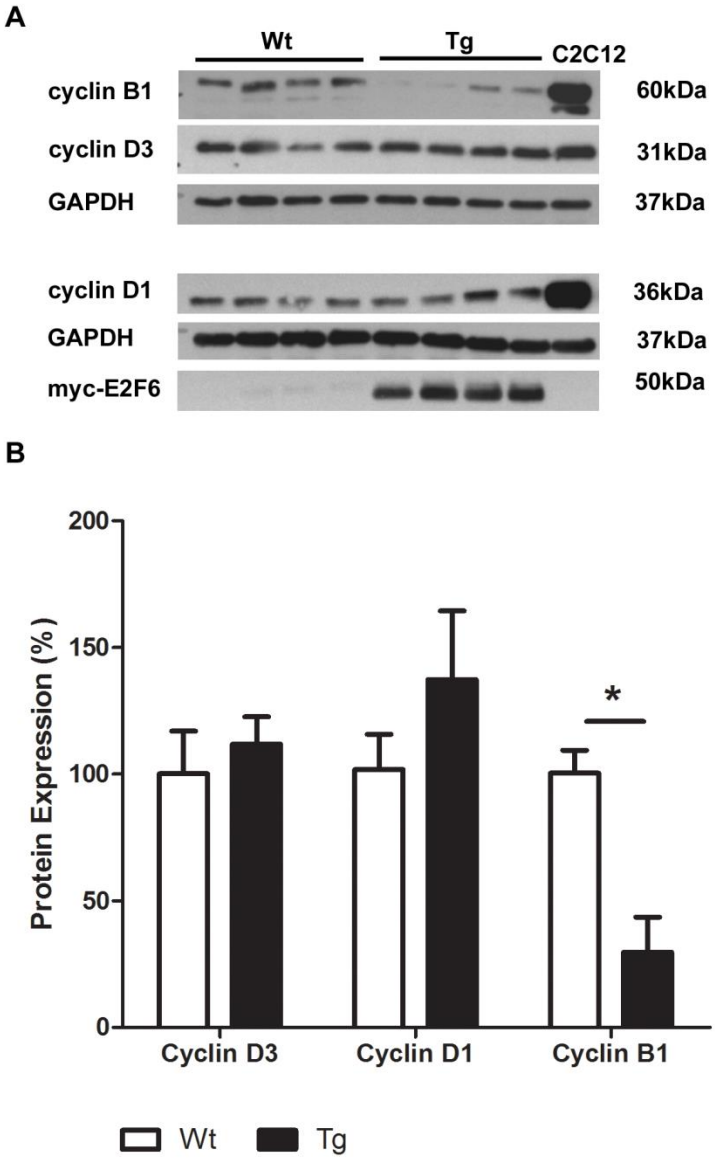

Figure 22. ***E2F6 Deregulates Cyclin B1 Expression in Myocardium.*** (**A)** Representative immunoblot of protein isolated from Wt and Tg myocardium at post-natal day 1 with anti- cyclin D1, anti-cyclin D3, and anti-cyclin B1. (**B)** Densitometric quantification of cyclin immunoblots. Expression is normalized against GAPDH. Results represent mean±SEM values (n=4). *$P<0.05$.

Ketones Regulate Connexin-43 in Neonatal Cardiomyocytes

Recent evidence indicates that ketones can enhance CX-43 protein in endothelial cells via the Extracellular Receptor Kinase (ERK) pathway (145). We previously noted the deregulation of ERK activity and a loss of CX-43 protein in adult Tg mice (80), and in the present study we detected a 50% down-regulation of CX-43 protein at post-natal day 1 ($P<0.05$) **(Figure 23A and 23B)**.

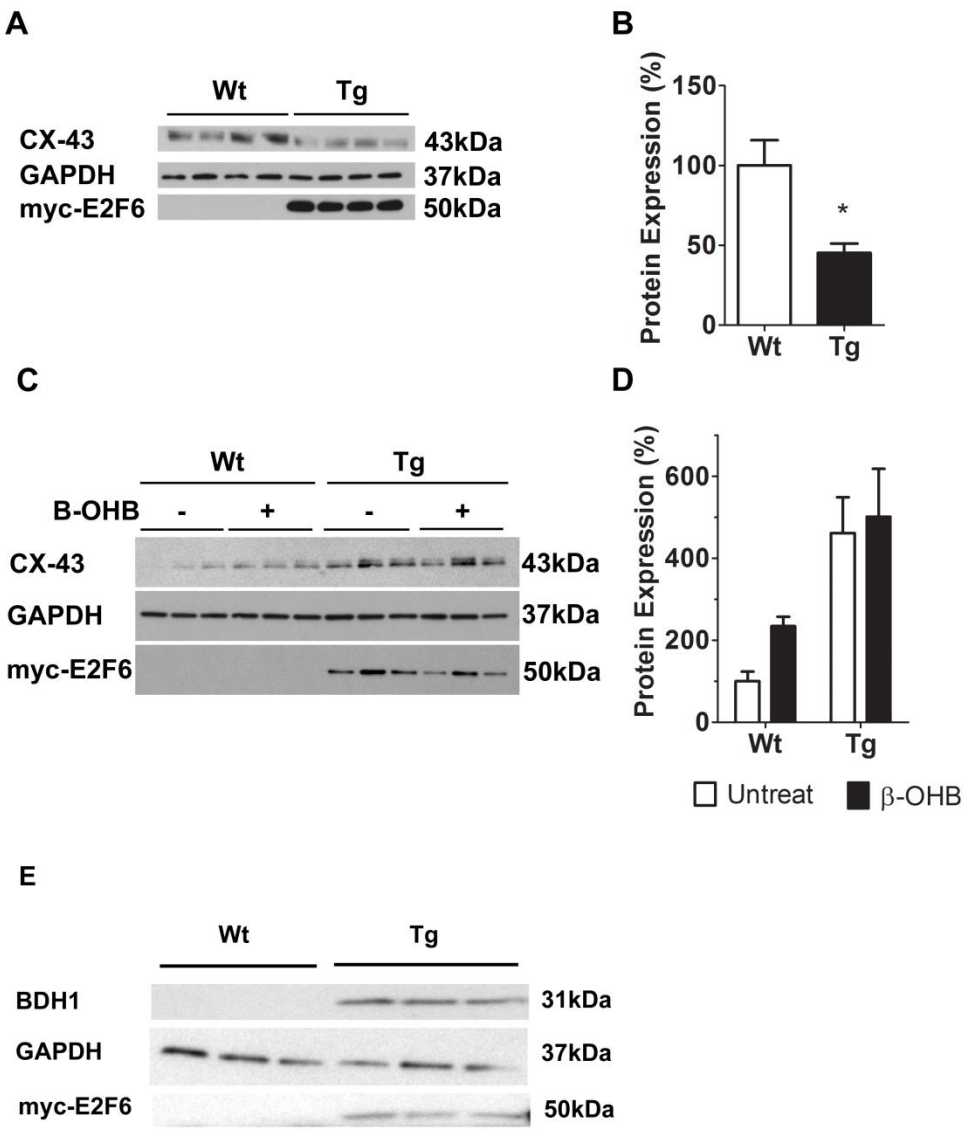

Figure 23. ***β-OHB Regulates CX-43 Protein Expression in Neonatal Cardiomyocytes.*** (**A)** Representative immunoblot of protein isolated from Wt and Tg myocardium at post-natal day 1 with anti-CX-43. (**B)** Densitometric quantification of CX-43 immunoblot. Expression is normalized against GAPDH. Results represent mean±SEM values (n=4). (**C)** Representative immunoblot analyses of protein from Wt and Tg neonatal cardiomyocytes following incubation with or without β-OHB (β-hydroxybutyrate). (**D)** Densitometric quantification of CX-43 in treated and non-treated neonatal

cardiomyocytes. Expression is normalized against GAPDH. Results represent the mean±SEM values (n=3-5). **(E)** Representative immunoblot analysis of BDH1 in Wt and Tg neonatal cardiomyocytes. *$P<0.05$.

We hypothesized that the excess BDH1present in Tg hearts could limit the amount of β-OHB in the cardiomyocyte via its conversion to acetoacetate and subsequent availability for the ketone catabolic pathway. This could in turn inhibit the signaling capacity of β-OHB (the most stable and abundant ketone) and thus may contribute to the observed down-regulation of CX-43 in Tg hearts. To test this we examined the amount of CX-43 in neonatal cardiomyocytes incubated with or without the β-OHB. Wt cardiomyocytes incubated with β-OHB showed a 100% increase of CX-43 ($P<0.05$) **(Figure 23C and 23D)**, similar to what was recently reported in endothelial cells (145). In contrast, β-OHB had no significant impact on CX-43 expression in Tg cardiomyocytes supporting our hypothesis that BDH1 reduces ketone signaling.

Surprisingly, the reduction of CX-43 noted *in vivo* **(Figure 23A)** was reversed in culture of Tg cardiomyocytes **(Figure 23B)**. In order to rule out the possibility that BDH1 was reduced in culture, thereby reversing its effect on CX-43 expression, we assessed its level in cultured cardiomyocytes. Western blot with anti-BDH1 detected its presence in neonatal cardiomyocytes cultured from Tg mice, but not Wt, indicating that its loss is not responsible for the rescue of CX-43 in culture **(Figure 23E)**. This suggests the presence of factors in the culture media which specifically promote expression of CX-43 in neonatal cardiomyocyte from Tg hearts. In support of this hypothesis, Tg cardiomyocytes showed an increase in CX-43 expression over time in culture **(Appendix 3: Sup Fig 6)**.

Discussion

The E2F pathway regulates early cardiac development through mechanisms that impact cell proliferation, hypertrophy, and death (47,53,146,55). We previously demonstrated that the E2F pathway can also impact post-natal cardiac function via manipulation of the pathway *in vivo* with the repressor E2F6 (80). E2F6 resulted in dose dependent DCM associated with inappropriate activation of E2F responsive genes, but without changes in cardiac growth or death (80). Further, our data also revealed that the E2F pathway can impact β-adrenergic signaling in the post-natal heart (118). Here we demonstrate that deregulation of the E2F pathway impairs glycolysis in the developing postnatal myocardium, and markedly enhances that expression of the ketogenic enzyme, BDH1, which was linked to the down-regulation of CX-43. Thus we present notable evidence that appropriate modulation of the E2F pathway is critical for regulating cardiac metabolism and, consequently, function of post-natal myocardium.

E2F6-Tg mice present with an early reduction of CX-43 and a defect in cardiac function potentially accounting for the noted DCM and sudden death (80). Recent studies demonstrated that β–OHB can enhance CX-43 expression in endothelial cells (145) which we have now also noted in Wt neonatal cardiomyocytes. This suggests that ketones may uniquely modulate the gap junction levels in different cell types. It should be noted that CX-43 expression was rescued in culture of Tg cardiomyocytes while BDH1 was still highly expressed. Thus other factors appear to have an effect on CX-43 expression in culture conditions. In this regard, multiple MAPK pathways have been implicated in the post-transcriptional regulation of CX-43, and these were deregulated in E2F6-Tg mice

(147), (145) (80). It is possible that deregulation of MAPKs may have sensitized E2F6-Tg cardiomyocytes to growth factors in the culture media.

Despite differences in vitro and in vivo both neonatal cardiomyocytes and hearts from Tg mice show a marked induction of BDH1 and a diminished capacity to regulate CX-43 expression. In the heart, Tg-mice do not enhance CX-43 levels to the appropriate level required for cardiac function, and in culture, Tg cardiomyocytes are unresponsive to CX-43 ketone signaling pathways. In both cases this likely involves the marked induction of BDH1 protein which could diminish the available β-OHB (via its conversion to a less stable ketone) thereby driving it towards the ketone catabolic pathway and reducing its ability to act as a signaling molecule to enhance the amount of CX-43. The resulting down-regulation of CX-43 in Tg myocardium would alter cardiomyocyte communication and function from a very young age, potentially leading to the early DCM noted. In this regard, CX-43 is reported to be down-regulated in the diabetic rat heart and in many types of heart failure (148,149,150,151). Further, metabolic remodeling is known to occur in heart failure with enhanced BDH1 and ketone signaling (65,66). Hence our data here may critically serve to link enhanced BDH1 and the loss of CX-43 in the adult failing heart as well. It has previously been demonstrated that an increase in BDH1 transcript levels in both mouse and human cardiac tissue is associated with enhanced BDH1 activity and ketone metabolism (66,65). While we have not measured BDH1 activity here, the robust increase in both transcript and protein levels induced by E2F6 imply an enhanced BDH1enzyme activity as early as postnatal day 1.

The relationship between E2F, BDH1, and CX-43 highlights the emerging idea that ketones not only serve as energy substrates, but are also important signaling

molecules which can regulate gene expression during nutrient scarcity/adaptation. Ketones can initiate undefined signaling cascades via binding to G-protein coupled receptors, or by direct interaction with and inhibition of HDACs (64,152). Rb recruits HDACs to repress E2F responsive genes (14,13), which we have shown to be inhibited by E2F6 expression in the heart (80). Furthermore, we found that E2F6 also regulates G-coupled protein receptor signaling pathways (118), suggesting a novel relationship between E2F/Rb, HDACs, and ketones which critically impacts myocardial growth, function, and metabolism.

It is plausible that BDH1 was induced by E2F6 in Tg myocardium to compensate for the impairment in glycolysis (which is the major source of energy in the neonatal heart). The decrease in GLUT4 protein could have limited glucose entry to E2F6-Tg cardiomyocytes, and when coupled with the observed decrease in AKT2 activation (which regulates glucose homeostasis) could account for the impaired glycolysis (153). Alterations in glucose metabolism have been previously linked to the E2F/Rb pathway as demonstrated by double knock-out of E2F1/E2F2 which impaired insulin production and caused diabetes (154). Additionally, studies have demonstrated that E2F/Rb promote glycolysis over oxidative phosphorylation in muscle and fat tissue via the deregulation of cyclin, in particular cyclin D1 (144,155). Thus it is a logical extension that E2F6, which inhibits E2F/Rb activity, would also inhibit glycolysis. E2F6-Tg mice express less cyclinB1 which could represent a delay in the cardiac cell cycle (i.e. not reaching mitosis) similar to what was observed in E2F6 expressing 3T3 cells which accumulated in S phase (27). Such a shift in the cell cycle could cause a shift in the metabolic profile as well. The specific change in cyclin B1 may involve the reduction of E2F3 in E2F6-Tg myocardium

since it is a critical regulator of the cell cycle during perinatal cardiac development (35,80). This suggests that E2F3 may also be a key regulator of cyclin B1 and glycolysis in the heart. Further, since fatty acid oxidation is not increased in response to the depression of glycolysis, ketolysis may be a necessary adaptation as an alternative energy source.

It is interesting to note that BDH1 levels were not increased in the adult (6wk old) Tg-myocardium which are experiencing heart failure. This may reflect the fact that fatty acids are the major energy substrate at this time and fatty acid metabolism appeared to be unaffected in E2F6 Tg mice. This implies that the induction of BDH1 may be an early marker for metabolic stress/changes in the myocardium that precede heart failure. There is a window of overlap between enhanced BDH1 expression and the early symptoms of DCM around 3 weeks supporting the correlative relationship (118). This may be particularly useful information for ~40% of cases of idiopathic dilated cardiomyopathy and early-onset of disease.

The robust increase of *Bdh1* transcript by E2F6 at birth and the lack of change in other ketogenic enzymes, such as OXCT1, imply a specific role for E2Fs through a transcriptional mechanism. A basic promoter analysis did not detect an E2F consensus binding site in the *Bdh1* promoter **(Appendix 3: Sup Fig 7)**. This does not rule out direct transcriptional regulation as E2F6 has been demonstrated to bind to DNA at non-consensus sites and activate transcription (25,29). A nuclear-factor (NF)-kappaB site was predicted by the promoter analysis 1938bp upstream of the BDH1 transcription start site (core score 1.00). This is of particular interest because E2Fs can bind to and de-regulate NF-kappaB in the context of inflammation and metabolism (156,157). Thus it is possible

that the deregulation of E2Fs in E2F6-Tg myocardium may have enabled NF-kappaB to flip a metabolic switch activating BDH1 in the neonatal heart. In support of this, E2F1-3 levels normally drop in the adult myocardium (8) when we have demonstrated that BDH1 is normally expressed.

The data here demonstrate a novel role for the E2F pathway in regulating metabolism in post-natal myocardium since its perturbation by E2F6 leads to aberrant glycolysis and the induction of the ketogenic enzyme: BDH1. These changes appear to impact ketogenic signaling to deregulate CX-43 levels and thereby disrupt cardiac function. The potent early induction of BDH1 prior to a discernable cardiac pathology implies that BDH1 is an early biomarker of metabolic stress and DCM. The information here could provide new insight into the early diagnosis and potential treatment options in idiopathic cases of DCM.

Acknowledgements

We thank Dr. Mary Ellen Harper for kind use of the Flux Analyzer/ Sea Horse platform.

Disclosures

None.

GENERAL DISCUSSION

The works in this thesis elucidate the *in vivo* capacity for the E2F pathway to regulate cell death, hypertrophy, and differentiation in the post-natal heart by manipulating its activity with E2F6 in a cardiac specific Tg mouse model. E2F6-Tg mice developed early onset DCM without hypertrophy or apoptosis suggesting that E2F6 had protective properties against these pathological processes. My data clearly shows that E2F6 deregulates E2F3 which is a master regulator of the cardiac cell cycle and the only E2F family member required for viability. I propose that via alteration of E2F3 (and subsequently its association with Rb), E2F6 altered the dynamics of cell cycle withdrawal in Tg myocardium leading to metabolic changes which impact differentiation and function leading to DCM **(summarized in Figure 24)**. Use of the E2F6-Tg model may aid in the understanding of idiopathic cases of DCM which may prove to be of significance in the field.

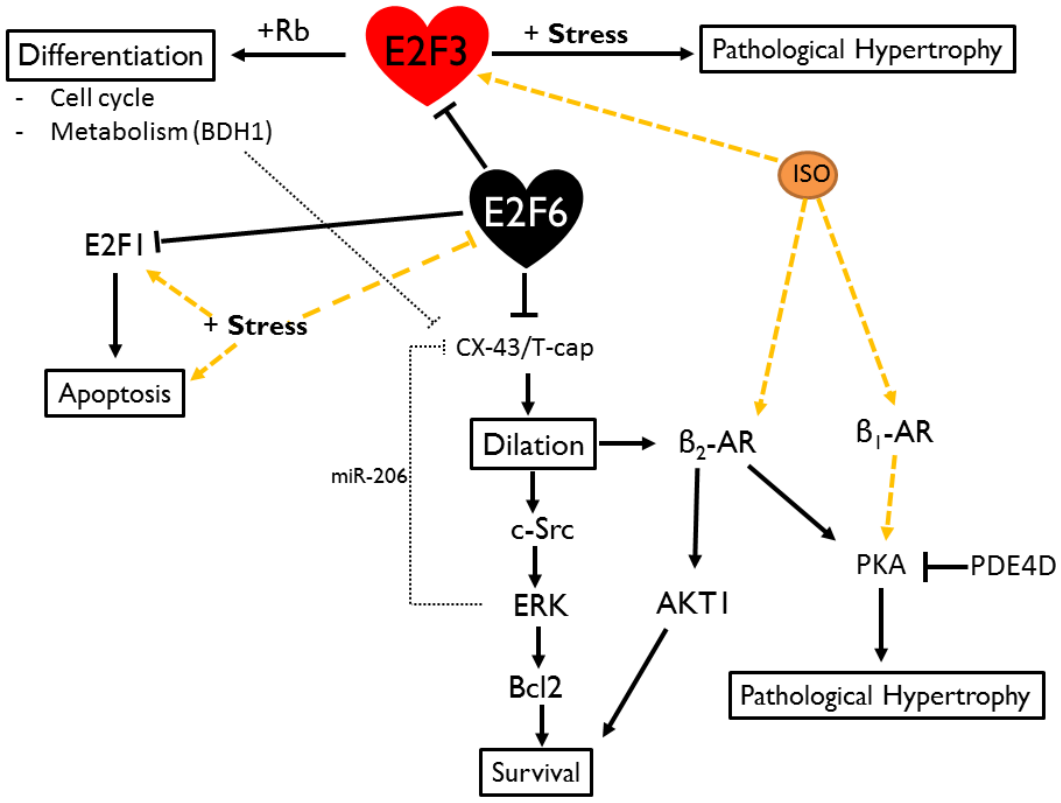

Figure 24: ***A summary model for E2F6 induced dilated cardiomyopathy***. E2F6 expression inhibits E2F3 with impacts on cell cycle/metabolism and thereby cardiac differentiation via inhibition of E2F3/Rb. These changes cause the down-regulation of CX-43 and T-Cap leading to cardiac remodeling which proceeds directly to dilation without hypertrophy or apoptosis via inhibition of E2F3 and E2F1. Dilation activates the stretch sensitive c-src and a β_2-AR survival pathway, which protects Tg myocardium from apoptosis. Activation of the β_2 pathway sensitizes the heart to isoproterenol leading to the rescue of E2F3 and the induction of pathological hypertrophy. The increased activity of ERK may also impact the post-transcriptional loss of CX-43 via miR-206 (80) which enhances disease progression.

E2F6: a potential therapeutic tool in heart failure

The lack of hypertrophy and apoptosis in E2F6-Tg mice is particularly curious given that these are hallmarks of heart failure and DCM. Cell growth and apoptosis are well known to be regulated by the E2F pathway thus I hypothesized that E2F6 had repressed them. When challenged with the hypertrophic agent, isoproterenol, E2F6-Tg mice were not resilient, but instead were twice as sensitive as their Wt counterparts. Their increased sensitivity can likely be attributed to activation of a β_2 adrenergic receptor pathway. Intriguingly, E2F3 was downregulated in Tg myocardium and was rescued by isoproterenol, suggesting that E2F activity is central and necessary for cardiac pathological hypertrophy to occur **(Figure 24)**. In support of this notion, Bicknell and colleagues found that E2F/DP activity was necessary for pathological hypertrophy in NCM (55). Thus it seems that the E2F pathway, in particular E2F3, is critical to regulate cardiac pathological hypertrophy *in vitro* and *in vivo*.

The β_2 adrenergic pathway described in Chapter 1 was previously demonstrated to activate cell survival in cardiomyocytes (95). Thus I hypothesized that its activation could explain the lack of apoptosis in Tg mice despite their advanced disease. In support of its anti-apoptotic properties, E2F6 was capable of attenuating the apoptotic response to cobalt chloride in cardiomyocytes. In contrast to the adult heart, the protection conferred to NCM by E2F6 did not include an increase in Bcl-2. In cancer cell lines E2F6 inhibited apoptosis via inhibition of E2F1 **(Figure 24)** (75,78). E2F6 was able to out-compete E2F1 for DNA binding in *in vitro* assays (15,17), and we previously detected the presence of myc-E2F6 on gene promoters in adult Tg myocardium (80). This suggests that E2F6 has the capacity to out-compete pro-apoptotic E2F family members in the

heart. Unlike in cancer cell lines (such as HeLa used in Chapter 2), my preliminary data suggests that E2F1 was not up-regulated in cardiomyocytes in response to doxorubicin **(Appendix 4: Sup Fig 8)**. This suggests that another E2F family member may be responsible for inducing apoptosis. In addition to E2F1, E2F3 was also capable of inducing apoptosis in neonatal cardiomyocytes (53). Furthermore, I demonstrated that E2F3 expression was enhanced by isoproterenol along with the β_1-AR which can induce cardiomyocyte cell death (95). Since E2F6 repressed E2F3 expression in Tg myocardium it is possible that E2F6 may exert protection against apoptosis in cardiomyocytes via inhibition of E2F3. Thus future experiments should focus on the balance between the repressor E2F6 and activators: E2F1 and E2F3 in cardiomyocytes.

Although E2F6 holds promise for battling apoptosis in the heart, my studies were limited by the reduction of myc-E2F6 in response to drug exposure. In the case of doxorubicin the loss of E2F6 was similar (albeit more rapid) to what I observed in HeLa cells treated with dox, but via completely different mechanisms. In HeLa and Wt-NCM *e2f6* transcript levels did not change in response to dox, implying that endogenous E2F6 protein was deregulated at the post-transcriptional level by dox. Post-transcriptional regulation of E2F6 also appears to be important in cardiac development in which its transcript is maintained while protein is decreased **(Appendix 4: Sup Fig 9)**. Unlike other E2F family members, E2F6 is not targeted to the proteasome via $p19^{ARF}$, and the mechanisms which regulate its turn-over are not known. Bertoli and colleagues found that E2F6 was phosphorylated by Chk1 in HEK cells which were subjected to DNA replication stress (121). Chks have also been demonstrated to phosphorylate and stabilize pro-apoptotic E2F1. Thus it is possible that E2F6 was down-regulated and E2F1 was up-

regulated at the post-transcriptional level by Chk1 phosphorylation. Phosphorylation of E2F6 could signal for its degradation, or its dissociation from DNA could destabilize it, thereby leaving E2F1 (which is stabilized by Chk) free to induce apoptosis. The use of commercially available Chk1/2 inhibitors could be used to test this hypothesis.

In cardiomyocytes, Chk1 is unlikely to regulate E2Fs given the fact that it is undetectable following dox exposure. Since E2F1 does not appear to be up-regulated by dox **(Appendix 4: Sup Fig 8)**, and E2F6 is normally expressed at very low levels in the post-natal heart, this is not particularly surprising. In fact, it is reasonable to propose that the lack of E2F6 in adult myocardium may actually sensitize it to doxorubicin exposure resulting in cardiomyopathy. Additionally, the interruption of *α-mhc* by dox, which caused the loss of the E2F6 transgene (via its promoter), may also sensitize the heart to dox (120).

In contrast to dox, cobalt chloride did not deregulate E2F6 protein levels and decreased the pro-apoptotic E2F1 in HeLa. Although myc-E2F6 was retained in Tg cardiomyocytes for a longer period of time (than in response to dox) and did convey some resilience to apoptosis it was still down-regulated. Since E2F6 protein is stable in HeLa in response to $CoCl_2$, it is compelling to predict that myc-E2F6 is down-regulated at the level of its αMHC promoter (which is reduced by dox and in heart failure), but this remains to be confirmed by RT-qPCR. If it is merely a problem of promoters, the potential to use E2F6 as a therapeutic target to reduce apoptosis in the heart would be increased. Future experiments should also explore the response of Tg cardiomyocytes (or perhaps rat cardiomyocytes transfected with E2F6 under the control of a different

promoter) with other apoptotic agents and hypoxia/re-oxygenation to determine if E2F6 could be a useful tool for cardio-protection.

Similarly, the ability of E2F6 to protect against other hypertrophic agents should also be evaluated. In particular, the ability for E2F6 to regulate the alpha adrenergic response could be tested (via administration of angiotensin or endothelin) which could prove a valuable tool against hypertension. Another useful model of hypertrophy in mice is trans-aortic constriction (TAC). This could prove problematic in Tg mice since TAC is usually performed on adult mice due to the difficulty of the surgery on such a small animal, and the Tg mouse heart is already compromised by DCM. In support of this, the pre-existing DCM likely contributed to the increased sensitivity of Tg mice to isoproterenol. It is probable that since Tg myocardium was already remodeled it could not remodel itself any further upon stimulation. In support of this, while Wt mice showed an activation of the fetal gene program after iso administration, the program was already activated in Tg mice and was not further increased by drug exposure.

An alternative to using adult Tg mice would be to treat neonatal cardiomyocytes from Wt and Tg mice. It would also be beneficial to extract normal adult cardiomyocytes (using the Langendorf system) and infect them with E2F6 (via adenovirus). This way the cells would not be initially compromised and would be more similar to the adult diseased heart. To take it one step further, E2F6 could also be delivered to adult mice prior to the administration of hypertrophic and/or apoptotic reagents and tested for increased survival and cardiac performance *in vivo*.

Mechanisms for E2F6 induced dilated cardiomyopathy

While it is astounding that E2F6-Tg mice develop DCM without preceding hypertrophy and the limited induction of apoptosis, the question still remains: why do they develop DCM? I believe the answer to this question is hidden in the cell cycle during early post-natal cardiac development. When one thinks of the E2F pathway, the cell cycle immediately comes to mind as E2F regulates virtually all facets of it including: cell cycle gene repression during G_0, the induction of genes involved in growth during G_1 and DNA replication during S-phase, and checkpoint control. As mentioned, the exact role of E2F6 in the cell cycle remains undefined although evidence has demonstrated that E2F6 can cause an accumulation of cells in S-phase and delay cell cycle re-entry (27).

My initial microarray/qPCR analysis of Tg hearts (P7) during my MSc revealed alterations in cell cycle related genes, in particular those involved in S phase implying a potential accumulation (80). We did observe an increase in BrdU incorporation in adult Tg- myocardium (a common observation in HF) but there was no increase in neonatal pup hearts (80). The BrdU experiment was performed at P7 to mirror the micro-arrays, but it is possible that a difference could be observed at an earlier time, especially when considering that cardiomyocytes withdraw from the cell cycle a few days after birth (day 5). Thus, a potential defect or delay in cell cycle withdrawal could have occurred which was no longer detectable at P7. I did observe an increase in the S-phase cyclin (cyclin E1) and a decrease in the G_2/M phase cyclin (cyclin B1) in younger Tg hearts, which would imply a prolonged S phase. In order to fully assess this possibility, future studies should include the evaluation of more cell cycle markers and fluorescent activated cell sorting in Wt vs. Tg NCM.

As alluded to in the manuscripts, a defect in the cell cycle of Tg mice would likely be related to the down-regulation of E2F3 **(Figure 24)**. In embryonic stem cells, Oct3/4 expression inhibited proliferation with increased expression of E2F6 and reduced E2F3, and was reversible by the addition of E2F3 (158). In post-natal myocardium growth does not include cardiomyocyte proliferation, but a similar phenomenon was observed in the context of hypertrophy. In essence, E2F6 inhibited pathological growth in the diseased heart with a reduction of E2F3 and this was reversed by iso and the rescue of E2F3 expression.

In addition to growth and proliferation, E2F3 was demonstrated to regulate early cardiac development (35,129). Furthermore, in a partial mixed strain of $E2F3^{-/-}$ in which a quarter of mice survive into adulthood, 85% of those go on to develop late-onset DCM (35). This implies that E2F3 is also important to adult cardiac structure and function. It was suggested by the authors that this phenotype could be caused by the disorganization of sarcomere proteins. This is quite feasible as mutations in sarcomere proteins make up about one third of all cases of DCM. In our study, I demonstrated a 70% decrease in the amount of the sarcomere protein: Titin-cap. This protein is important for recruiting proteins like muscle lim protein to the z-line, and point mutations which inhibit T-cap function cause DCM (127).

It is interesting to note that the time of contractile perturbation is also important, as exemplified by the over-expression of tropomodulin which caused early onset DCM when it accumulated shortly after birth, but was asymptomatic when expressed later on in development (159). This suggests that the cardiomyocyte is particularly sensitive during this critical time-point of peri-natal development and cell cycle withdrawal. Thus, if E2F6

caused an alteration in cardiac function early on it could have major consequence like early-onset DCM. I noted a significant decrease in connexin43 in E2F6-Tg mice which occurred as early as P1. The loss of CX-43 was demonstrated in a desmin model of DCM (160), and generally speaking its down-regulation is a hallmark of HF (89). Thus the down-regulation of critical players in cardiac function and contraction (such as CX-43 and T-cap) at an early age could imply a defect or delay in cell cycle withdrawal which leads to aberrant differentiation and DCM **(Figure 24)**.

E2F3 was also demonstrated to be an important player in skeletal muscle differentiation and development (161). I attempted to explore the role of E2F6 in muscle development by expressing E2F6 in C2C12 cells (murine myoblast cell line) and inducing differentiation via serum starvation (replacing feeding media with 2% horse serum induces myotube formation). This resulted in a 30% reduction in the fusion index (measure of differentiation) of myc-E2F6 transfected C2C12 in comparison to 6myc-empty vector transfected cells **(Appendix 4: Sup Fig 10)**. Unfortunately, the mechanisms for this defect could not be fully explored because myc-E2F6 expression was lost on the first day of serum starvation (when selection media was removed). These results imply that E2F6 has a negative effect on differentiation, which is supported by its reduced expression during C2C12 differentiation **(Appendix 4: Sup Fig 11)** and cardiac development (80).

To maintain a differentiated state E2F3 would impart its activity via the recruitment of the pocket proteins. In fact, deletion of Rb and p130 in myocardium led to hyperplasia *in vivo* (47), and in cardiomyocytes inhibited post-mitotic differentiation (143). It is also interesting to note that Rb's repressor function was inhibited in an

emerin model of DCM due to its inappropriate nuclear docking and subsequent E2F gene activation (162,163). Since E2F6 can out-compete for DNA binding (we detected it at E2F responsive gene promoters in Tg hearts), and it does not interact with pocket proteins it is logical that E2F6 would inhibit pocket protein mediated repression and differentiation, especially when considering that Rb's localizer, E2F3, is down-regulated. This is supported by the transcriptional activation of hundreds of genes in E2F6-Tg hearts, in particular E2F responsive genes (80). Chromatin Immunoprecipitation (ChIP) of Rb would be required to validate its displacement in Tg myocardium, but this has proven difficult since the antibodies which best detect Rb in the heart target its binding domains which are inaccessible during ChIP.

Rb and E2F1 have also been implicated in regulating cellular metabolism. In general, they tend to drive glycolysis over oxidative phosphorylation. Given that E2F6 seems to impair E2F/Rb function in Tg myocardium it was perhaps not surprising that we observed metabolic changes in E2F6-Tg neonates. Metabolic shifts, or "metabolic remodeling" has been recognized as an important change during HF and connected to the cell cycle. E2F6-Tg mice present with impaired glycolysis without a compensatory increase in fatty acid oxidation. Since glucose is still an important energy source for the young cardiomyocyte (and the failing heart), this could have a detrimental effect on Tg hearts shortly after birth as well as in their diseased state. We detected the expression of the ketogenic enzyme: BDH1 at post-natal day 1, six weeks prior to when it is detectable in the normal heart. The potent early induction of this enzyme implies that it could increase ketone metabolism and affect ketone signaling pathways. Of particular interest, is the potential for BDH1expression in the down-regulation of CX-43 **(Figure 24)**.

Unfortunately, we were not capable of fully assessing our hypothesis (that excess BDH1 reduced β-OHB and thereby CX-43- **Figure 24**) since CX-43 was rescued in culture conditions. Despite this complication, Tg-cardiomyocytes did not increase CX-43 in response to β-OHB like their Wt counterparts, thereby implying that BDH1 could have inhibited β-OHB signaling in Tg NCM. Future studies should focus on the mechanism for the transcriptional up-regulation of BDH1. Co-transfection of cells with a BDH1 luciferase construct and E2F family members could be used to determine if it is a direct transcriptional target of E2F.

Perspective

In summary, E2F6 appears to impact multiple facets which determine cardiac development and function, ultimately causing DCM in Tg mice. Given these results it would be beneficial to screen human samples of DCM for mutations in E2F coding regions and upstream sequences to determine if mutations in E2F occur in DCM. Further, our results imply that BDH1 may be an early biomarker of the disease, and that further investigation of the interplay between the cell cycle and metabolism could be useful in the detection and treatment of DCM. This is especially important since DCM has no cure and its cause remains unknown in one third of patients. Finally, the studies reported in this thesis have unveiled the potential for E2F6 in promoting cell survival via multiple mechanisms throughout post-natal cardiac development implying a therapeutic potential for E2F6 in a wide range of cardiac diseases.

REFERENCES

1. Organization WH. World Health Organization. [Online].; 2016. Available from: http://www.who.int/gho/ncd/mortality_morbidity/cvd/en/.

2. Foundation HaS. Statistics. [Online].; 2012 [cited 2016 09 29. Available from: http://www.heartandstroke.com/site/c.ikIQLcMWJtE/b.3483991/k.34A8/Statistics.htm.

3. Senyo SE, Lee RT, Kuhn B. Cardiac regeneration based on mechanisms of cardiomyocyte proliferation and differentiation. Stem Cell Research. 2014; 13: p. 532-541.

4. Bergmann O, Bhardwaj RD, Bernard S, Zdunek S,BHF, Walsh S, Zupicich J, et al. Evidence for cardiomyocyte renewal in humans. Science. 2009; 324: p. 98–102.

5. Singh A, Singh A, Sen D. Mesenchymal stem cells in cardiac regeneration: a detailed progress report of the last 6 years (2010–2015). Stem Cell Research and Therapy. 2016; 7: p. 82.

6. Porello ER, Mahmoud AI, Simpson E, Hill JA, Richardson JA, Olson EN, et al. Transient Regenerative Potential of the Neonatal Mouse Heart. Science. 2011; 331(6020): p. 1078-1080.

7. Senyo SE, Steinhauser ML, Pizzimenti CL, Cai L, Wang M, Wu TD, et al. Mammalian heart renewal by pre-existing cardiomyocytes. Nature. 2013; 493(7432): p. 433-436.

8. Ahuja P, Sdek P, MacLellan WR. Cardiac myocyte cell cycle control in development, disease, and regeneration. Physiological Reviews. 2007; 87: p. 521-544.

9. DiStefano L, Rugaard Jensen M, Helin K. E2F7, a novel E2F featuring DP-independent repression of a subset of E2F-regulated genes. EMBO Journal. 2003; 22: p. 6289-6298.

10. Maiti B, Li J, de Bruin A, Gordon F, Timmers C, Opavsky R, et al. Cloning and characterization of mouse E2F8, a novel mammalian E2F family member capable of blocking cellular proliferation. The Journal of Biological Chemistry. 2005; 280(18): p. 18211-18220.

11. Rueger J, Tuana BS. The E2F Pathway in Cardiac Developement and Disease. In Ostadal B, editor. Genes and Cardiovascular Function.: Springer Science ; 2011. p. 29-41.

12. Taubert S, Forrini C, Frank SR, Parisi T, Fuchs M, Chan HM, et al. E2F-dependent histone acetylation and recruitment of the Tip60 acetyltransferase complex to chromatin in late G1. Molecular and Cellular Biology. 2004; 24: p. 4564-4556.

13. Ferreira R, Magnaghi-Jaulin L, Robin P, Harel-Bellan A, Trouche D. The three members of the pocket proteins family share the ability to repress E2F activity through recruitment of a histone deacetylase. Proceedings of the National Academy of Sciences of the United States of America. 1998; 95: p. 10493-10498.

14. Brehm A, Miska EA, McCance DJ, Reid JL, Bannister AJ, Kouzarides T. Retinoblastoma protein recruits histone deacetylase to repress transcription. Nature. 1998; 391: p. 597-601.

15. Cartwright P, Muller H, Wagener C, Holm K, Helin K. E2F-6: a novel member of the E2F family is an inhibitor of E2F-dependent transcription. Oncogene. 1998; 17: p. 611-623.

16. Gaubatz S, Wood JG, Livingston DM. Unusual proliferation arrest and transcriptional control properties of a newly discovered E2F family member, E2F-6. Proceedings of the National Academy of Sciences of the United States of America. 1998; 95: p. 9190-9195.

17. Trimarchi JM, Fairchild B, Verona R, Moberg K, Andon N, Lees JA. E2F-6, a member of the E2F family that can behave as a transcriptional repressor. Proceedings of the National Academy of Sciences of the United States of America. 1998; 95: p. 2850-2855.

18. Dahme T, Wood J, Livingston JM, Gaubatz S. Two different E2F6 proteins generated by alternative splicing and internal translation initiation. European Journal of Biochemistry. 2002; 269: p. 5030-5036.

19. Sparmann A, van Lohuizen M. Polycomb silencers control cell fate, development and cancer. Nature Reviews Cancer. 2006; 6: p. 846-856.

20. Trimarchi JM, Fairchild B, Wen J, Lees JA. The E2F6 transcription factor is a component of the mammalian Bmi1-containing polycomb complex. Proceedings of the National Academy of Sciences of the United States of America. 2001; 98: p. 1519-1524.

21. Atwool C, Oddi S, Cartwright P, Prosperini E, Agger K, Steensgaard P, et al. A noevl repressive E2F6 complaex containing the polycomb group protein, EPC1, that interacts with EZH2 in a proliferation-specific manner. Journal of Biological Cehmistry. ; 280.

22. Takahashi Y, Rayman J, Dynlacht B. Analysis of promoters binding by the E2F and pRB families in vivo: distinct E2F proteins mediate activation and repression. Genes and Developement. 2000; 14: p. 804-816.

23. Giangrande PH, Zhu W, Schlisio S, Sun X, Mori S, Gaubatz S. A role for E2F6 in distinguishing G1/S- and G2/M-specific transcription. Genes and Developement. 2004; 18: p. 2941-2951.

24. Lyons TE, Salih M, Tuana BS. Activating E2Fs mediate transcriptional regulation of human E2F6 repressor. American Journal of Physiology. Cell Physiology. 2006; 290: p. C189-C199.

25. Ogawa H, Ishiguro K, Gaubatz S, Livingston DM, Nakatani Y. A complex with chromatin modifiers that occupies E2F-and myc-responsive genes in G0 cells. Science. 2002; 296: p. 1132-1136.

26. Deshpande AM, Akunowicz JD, Reveles XT, Patel BB, Saria EA, Gorlick AG, et al. PHC3, a component of the hPRC-H complex, associates with E2F6 during G0 and is lost in osteosarcoma tumors. Oncogene. 2007; 26: p. 1714-1722.

27. Gaubatz S, Wood JG, Livingston DM. Unusual proliferation arrest and transcriptional control properties of a newly discovered E2F family member, E2F-6. Proceedings of the National Academy of Sciiences of the United States of America. 1998; 95: p. 9190-9195.

28. Storre J, H. E, Fuchs M, Ullmann D, Livingston D, S. G. Homeotic transformations of the axial skeleton that accompany a targeted deletion of E2f6. EMBO Reports. 2002; 3: p. 695-700.

29. Xu X, Bedia M, Jin VX, Rabinovich A, Oberley MJ, Green R, et al. A comprehensive ChIP-chip analysis of E2F1, E2F4, and E2F6 in normal and tumor cells reveals interchangeable roles of E2F family members. Genome Research. 2007; 17: p. 1550-1561.

30. Field SJ, Tsai F, Kuo F, Zubiaga AM, Kaelin WGJ, Livingston DM, et al. E2F-1 Functions in Mice to Promote Apoptosis and Suppress Prolioferation. Cell. 1996; 85(4): p. 549-561.

31. Yamasaki L, Jacks T, Bronson R, Goillot E, Harlow E, Dyson NJ. Tumor Induction and Tissue Atrophy in Mice Lacking E2F-1. Cell. 1996; 85: p. 537-548.

32. Murga M, Fernandez-Capetillo O, Field SJ, Moreno B, Borlado LR, Fuijwara Y, et al. Mutation of E2F2 in mice causes enhanced T lymphocyte proliferation, leading to the development of autoimmunity. Immunity. 2001; 15: p. 959-970.

33. Humbert PO, Verona R, Trimarchi JM, Rogers C, Dandapani S, Lees JA. E2f3 is critical for normal cellular proliferation. Genes and Developement. 2000; 14(6): p. 690-703.

34. Cloud JE, Rogers C, Reza TL, Ziebold U, Stone JR, Picard MH, et al. Mutant Mouse Models Reveal the Relative Roles of E2F1 and E2F3 In Vivo. Molecular and Cellular Biology. 2002; 22(8): p. 2663-2672.

35. King JC, Moskowitz IPG, Burgon PG, Ahmad F, Stone JR, Seidman JG, et al. E2F3 plays an essential role in cardiac development and function. Cell Cycle. 2008; 7: p. 3775-3780.

36. Humbert PO,RC, Ganiastas S, Landsberg RL, Trimarchi JM, Dandapani S, Brugnara C, et al. E2F4 is essential for normal erythrocyte maturation and neonate viability. Molecular Cell. 2004; 6: p. 281-291.

37. Lindeman J, Dagnino L, Gaubatz S, Xu Y, Bronson RT, Warren HB, et al. A specific, non-proliferative role for E2F-5 in choroid plexus function revealed by gene targeting. Genes and Developement. 1998; 12: p. 1092-1098.

38. Li J, Ran C, Li E, Gordon F, Comstock G, H. S, et al. Synergistic Function of E2F7 and E2F8 is Essential for Cell Survival and Embryonic Develeopment. Developemental Cell. 2008; 14(1): p. 62-75.

39. Jacks T, Fazeli A, Schmitt EM, Bronson RT, Goodell MA, Weinberg RA. Effects of an rb mutation in the mouse. Nature. 1992; 359: p. 295-300.

40. Lee EYP, Chang C, N. H, Wang YJ, Lai C, Herrup K, et al. Mice deficient for Rb are nonviable and show defects in neurogenesis and haematopoiesis. Nature. 1992; 359(6393): p. 288-294.

41. Cobrinik D, Lee MH, Hannon G, Mulligan G, Bronson RT, Dyson N, et al. Shared role of the pRB-related p130 and p107 proteins in limb development. Genes and Developement. 1996; 10: p. 1633-1644.

42. Lee MH, Williams BO, Mulligan G, Mukai S, Bronson RT, Dyson N, et al. Targeted disruption of p107: functional overlap between p107 and Rb. Genes and Developement. 1996; 10: p. 1621-1632.

43. Tsai SY, Opavsky R, Sharma N, Wu L, Naidu S, Nolan E, et al. Mouse developement with a single E2F activator. Nature. 2008; 458(137): p. 1142.

44. Rempel R, Saenez-Robels M, Storms R. Loss of E2F4 Activity Leads to Abnormal Developement of Multiple Cell Lineages. Moecular Cell. 2000; 6: p. 270-281.

45. Dannenberg JH, Schuijff L, Dekker M, vdVM, te Riele H. Tissue-specific tumor suppressor activity of retinoblastoma gene homologs p107 and p130. Genes and Developement. 2004; 18: p. 2952-2962.

46. Berman SD, West JC, Danielan PS, Caron AM, Stone JR, Lees JA. Mutations of p107 exacerbates the consequences of Rb loss in embryonic tissues and causes cardian and blood vessel defects. Proceedings of the National Academy of Sciences of the UnitedStates of America. 2009; 106: p. 14932-14936.

47. MacLellan WR, Garcia A, Oh H, Frenkel P, Jordan M, Roos KP, et al. Overlapping roles of pocket proteins in the myocardium are unmasked by germ line deletion of p130 plus heart-specific deletion of Rb. Molecular and Cellular Biology. 2005; 25: p. 2486-2497.

48. Sdek P, Zhao P, Wang Y, Huang C, Ko CY, Butler PC, et al. Rb and p130 control cell cycle gene silencing to maintain the postmitotic phenotype in cardiac myocytes. Journal of Cell Biology. 2011; 194: p. 407-423.

49. Shimizua I, Minaminoa T. Physiological and pathological cardiac hypertrophy. Journal of Molecular and Cellular Cardiology. 2016; 97: p. 245-262.

50. Bernardo BC, Weeks KL, Pretorius L, McMullen JR. Molecular distinction between physiological and pathological cardiac hypertrophy: Experimental findings and therapeutic strategies. Pharmacology & Therapeutics. 2010; 128(1): p. 191-227.

51. Barry SP, Davidson SM, Townsend PA. Molecular regulation of cardiac hypertrophy. International Journal of Biochemistry and Cell Biology. 2008; 40: p. 2023-2039.

52. Rohini A, Agrawal N, Koyani CN, Singh R. Molecular targets and regulators of cardiac hypertrophy. Pharmacology Research. 2010; 61: p. 269-280.

53. Ebelt H, Hufnagel N, Neuhaus P, Neuhaus H, Gajawada P, Simm A, et al. Divergent siblings: E2F2 and E2F4 but not E2F1 and E2F3 induce DNA synthesis in cardiomyocytes without activation of apoptosis. Circulation Research. 2005; 96: p. 509-517.

54. Ebelt H, Zhang Y, Kampke A, Xu J, Schlitt A, Buerke M. E2F2 expression induces proliferation of terminally differentiated cardiomyocytes in vivo. Cardiovascular Research. 2008; 80: p. 219-226.

55. Vara D, Bicknell KA, Coxon CH, Brooks G. Inhibition of E2F Abrogates the Development of Cardiac Myocyte Hypertrophy. The Journal of Biological Chemistry. 2003; 278: p. 21388-21394.

56. Wohlschlaeger J, Schmitz KJ, Takeda A, Takeda N, Vahlhaus C, Stypmann J, et al. Reversible regulation of the retinoblastoma protein/E2F-1 pathway during "reverse cardiac remodelling" after ventricular unloading. J Heart Lung Transplant. 2010; 29: p. 117-124.

57. Aguilar V, Lluis Fajas L. Cycling through metabolism. EMBO Molecular Medicine. 2010; 2(9): p. 338-348.

58. Kaplon J, van Dam L, Peeper D. Two-way communication between the metabolic and cell cycle machineries: the molecular basis. Cell Cycle. 2015; 14(13): p. 2022-2032.

59. Tuunanen H, Knuuti J. Metabolic remodelling in human heart failure. Cardiovascular Research. 2011; 90: p. 251-257.

60. McClave SA, Sinder HL. Dissecting the energy needs of the body. Current Opinion in Clinical Nutrition and Metabolic Care. 2001; 4(2): p. 143-147.

61. Stanley WC, Recchia FA, Lopaschuk GD. Myocardial Substrate Metabolism in the Normal and Failing Heart. Physiological Reviews. 2005; 85: p. 1093-1129.

62. Doenst T, Nguyen TD, Abel ED. Cardiac Metabolism in Heart Failure Implications Beyond ATP Production. Circulation Research. 2013; 113: p. 709-724.

63. van Bilsen M, van Nieuwenhoven FA, van der Vusse GJ. Metabolic remodelling of the failing heart: beneficial or detrimental? Cardiovascular Research. 2009; 81: p. 420-428.

64. Newman JC, Verdin E. Ketone bodies as signaling metabolites. Trends in Endocrinology and Metabolism. 2014; 25: p. 42-52.

65. Bedi KCJ, Snyder WD, Brandimarto J, Moez A, Mesaros C, Worth AJ, et al. Evidence for Intramyocardial Disruption of Lipid Metabolism and Increased Myocardial Ketone Utilization in Advanced Human Heart Failure. Circulation. 2016; 133: p. 706-716.

66. Aubert G, Martin OJ, Horton JL, Lai L, Vega RB, Leone TC, et al. The Failing Heart Relies on Ketone Bodies as a Fuel. Circulation. 2016; 133: p. 698-705.

67. Elmore S. Apoptosis: A Review of Programmed Cell Death. Toxicologic Pathology. 2007; 35: p. 495-516.

68. Polager S, Ginsberg D. E2F - at the crossroads of life and death. Trends in Cell Biology. 2008; 18: p. 528-535.

69. Nahle Z, Polakoff J, Davuluri RV, McCurrach ME, Jacobson MD, Narita M, et al. Direct coupling of the cell cycle and cell death machinery by E2F. Nature Cell Biology. 2002; 4: p. 859-864.

70. Haupt Y, Maya R, Kazaz A, Oren M. Mdm2 promotes the rapid degradation of p53. Nature. 1997; 387: p. 296-299.

71. Hiebart SW, Packham G, Strom D, Haffner R, Oren M, Zambetti G, et al. E2F1:Dp1 induces p53 and overrides survival factors to trigger apoptosis. Molecular and Cellular Biology. 1995; 5: p. 6864-6874.

72. Hseih J, Yap D, O'Connor DJ, Fogal V, Fallis L, Chan F, et al. Novel Functions of the Cyclin A Binding Site of E2F in Regulating p-53 Induced Apoptosis in Response to DNA Damage. Molecular Cell Biology. 2002; 22: p. 78-93.

73. Yurkova N, Shaw J, Blackie K, Weidman D, Jayas R, Flynn B, et al. The Cell Cycle Factor E2F-1 Activates Bnip3 and the Intrinsic Death Pathway in Ventricular Myocytes. Circulation Research. 2008; 102: p. 472-479.

74. Yang W, Wang Z, Zhu Y, Yang H. E2F6 negatively regulates ultraviolet-induced apoptosis via modulation of BRCA1. Cell Death and Differentiation. 2006; 14: p. 807-817.

75. Yang WW, Shu B, Zhu Y, Yang HT. E2F6 Inhibits Cobalt Chloride-Mimetic Hypoxia-induced Apoptosis through E2F1. Molecular Biology of the Cell. 2008; 19: p. 3691-3700.

76. Bhatnagar N, Li X, Padi SK., Zhang Q, Tang MS, Guo B. Downregulation of miR-205 and miR-31 confers resistance to chemotherapy-induced apoptosis in prostate cancer cells. Cell Death Discovery. 2010; 1: p. e105.

77. Zhang Q, Sun M, Zhou S, Guo B. Class I HDAC inhibitor mocetinostat induces apoptosis by activation of miR-31 expression and suppression of E2F6. Cell Death Discovery. 2016; 2: p. 16036.

78. Tang H, Liu P, Yang L, Xie X, Ye F, Wu M, et al. miR-185 Suppresses Tumor Proliferation by Directly Targeting E2F6 and DNMT1 and Indirectly Upregulating BRCA1 in Triple-Negative Breast Cancer. Molecular Cancer Therapeutics. 2014; 13(12): p. 3185-3197.

79. Agah R, Kirschebaum LA, Abdellatif M, Truong LD, Chakraborty S, Michael LS, et al. Adenoviral Delivery of E2F-1 Directs Cell Cycle Reentry and p53-independent Apoptosis in Post Mitotic Adult Myocardium. Journal of Clinical Investigation. 1997; 100: p. 2722-2728.

80. Westendorp B, Major JL, Nader M, Salih M, Leenen FHH, Tuana BS. The E2F6 repressor activates gene expression in myocardium resulting in dilated cardiomyopathy. FASEB Journal. 2012; 26(6): p. 2569-2579.

81. Mozaffarian D, Benjamin EJ, Go AS, Arnett DK, Blaha MJ, Cushman M, et al. Heart Disease and Stroke Statistics—2016 Update. Circulation. 2016;: p. e1-e323.

82. McNally EM, Golbus JR, Puckelwartz MJ. Genetic mutations and mechanisms in dilated cardiomyopathy. Journal of Clinical Investigation. 2013; 123(1): p. 19-26.

83. Hershberger RE, Morales A. Dilated Cardiomyopathy Overview [internet]. Seattle: University of Washington; 1993-2017 [cited 2017 1 24. Available from: https://www.ncbi.nlm.nih.gov/books/NBK1309/.

84. Luk A, Ahn E, Soor GS, Butany J. Dilated cardiomyopathy: a review. Journal of Clinical Pathology. 2009; 62(3): p. 219-225.

85. McKinsey TA, Olson EN. Toward transcriptional therapies for the failing heart: chemical screens to modulate genes. Journal of Clinical Investigation. 2005; 115: p. 538-546.

86. Demos-Davies KM, Ferguson BS, Cavasin MA, Mahaffey JH, Williams SM, Spiltoir JI. HDAC6 contributes to pathological responses of heart and skeletal muscle to chronic angiotensin-II signaling. American Journal of Physiology. Heart Circulation Physiology. 2014; 307: p. H252-H258.

87. Mori J, Basu R, McLean BA, Das SK, Zhang L, Patel VB. Agonist-induced hypertrophy and diastolic dysfunction are associated with selective reduction in glucose oxidation: a metabolic contribution to heart failure with normal ejection fraction. Circulation Heart Failure. 2012; 5: p. 493-503.

88. Gustein DE, Morley GE, Tamaddon H, Vaidya D, Schneider MD, Chen J. Conduction slowing and sudden arrhythmic death in mice with cardiac-restricted inactivation of Connexin43. Circulation Research. 2001; 88: p. 333-339.

89. Severs NJ, Dupont E, Coppen SR, Halliday D, Inett E, Baylis D,ea. Remodelling of gap junctions and connexin expression in heart disease. Biochimica et Biophysica Acta Biomembranes. 2004; 1662: p. 138-148.

90. Song K, Backs J, McAnally J, Qi X, Gerard RD, Richardson JA, et al. The transcriptional coactivator CAMTA2 stimulates cardiac growth by opposing class II histone deacetylases. Cell. 2006; 125: p. 453-466.

91. Fielitz J, van Rooij E, Spencer JA, Shelton JM, Latif S, van der Nagel R, et al. Loss of muscle-specific RING-finger 3 predisposes the heart to cardiac rupture after myocardial infarction. Proceedings of the National Academy of Sciences of the United States of America. 2007; 104: p. 4377-4382.

92. Merlet N, Piriou N, Rozec B, Grabherr A, Lauzier B, Trochu JN, et al. Increased beta2-adrenoreceptors in doxorubicin-induced cardiomyopathy in rat. PLos One. 2013; 8: p. e64711.

93. Richter W, Catherine SL, Conti M. Splice variants of the cyclic nucleotide phosphodiesterase PDE4D are differentially expressed and regulated in rat tissue. Biochemical Journal. 2005;: p. 803-811.

94. Luttrell LM, Ferguson SSG, Daaka Y, Miller WE, Maudsley S, Della Rocca GJ, et al. B-arrestin-dependent formation of B2 adrenergic receptor-Src protein kinase complexes. Science. 1999; 283: p. 655-661.

95. Shin S, Kim T, Ho-Sung L, Ho-Sun K, Jun Hyuk KJ, Lee JY, et al. The switching role of b-adrenergic receptor signaling in cell survival or death decision of cardiomyocytes. Nature Communications. 2014; 5: p. 5777.

96. Corre I, Baumann HS. Regulation of Gi2 proteions of v-fms-induced proliferation and transformation via Src-kinase and STAT3. Oncogene. 1999; 18: p. 6335-6342.

97. Bueno OF, Molkentin JD. Involvement of extracellular signal-regulated kinases 1/2 in cardiac hypertrophy and cell death. Circulation Research. 2002; 91: p. 776-781.

98. Wang S, Gong H, Jiang G, Ye Y, Wu J, You J, et al. Src is required for mechanical stretch-induced cardiomyocyte hypertrophy through angiotenisin II type 1 receptor-dependent B-arrestin2 pathways. PLos One. 2014;: p. e92926.

99. Scott JD, Santana LF. A-kinase anchoring proteins: getting to the heart of the matter. Circulation. 2010; 121: p. 1264-1271.

100. Beca S, Heli PB, Simpson JA, Zhao D, Farman GP,JPP, al e. Phosphodiesterase 4D regulates baseline sarcoplasmic reticulum Ca2+ release and cardiac contractility, independently of L-type Ca2+ current. Circulation Research. 2011; 109: p. 1024-1030.

101. Chang Z, Zhang Q, Feng Q, Xu J, Teng Q, al e. Deletion of Akt1 causes heart defects and abnormal cardiomyocyte proliferation. Developemental Biology. 2010; 347: p. 384-391.

102. Wu Y, Ouyang W, Lazorchak AS, Liu D, Shen H, Su B. mTOR complex 2 tragets Akt for proteasomal degradation via phosphorylation at the hydrophobic motif. Journal of Biological Chemistry. 2011; 286: p. 14190-14198.

103. Liao Y, Hung MC. Physiological regulation of Akt activity and stability. American Journal of Translational Research. 2012; 2: p. 19-42.

104. Fang X, Yu SX, Lu Y, Bast RC, Woodgett JR, Mills GB. Phosphorylation and inactivation of glycogen synthase kinase 3 by protein kinase A. Proceedings of the National Academy of Sciences of the United States of America. 2000; 97: p. 11960-11965.

105. Tomita H, Nazmy M, Kajimoto K, Yehia G, Molina CA, Sadoshima J. Inducible cAMP early repressor (ICER) is a negative-feedback regulator of cardiac hypertrophy and an important mediator of cardiac myocyte apoptosis in response to B-adrenergic receptor stimulation. Circulation Research. 2003; 93: p. 12-22.

106. Shaw J, Yurkova N, Zhang T, Gang H, Aguilar F, Weidman D, et al. Antagonism of E2F-1 regulated Bnip3 transcription by NFKB is essential for basal cell survival. Proceedings of the National Academy of Scienec of the United Staes of America. 2008; 105: p. 20734-20739.

107. D. D, Konecny F, Zou J, Sun X, von Harsdorf R. Anti-apoptotic of the E2F transcription factor 4 (E2F4)/p130, a member of retinoblastoma gene family in cardiac myocytes. Journal of Molecular and Cellular Cardiology. 2012; 53: p. 820-828.

108. Shenoy SK, Drake MT, Nelson CD, Houtz DA, Xiao K, S. M, et al. B-Arrestin-dependent, G protein-independent ERK1/2 activation by the B2 adrenergic receptor. Journal of Biological Chemistry. 2006; 281: p. 1261-1273.

109. Ruwhof C, van der Laarse A. Mechanical stress-induced cardiac hypertrophy: mechanisms and signal transduction pathways. Cardiovascular Research. 2000; 47: p. 23-27.

110. Purcell NH, Wilkins BJ, York A, Saba-El-Leil MK, Meloche S, Robbins J, et al. Genetic inhibition of cardaic ERK1/2 promotes stress-induced apoptosis and heart failure but has no effect on hypertrophy in vivo. Proceedings of the National Academy of Sciences of the United States of America. 2007; 104: p. 14074-14079.

111. Travers JG, Kamal FA, Robbins J, Yutzey KE, Blaxall BC. Cardiac Fibrosis: The Fibroblast Awakens. Circulation Research. 2016; 118(6): p. 1021-1040.

112. Trimarchi JM, Lees JA. Sibling rivalry in the E2F family. Nature Reviews Molecular Cell Biology. 2002; 3: p. 11-20.

113. Dyson DK, Dimova NJ. The E2F transcriptional network: old acquaintances with new faces. Oncogene. 2005; 24: p. 2810-2826.

114. Bhatnagar N, Li X, Padi SK, Zhang Q, Tang MS, Guo B. Downregulation of miR-205 and miR-31 confers resistance to chemotherapy-induced apoptosis in prostate cancer cells. Cell Death and Disease. 2010; 1: p. e105.

115. Zhang Q, Padi SK, Tindall DJ, Guo B. Polycomb protein EZH2 suppresses apoptosis by silencing the proapoptotic miR-31. Cell Death and Disease. 2014; 5: p. e1486.

116. Pei Y, Banerjee S, Sun Z, Chandra Jha H, Saha A, Robertson ES. EBV Nuclear Antigen 3C Mediates Regulation of E2F6 to Inhibit E2F1 Transcription and Promote Cell Proliferation. PLOS Pathogens. 2016; 12(8): p. e1005844.

117. Major JL, Dewan A, Salih M, Leddy JJ, Tuana BS. E2F6 Impairs Glycolysis and Activates BDH1 Expression Prior to Dilated Cardiomyopathy. PLOS One. 2017; 12(1): p. e0170066.

118. Major JL, Salih M, Tuana BS. Interplay between the E2F pathway and β-adrenergic signaling in the pathological hypertrophic respnse of myocardium. Journal of Molecular and Cellular Cardiology. 2015; 84: p. 179-190.

119. Shu B, Yang WW, Yang HT. Expression pattern of E2F6 in physical and chemical hypoxia-induced apoptosis. Acta Physiologican Sinica. 2008; 60(1): p. 1-10.

120. Chatterjee K, Zhang J, Honbo N, Karliner JS. Doxorubicin Cardiomyopathy. Cardiology. 2010; 115(2): p. 155-162.

121. Bertoli C, Klier S, McGowan C, Wittenberg C, de Bruin RA. Chk1 inhibits E2F6 repressor function in response to replication stress to maintain cell-cycle transcription. Current Biology. 2013; 23: p. 1629-1637.

122. Cimprich KA, Cortez D. ATR: An Essential Regulator of Genome Integrity. Nature Reviews Molecular and Cellular Biology. 2008; 9(8): p. 616-627.

123. Chen H, Tsai S, Leone G. Emerging roles of E2Fs in cancer: An exit from cell cycle control. Nature Reviews Cancer. 2009; 9(11): p. 785-797.

124. Knudsen ES, Wang JYJ. Targeting the RB-pathway in cancer therapy. Clinical Cancer Research. 2010; 16(4): p. 1094-1099.

125. Stevens C, Smith L, La Thangue NB. Chk2 activates E2F-1 in response to DNA damage. Nature Cell Biology. 2003; 5(5): p. 401-409.

126. Urist M, Tanaka T, Poyurovsky MV, Prives C. p73 induction after DNA damage is regulated by checkpoint kinases Chk1 and Chk2. Genes and Developement. 2004; 18(24): p. 3041-3054.

127. Hayashi T, Arimura T, Itoh-Satoh M, Ueda K, Hohda S, Inagaki N, et al. Tcap gene mutations in hypertrophic cardiomyopathy and dilated cardiomyopathy. Journal of the American Academy of Cardiology. 2004; 44(11): p. 2192-2201.

128. Bos JM, Poley RN, Ny M, Tester DJ, Xu X, Vatta M, et al. Genotype-phenotype relationships involving hypertrophic cardiomyopathy-associated mutations in titin, muscle LIM protein, and telethonin. Molecular Genetics and Metabolism. 2006; 88(1): p. 78-85.

129. Asp P, Acosta-Alvear D, Tsikitis M, van Oevelen C, Dynlacht BD. E2f3b plays an essential role in myogenic differentiation through isoform-specific gene regulation. Genes and Developement. 2009; 23: p. 37-53.

130. Sdek P, Zhao P, Wang Y, Huang C, Ko CY, Butler PC, et al. Rb and p130 control cell cycle gene silencing to maintain the postmitotic phenotype in cardiac myocytes. Journal of Cell Biology. 2011; 194(3): p. 407-423.

131. Baskin KK, Winders BR, Olson EN. Muscle as a "mediator" of systemic metabolism. Cell Metabolism. 2015; 21: p. 237-248.

132. Kolwicz Jr SC, Purohit S, Tian R. Cardiac Metabolism and its Interactions With Contraction, Growth, and Survival of Cardiomyocytes. Circulation Research. 2013; 113: p. 603-613.

133. Janardhan A, Chen J, Crawford PA. Altered Systemic Ketone Body Metabolism in Advanced Heart Failure. Texas Heart Institute Journal. 2011; 38: p. 533-538.

134. Kolwicz SC, Airhart S, Tian R. Ketones Step to the Plate: A Game Changer for Metabolic Remodeling in Heart Failure? Circulation Research. 2016; 133: p. 689.

135. Dedkova EN, Blatter LA. Role of β-hydroxybutyrate, its polymer poly-β-hydroxybutyrate and inorganic polyphosphate in mammalian health and disease. Frontiers in Physiology. 2014; 5: p. 260.

136. Kanikarla-Marie P, Jain SK. Hyperketonemia and ketosis increase the risk of complications in type 1 diabetes. Free Radical Biology and Medicine. 2016; 95: p. 268-277.

137. Palomer X, Álvarez-Guardia D, Davidson MM, Chan TO, Feldman AM, Vázquez-Carrera M. The Interplay between NF-kappaB and E2F1 Coordinately Regulates Inflammation and Metabolism in Human Cardiac Cells. PLOS One. 2011; 6: p. e19724.

138. Hsieh MCF, Das D, Sambandam N, Zhang MQ, Nahlé Z. Regulation of the PDK4 Isozyme by the Rb-E2F1 Complex. The Journal of Biological Chemistry. 2008; 283: p. 27410-27417.

139. Ramjiawan A, Bagchi RA, Blant A, Albak L, Cavasin MA, Horn T, et al. Roles of histone deacetylation and AMP kinase in regulation of cardiomyocyte PGC-1α gene expression in hypoxia. American Journal of Physiology. Cell Physiology. 2013; 304: p. C1064-72.

140. Ferguson BS, McKinsey TA. Non-sirtuin histone deacetylases in the control of cardiac aging. Journal of Molecular and Cellular Cardiology. 2015; 83: p. 14-20.

141. Fajas L, Annicotte JS. E2F1 at the crossroad of proliferation and oxidative metabolism. Cell Cycle. 2011; 10: p. 4193-4194.

142. Wu M, Seto E, Zhang J. E2F1 enhances glycolysis through suppressing Sirt6 transcription in cancer cells. Oncotarget. 2015; 6: p. 11252-11263.

143. Sdek P, Zhao P, Wang Y, Maclellan R. Rb and p130 control cell cycle gene silencing to maintain the postmitotic phenotype in cardiac myocytes. Journal of cell Biology. 2011; 194: p. 407-423.

144. Sakamaki T, Casimiro MC, Ju X, Quong AA, Katiyar S, Liu M, et al. Cyclin D1 determines mitochondrial function in vivo. Molecular and Cellular Biology. 2006; 26: p. 5449-5569.

145. Ho CF, Chan KW, Yeh HI, Kuo J, Liu HJ, Wang CY. Ketone bodies upregulate endothelial connexin43 (Cx43) gap junctions. The Veterinary Journal. 2013; 198: p. 696-701.

146. Kirshenbaum LA, Abdellatif M, Chakraborty S, Schneider MD. Human E2F-1 reactivates cell cycle progression in ventricular myocytes and represses cardiac gene transcription. Developemental Biology. 1996; 179: p. 402-411.

147. Kalma Y, Granot I, Galiani D, Barash A, Dekel N. Luteinizing Hormone-Induced Connexin 43. Endocrinology. 2004; 145: p. 1617-1624.

148. Kostin S, Dammer S, Hein S, Klovekorn WP, Baure EP, Schaper J. Connexin 43 expression and distribution in compensated and decompensated cardiac hypertrophy in patients with aortic stenosisConnexin 43 expression and distribution in compensated and decompensated cardiac hypertrophy in patients with aortic stenosis. Cardiovascular Research. 2004; 62(1): p. 426-436.

149. Ai X, Pogwizd SM. Connexin 43 Downregulation and Dephosphorylation in Nonischemic Heart Failure Is Associated With Enhanced Colocalized Protein Phosphatase Type 2A. Circulation Research. 2005; 96: p. 54-63.

150. Boulaksil M, Winckels SK, Engelen MA, Stein M, van Veen TA, Jansen JA, et al. Heterogeneous Connexin43 distribution in heart failure is associated with dispersed conduction and enhanced susceptibility to ventricular arrhythmias. European Journal of Heart Failure. 2010; 12(9): p. 913-921.

151. Lin H, Ogawa K, Imanaga I, Tribulova N. Remodeling of connexin 43 in the diabetic rat heart. Molecular and Cellular Biochemistry. 2006; 290(1): p. 69-78.

152. Shimazu T, Hirschey MD, Newman J, He W, Shirakawa K, Le Moan N, et al. Suppression of oxidative stress by β-hydroxybutyrate, an endogenous histone deacetylase inhibitor. Science. 2013; 339: p. 211-214.

153. Gonzalez E, McGraw TE. The Akt kinases: isoform specificity in metabolism and cancer. Cell Cycle. 2009; 8: p. 2502-2508.

154. Iglesias A, Murga M, Laresgoiti U, Skoudy A, Bernales I, Fullaondo A, et al. Diabetes and exocrine pancreatic insufficiency in E2F1/E2F2 double-mutant mice. The Journal of Clinical Investigation. 2004; 113: p. 1398-1407.

155. Dali-Youcef N, Mataki C, Coste A, Messaddeq N, Giroud S, Blanc S, et al. Adipose tissue-specific inactivation of the retinoblastoma protein protects against diabesity because of increased energy expenditure. Proceedings of the National Academy of Sciences of the United States of Amreica. 2008; 104: p. 10703–10708.

156. Chen M, Capps C, Willerson JT, Zoldhelyi P. E2F-1 regulates nuclear factor-kappaB activity and cell adhesion: potential antiinflammatory activity of the transcription factor E2F-1. Circulation. 2002; 106: p. 2707-2713.

157. Palomer X, Álvarez-Guardia D, Davidson MM, Chan TO, Feldman AM, Vazquez-Carrera M. The Interplay between NF-kappaB and E2F1 Coordinately Regulates Inflammation and Metabolism in Human Cardiac Cells. PLOS One. 2011; 6: p. e19724.

158. Kanai D, Ueda A, Akagi T, Yokota T, Koide H. Oct3/4 directly regulates expression of E2F3a in mouse embryonic. Biochemical and Biophysical Research Communications. 2015; 459: p. 374-378.

159. Sussman MA, Welch S, Cambon N, Klevitzky R, Hewett T, Price R, et al. Myofibril degeneration caused by tropomodulin overexpression leads to dilated cardiomyopathy in juvenile mice. Journal of Clinical Investigation. 1998; 101(1): p. 51-61.

160. Gard JJ, Yamada K, Green KG, Eloff BC, Rosenbaum DS, Wang X, et al. Remodeling of gap junctions and slow conduction in a mouse model of desmin-related cardiomyopathy. Cardiovascular Research. 2005; 67(3): p. 539-547.

161. Asp P, Acosta-Alvear D, Tsikitis M,vOC, Dynlacht BD. E2f3b plays an essential role in myogenic differentiation through isoform-specific gene regulation. Genes and Developement. 2009; 23: p. 37-53.

162. Markiewicz E, Dechat T, Foisner R, Quinlan RA, Hutchiinson CJ. Lamin A/C Binding Protein LAP2 is Required for Nuclear Anchorage of Retinoblastoma Protein. Molecular Biology of the Cell. 2002; 13: p. 4401-4413.

163. Melcon G, Koslov S, Cutler DA, Sullivan T, Hernandez L, Zhao P, et al. Loss of emerin at the nuclear envelope disrupts the Rb1/E2F and MyoD pathways during muscle regeneration. Human Molecular Genetics. 2006; 15: p. 637-651.

164. Clarke AR, Maandag ER, van Roon M, van der Lugt NMT, van der Valk M, Hooper ML, et al. Requirement for a functional rb-1 gene in murine development. Nature. 1992; 359(6393): p. 328-330.

165. Courel M, Friesenhahn L, Lees JA. E2f6 and Bmi1 cooperate in axial skeletal development. Development Dynamics. 2008; 237: p. 1232-1242.

APPENDICES

Appendix 1: Supplemental Information for Chapter 1

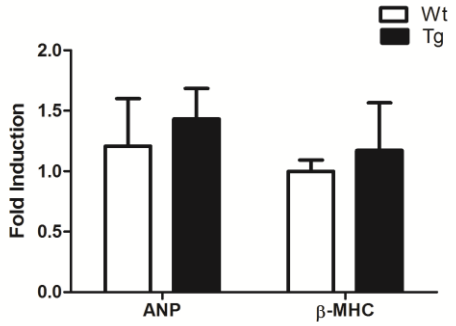

Supplemental Figure 1. ***Fetal gene program is not activated in 2 Week old Tg Hearts*****.** Fold induction of ANP and β–MHC transcripts in 2 week old Wt (white) and Tg (black) myocardium calculated by qPCR in relation to 18SrRNA. Results are presented as the mean ± SEM. (n=5-6).

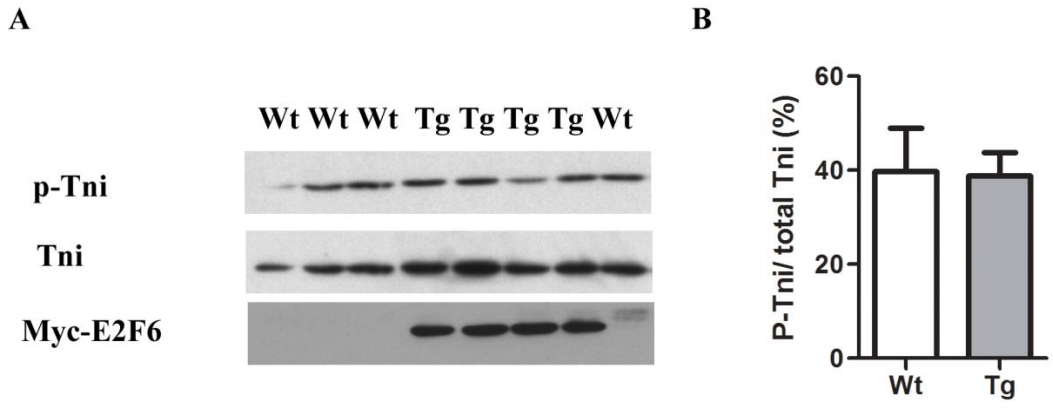

Supplemental Figure 2. ***Phosphorylation status of troponin I (TnI) is not changed in Tg myocardium.*** (A) Western blot analysis of phosphorylated (p-Tni) and total (Tni) in Wt and Tg cardiac lysates. (B) Densitometric quantification of p-Tni/Tni. Results are presented as the mean ± SEM. (n=4).

Appendix 2: Supplemental Information for Chapter 2

Online Materials and Methods Supplement

Mice & Genotyping

Transgenic (Tg) mice with cardiac specific expression of E2F6 (B6C3F1) under control of the α-MHC promoter were bred with WT B6C3F1 (80). All animal work was performed in accordance with the Guide for the Care and Use of Laboratory Animals published by the US National Institutes of Health (NIH Publication No. 85-23, revised 2011). The protocols were approved by the University of Ottawa's institutional animal care committee: cmm-1725, cmm-1723. All possible steps were taken to ameliorate animal suffering. Mouse pups were euthanized by decapitation.

Genotyping was performed via DNA extraction from mouse ear (adult) or tail (pup) clip and PCR using the Phire Tissue Direct (Thermo Scientific) kit as per the manufacturer's instructions. Primers spanning the 6^{th} intron of E2F6 were used (ATCACAGTACATATTAGGAGCAC- sense, and GGTGCGGCTACCAGTCTACA– anti-sense) which result in the amplification of a long fragment (988bp) in Wt mice and a long and short fragment (342bp) in E2F6-Tg mice.

Neonatal Cardiomyocyte Isolation

Neonatal cardiomyocytes isolation was performed as previously described (117). Briefly, hearts were collected from Wt and Tg mice at P1, rinsed in HBSS, and incubated in 0.5% trypsin dissolved in HBSS overnight at 4^{o}C. Hearts were digested in 0.5% Collagenase type II (Gibco) dissolved in HBSS and cells were collected after each digestion via centrifugation at 3000g for 3 minutes and resuspended in feeding media (DMEM, 16% media-199,10% horse serum, 5% FBS, 1% penicillin/streptomycin, and 1% non-essential amino acids). Total suspensions were plated on uncoated 10cm dishes to remove fibroblasts. Cardiomyocytes were seeded ($1x10^{6}$/well on 6 well plates for

protein analysis or $1x10^5$/well on 96 well plate for viability assay) onto 0.1% gelatin coated plates and allowed to attach for 48 hours in a 37^oC incubator with 5% CO_2.

HeLa Cell Culture

HeLa (passage 3) were obtained from ATCC and suspended in feeding media (DMEM supplemented with 10% FBS and 1% penicillin/streptomycin). Cells were kept in a 37^oC incubator with 5% CO_2.

Induction of Apoptosis and Cell Viability Assay

Cardiomyocyte and/or HeLa feeding media was replaced with starving media (DMEM, 16% media-199, 1% FBS, 1% penicillin/streptomycin) for 24hr prior to the addition of doxorubicin (0.25μM-1μM) or cobalt-chloride (250μM -1000μM) for 24 hours except where indicated. For the cell viability analysis cell titer blue reagent (resazurin-10ul) was added to each well and cells were incubated at 37^oC with 5% CO_2 for 3 hours as per the manufacturer's protocol (Promega). Absorbance at 570nm and 590nm were recorded by the Synergy H1 plate-reader (Biotek). Percent viability was calculated as the difference between 570 and 590nM readings in treated cells compared to their own untreated controls. Viability experiments were performed in triplicate (n=8).

Protein Extraction and Western Blot

Protein extraction and western blot was performed as previously described (117). Briefly, lysates were collected in RIPA (50mM Tris (pH 7.4), 1mM EDTA, 150μM NaCl, 0.25% deoxycholic acid, 1% NP-40) containing protease and phosphatase inhibitors (Roche) and 5mM sodium butyrate to inhibit histone deacetylases. Lysates were centrifuged at 12800g for 10min at 4^oC and protein concentrations were determined using the BCA assay (Thermo Scientific). Lysates (20-40ug) were run on gradient (5-15%) SDS-PAGE gels in 3X loading dye (Cell Signaling). Gels were transferred to PVDF membrane (Millipore) in transfer buffer (25mM Tris, 190mM Glycine, 20% methanol) overnight at 4^oC. Membranes were blocked and antibodies were diluted in TBST (1M Tris, 290mM NaCl, 0.1% Tween, pH7.2) containing 5% milk. Following

ECL (Roche), band signals were assessed by densitometry using Image Lab Software 4.0.1 (Bio-Rad).

The following primary antibodies were used: p53(2524, 1:1000, mouse), acetyl p53 (lys379) (2570, 1:1000, rabbit), caspase 3 (9662,1:1000, rabbit), Chk1(2G1D5) (2360, mouse, 1:1000), p-Chk1(Ser345) (2348,1:1000, rabbit), and cyclin E1 (HE12) (4129, 1:1000, mouse) were purchased from Cell Signaling, Bcl2 (sc-3782, 1:500, mouse) and E2F1 (sc-251, 1:1000, mouse) were purchased from Santa Cruz Biotechnology, α-Tubulin (ab176560, 1:30000, rabbit) and Teliothenin (T-cap) (ab133646, mouse, 1:1000) were purchased from Abcam, GAPDH (MA5-15738, 1:5000, mouse) was purchased from Thermo-Scientific, anti-E2F6 (MABE57, 1:500, mouse) was purchased from Millipore, and myc (11667149001, 1:2000, mouse) was purchased from Roche. Secondary antibodies: anti-mouse (115-035-003, 1:20000) and anti-rabbit (111-035-045, 1:20000) were purchased from Jackson Immunochemicals.

RNA isolation and Reverse Transcription real time PCR

Total RNA extraction, first-strand cDNA synthesis, and qRT-PCR were performed as previously described (80). Briefly, RNA was extracted from HeLa and NCM using the RNEasy kit (Qiagen) and from cardiac lysate using the RNEasy Fibrous Tissue Mini Kit as per the manufacturer's protocol (Qiagen). First-strand cDNA was synthesized from 1μg RNA and oligoDT with SuperScriptII reverse transcriptase (Invitrogen) as per the manufacturer's protocol. qPCR was performed in the q-Rotor (Qiagen) using Fast Start SYBR Green (Roche). Gene expression was normalized against *18S* rRNA or *gapdh* as indicated, and fold inductions were calculated using the $\Delta\Delta C_t$ method. Primer pairs used for qPCR are:

18S: 5'-CAGTTTCAGAGAGGTCTATTGCAC-3' (sense) and 5'-GCACTCACATGCCCATACTACATA-3' (anti-sense),
Chk1: 5'-CGCCACATCAGGTGGTATGT-3' (sense) and 5'-GGACACGTAGGCTGGGAAAA (anti-sense),

Rad51: 5'- TGTACATTGACACCGAGGGC-3' (sense) and 5'-CCGCCCTGAGTAGTCTGTTC-3' (anti-sense),

Blm2: 5’-TAAGCCTGAGTGAGGATCATGGC-3’ (sense) and 5’-TTTGTGGAGTGGAGACTCAGTG-3’ (anti-sense),
E2F6: 5’-AAGGGGCGGAGATGATGACC-3’ (sense) and 5’-GCCCCAAAGTTGTTCAGGTCAGAT -3’ (anti-sense),
human E2F6: 5’-GTATGCAGCCTTGCTGTTGA-3’ (sense) and 5’-AGTCCCTCAAGGAGCTCACA -3’ (anti-sense),
human E2F1: 5’-GGGCTCTAACTGCACTTTCG-3’ (sense) and 5’-AGGGAGTTGGGGTATCAACC -3’ (anti-sense)

Statistics

Data were analyzed with a student t-test (Figures: 12, 13C/D, 14 C/D, 18), or ANOVA (one-way Figures: 15B/D. 16B/D, 17C) (two way Figures: 13A, 14A, 17A, 17D) with Bonferroni post-hoc test. The level of significance was set at $P<0.05$ in all cases.

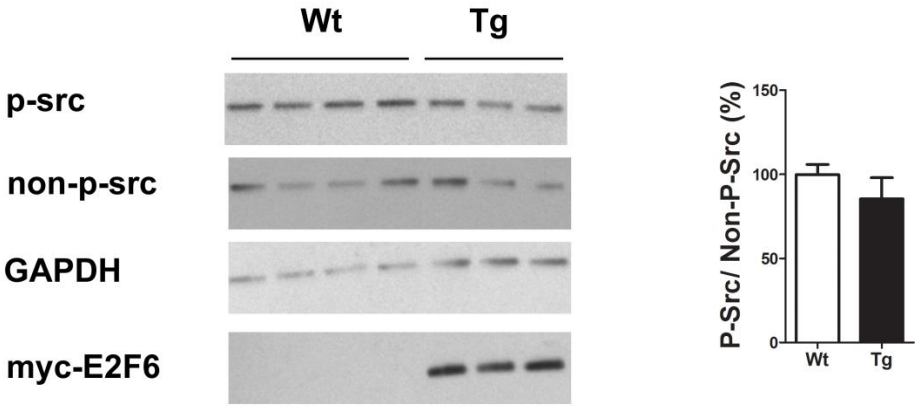

Supplemental Figure 3. ***Src not up-regulated in E2F6-Tg pup hearts.*** Representative immunoblot of Wt and Tg myocardium at postnatal day 1 probed with anti-src and p-src. (B) Quantification of p-src: non-p-src based on densitometry.

Appendix 3: Supplemental Information for Chapter 3

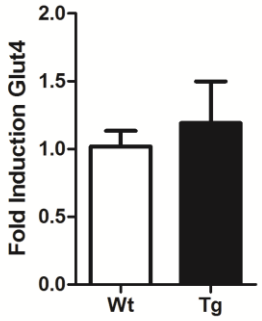

Supplemental Figure 4. ***GLUT4 Transcription is Not Altered in E2F6-Tg myocardium.*** *GLUT4* transcript levels from Wt and Tg myocardium 7 days after birth. Expression is normalized to *Gapdh*. Results represent mean±SEM values (n=5-7).

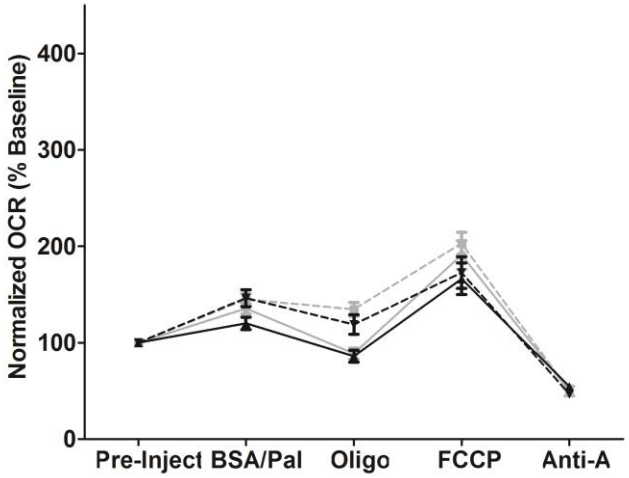

Supplemental Figure 5. ***Seahorse Method of OCR is Specific to Fatty Acids.*** Normalized oxygen consumption rate (OCR) of Wt and Tg neonatal cardiomyocytes following 24hr glucose starvation and treatment with etomoxir. Cardiomyocytes were treated with either BSA or palmitate, followed by the addition of oligomycin (Oligo), Carbonyl cyanide-4-phenylhydrazone (FCCP), and Antimycin-A (Anti-A). Results represent mean±SEM values (n=7-8).

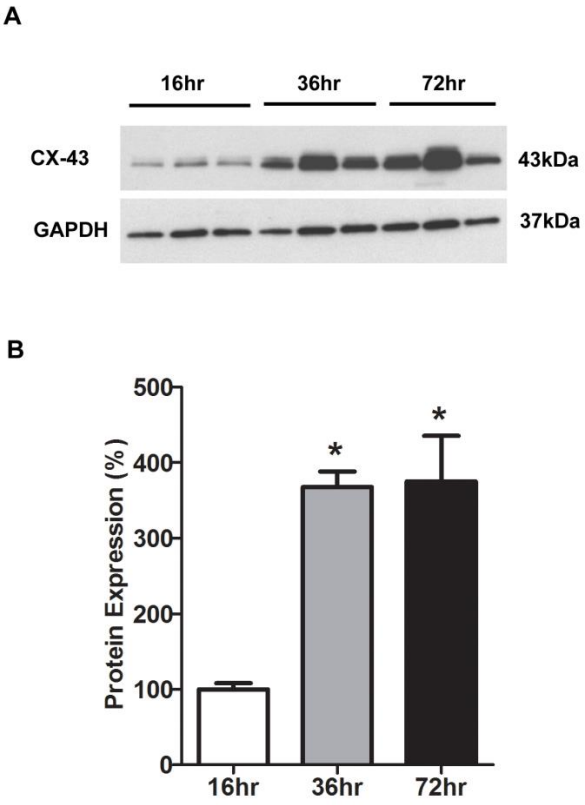

Supplemental Figure 6. ***CX-43 Expression is Increased in Tg Cardiomyocytes with Time in Culture.*** (A) Representative immunoblot of CX-43 in neonatal cardiomyocytes from Tg mice at 16, 36, and 72hr post-plating. (B) Quantification of CX-43 immunoblots. Results are presented as the mean ± SEM (n=3). **P*<0.05.

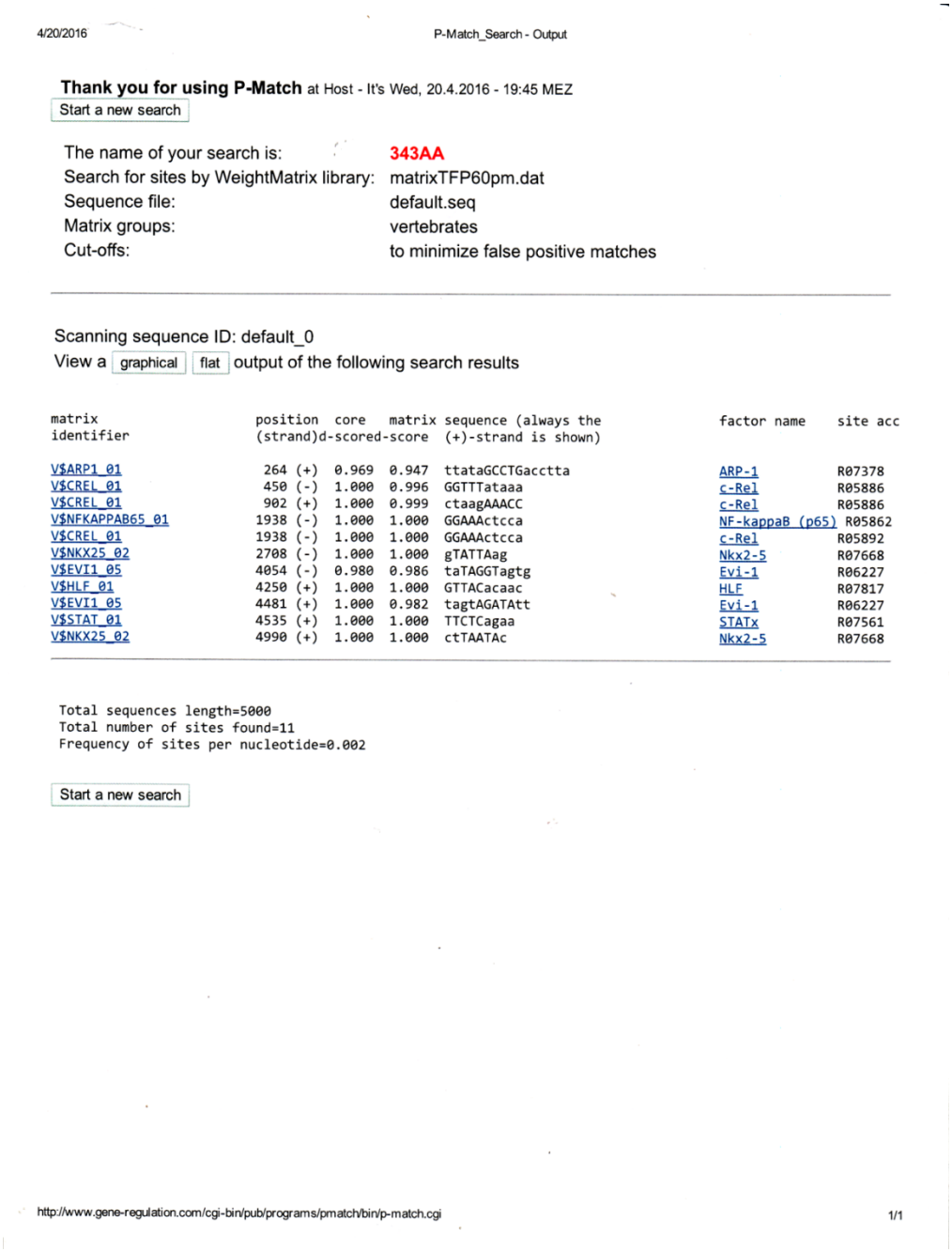

4/20/2016 P-Match_Search - Output

Thank you for using P-Match at Host - It's Wed, 20.4.2016 - 19:45 MEZ

Start a new search

The name of your search is:	343AA
Search for sites by WeightMatrix library:	matrixTFP60pm.dat
Sequence file:	default.seq
Matrix groups:	vertebrates
Cut-offs:	to minimize false positive matches

Scanning sequence ID: default_0

View a graphical flat output of the following search results

matrix identifier	position (strand)	core d-score	matrix d-score	sequence (always the (+)-strand is shown)	factor name	site acc
V$ARP1_01	264 (+)	0.969	0.947	ttataGCCTGacctta	ARP-1	R07378
V$CREL_01	450 (-)	1.000	0.996	GGTTTataaa	c-Rel	R05886
V$CREL_01	902 (+)	1.000	0.999	ctaagAAACC	c-Rel	R05886
V$NFKAPPAB65_01	1938 (-)	1.000	1.000	GGAAActcca	NF-kappaB (p65)	R05862
V$CREL_01	1938 (-)	1.000	1.000	GGAAActcca	c-Rel	R05892
V$NKX25_02	2708 (-)	1.000	1.000	gTATTAag	Nkx2-5	R07668
V$EVI1_05	4054 (-)	0.980	0.986	taTAGGTagtg	Evi-1	R06227
V$HLF_01	4250 (+)	1.000	1.000	GTTACacaac	HLF	R07817
V$EVI1_05	4481 (+)	1.000	0.982	tagtAGATAtt	Evi-1	R06227
V$STAT_01	4535 (+)	1.000	1.000	TTCTCagaa	STATx	R07561
V$NKX25_02	4990 (+)	1.000	1.000	ctTAATAc	Nkx2-5	R07668

Total sequences length=5000
Total number of sites found=11
Frequency of sites per nucleotide=0.002

Start a new search

http://www.gene-regulation.com/cgi-bin/pub/programs/pmatch/bin/p-match.cgi 1/1

Supplemental Figure 7. ***Promoter Analysis of Bdh1***. Analysis was performed using P-Match. The DNA sequence 5000bp upstream of the transcription start site of *Bdh1* was analyzed against the vertebrate core matrix.

Appendix 4: Supplemental Figures for Discussion

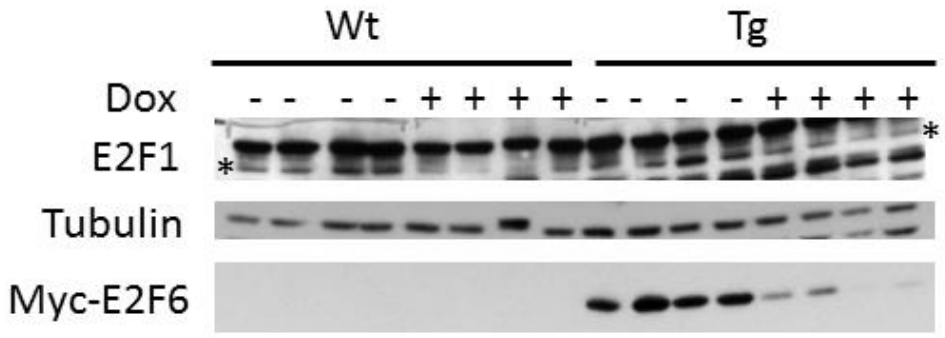

Supplemental Figure 8: ***E2F1 is decreased after dox (0.5μM 24hr) exposure in neonatal cardiomyocytes.*** Western blot examined with anti E2F1. E2F1 is denoted by the * (correct band determined by comparison to E2F1 expression vector).

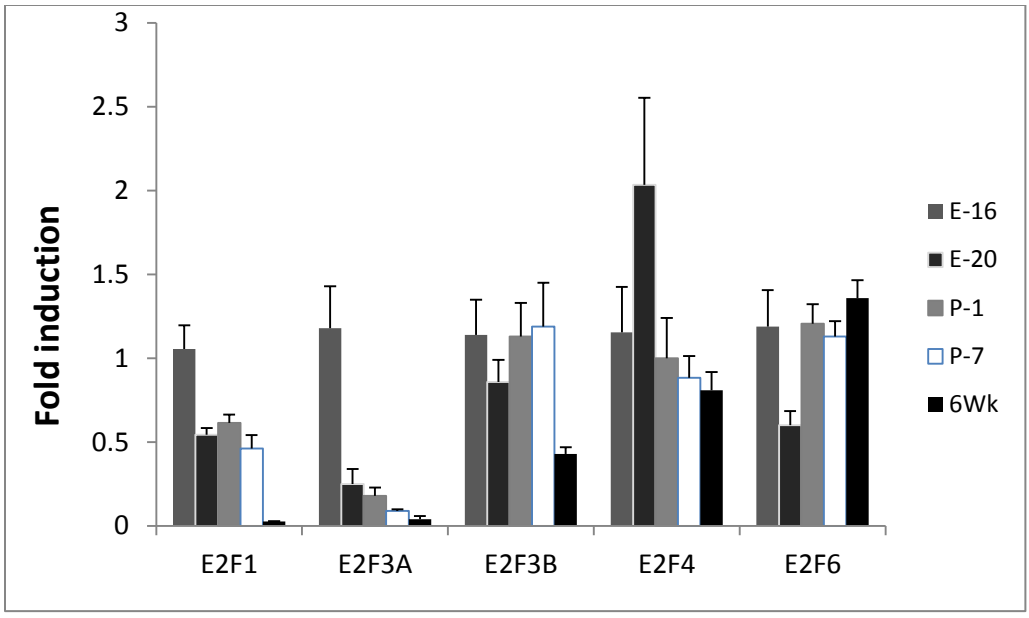

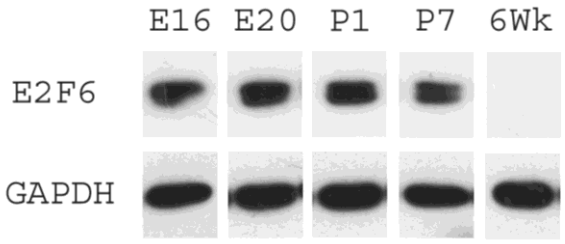

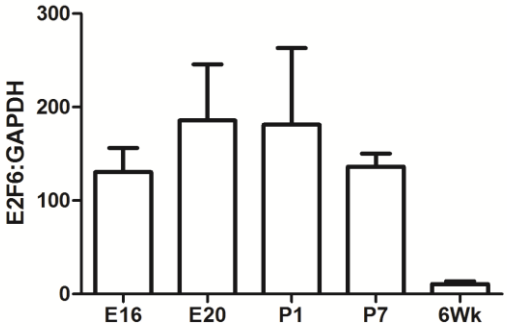

Supplemental Figure 9: ***E2F6 is down-regulated post-transcriptionally in the myocardium after birth.*** **(A)** Fold induction of E2F family members in the heart at various stages during murine development. Fold Inductions were calculated in reference to GAPDH (n=6). **(B)** Representative western blot of cardiac lysates from mice at various stages during development probed with anti-E2F6. **(C)** Quantification of E2F6 protein in the mouse heart in comparison to GAPDH.

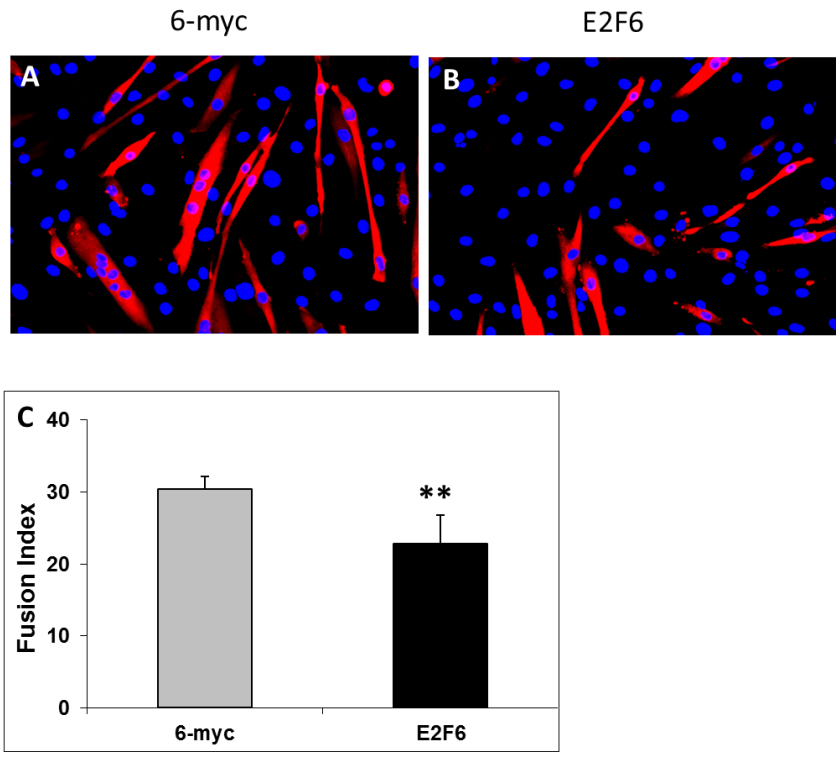

Supplemental Figure 10: ***E2F6 inhibits myoblast fusion.*** Transient transfection of C2C12 with (A) 6-myc or (B) E2F6. Cells were stained with mf20 (red) and DAPI (blue). Fusion index (C) n=8 fields of view. ** P-value<0.01

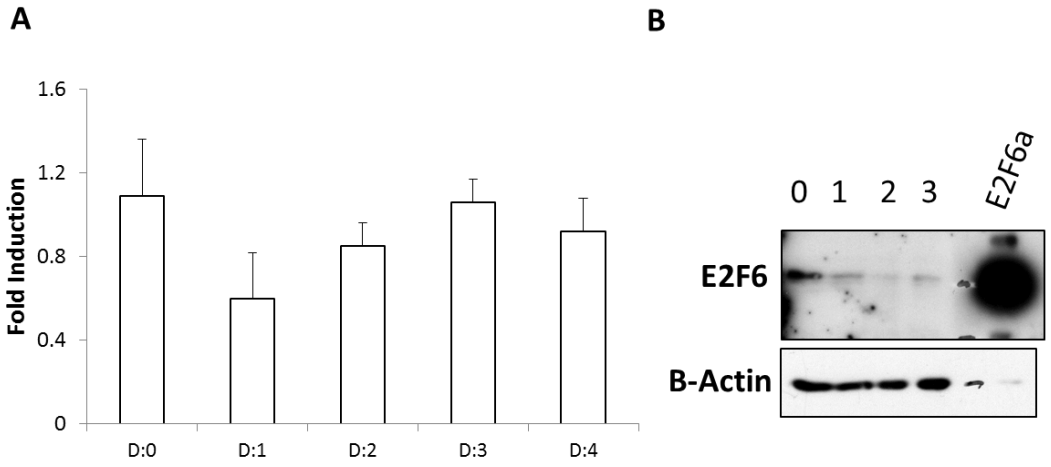

Supplemental Figure 11: ***E2F6 is down-regulated post-transcriptionally during C2C12 differentiation Day 0-Day 4.*** (A) Fold induction of E2F6 transcript relative to GAPDH (n=3). (B) Western blot analysis of E2F6 protein levels during differentiation. Over-expression of E2F6 in C2C12 is shown on the right as a positive control for anti-E2F6.